

Dynamic Surface Charge Distribution

Examining its effect on the electric double layer
using Molecular Dynamics simulation

Fenna Westerbaan van der Meij

Delft University of Technology

Cover picture:
*Artist's interpretation of the
silica-electrolyte interface*
by Julie van Vlerken, October 2020

Dynamic Surface Charge Distribution

Examining its effect on the electric double layer
using Molecular Dynamics simulation

by

Fenna Westerbaan van der Meij

in partial fulfillment of the requirements for the degree of

Master of Science
in Mechanical Engineering

at the Delft University of Technology,
to be defended publicly on Monday October 12, 2020 at 02:00 PM.

Supervisors:	Dr. R. M. Hartkamp Ir. M. F. Döpke
Thesis committee:	Prof. dr. ir. J. T. Padding Dr. B. P. Tighe Dr. R. M. Hartkamp Ir. M. F. Döpke

An electronic version of this thesis is available at <http://repository.tudelft.nl/>.

Preface and acknowledgements

Nine months ago, I started this thesis not knowing a pandemic would break out. Luckily for me, my simulations could be done from home, so in that regard I did not have the kind of setbacks my experimentally based colleagues experienced. However, it meant very little personal contact and long days in a never-changing environment (my room). I could not have done it without the help of some amazing people. I like to thank my supervisor Remco Hartkamp for his encouragement, his kindness when I felt a bit lost and our long and interesting discussions during the weekly meetings and via Slack. You made my thesis a lot more fun and interesting than I had imagined. I would also like to thank my second supervisor Max Döpke for helping me along in the scary world of command-line computing and for always being ready to answer my questions. And thank you Rintati Roza for being my buddy for the last couple of months. It was great to not be the only graduate student in this field anymore. I would also like to thank my friends for keeping me sane these last nine months. Especially, Mrigank Sinha, thank you for your emotional support. You helped me a lot, both with deep conversations and beer-induced fun. Thanks to Julie van Vlerken for our phone calls and movie nights, to Richelle van Capelleveen for the corona-walks and game breaks, and to Cynthia van den Anker for always thinking of me. Lastly, a big thank you to my boyfriend for your patience in enduring my numerous late-night monologues and joining me in my enthusiasm when I finally figured something out and in my frustration when the simulations kept crashing. You are the best.

Fenna Westerbaan van der Meij
Den Haag, October 2020

Abstract

In the pursuit of gaining a better understanding of the mechanisms of oxide-electrolyte interfaces, this thesis presents a working model that mimics a dynamic surface charge distribution by introducing protonation and deprotonation events using MD simulation. Due to the limitations of measurement equipment that operate on an atomic scale, literature cannot provide us with exact time scales for protonation and deprotonation events. Consequently, previous research simulated the surface charge distribution of oxide surfaces as being static and assumed the effect of local protonation and deprotonation to be negligible. This work shows that varying the (de)protonation event period τ significantly influences the characteristics of the electric double layer (EDL). Continuous protonation and deprotonation changes the diffusion coefficient and subsequently alters the structure of the Stern layer, screening function, and preferential adsorption type. As a whole, dynamic surface charge distribution has a considerable impact on the characteristics of the electric double layer depending on τ and should be considered in future MD simulations.

Contents

List of Figures	xi
List of Tables	xiii
List of Symbols	xv
List of Abbreviations	xvii
1 Introduction	1
1.1 Social relevance	1
1.2 Academic relevance	2
1.3 Scope of work	3
1.4 Research question	3
1.5 Hypothesis	4
1.6 Outline	4
2 Theoretical background	5
2.1 Silica-electrolyte interface	5
2.1.1 Amorphous silica	5
2.1.2 Silanol groups	6
2.1.3 Surface charge density	8
2.1.4 Electric double layer	9
2.2 Protonation and deprotonation	10
2.2.1 Equilibrium constant	10
2.2.2 (De)protonation rate constant	11
2.3 Properties of the EDL	14
2.3.1 Structure of the EDL	14
2.3.2 Adsorption type	14
2.3.3 Electrostatic screening	15
2.3.4 Water orientation	15
2.3.5 Diffusion	15
2.4 Experimental methods	16
2.4.1 Direct imaging	16
2.4.2 Indirect measurement	16
2.5 Conclusion	17
3 Methodology	19
3.1 Molecular dynamics simulation	19
3.1.1 Potentials	19
3.1.2 Velocity-Verlet integration	20
3.1.3 Periodic boundary conditions	21

3.2	Protonation and deprotonation model	21
3.2.1	Overview	21
3.2.2	Selection of random silanols	22
3.3	Simulation protocol.	23
3.3.1	Force field	24
3.3.2	Topology	24
3.3.3	Simulation conditions	25
3.4	Data analysis	26
3.4.1	Density profile as function of z-position	27
3.4.2	Density profile as function of distance	27
3.4.3	Screening function	27
3.4.4	Water orientation	27
3.4.5	Diffusion coefficient	27
4	Results and discussion	29
4.1	Structure of the EDL	29
4.2	Adsorption type	31
4.3	Electrostatic screening	33
4.4	Water orientation	33
4.5	Diffusion coefficient	34
5	Conclusion	37
6	Recommendations	39
6.1	Event periods.	39
6.2	Adsorption times	39
6.3	Effect of (de)protonation frequency on flow profiles	39
6.4	Protonation probability of silanols	39
	Bibliography	41
A	Derivations	45
A.1	Equation 2.9	45
B	Calculations	47
B.1	Number of ions in seawater	47
B.2	Number of deprotonated sites due to surface charge	47
C	Additional results	49
C.1	Density profiles as function of z-position	49
C.1.1	Average density profiles before symmetrization.	49
C.1.2	Density profiles for individual simulations.	50
C.2	Density profiles as function of distance	53
C.2.1	Zoomed-out density profile of Na^+	53
C.2.2	Density profiles for individual simulations.	54
C.3	Water orientation plots	56
C.4	MSD plots.	57
C.4.1	Visualization of bin sizes used for MSD calculation	57
C.4.2	Visualization of the curve-fitting range γ	58
C.4.3	Average MSD plots	59

D	LAMMPS scripts	65
D.1	in.forcefield	65
D.2	in.simulation	66
D.2.1	Initialization	66
D.2.2	Production	67
E	Python scripts	69
E.1	Creating initialization input files	69
E.2	Creating (de)protonation events input files	70
E.3	Generating MSD data	72

List of Figures

1.1	Composition of the earth's crust (Lutgens and Tarbuck [1])	1
2.1	Visualization of the atomic structure of amorphous silica, from Lunt <i>et al.</i> [2]	5
2.2	Visualization of the atomic structure of silica surface groups	6
2.3	Schematic overview of three pathways of silica surface group formation	7
2.4	Visualization of different silanol groups, inspired by Jal <i>et al.</i> [3]	8
2.5	Titration curve for silica, from Sonnefeld <i>et al.</i> [4] (+: 0.1 M NaCl, ■: 0.01 M NaCl, ★: 0.001 M NaCl)	9
2.6	Visualization of the EDL model	9
2.7	Schematic representation of protonation and deprotonation	10
2.8	Visualization of different adsorption types	14
3.1	Visualization of the periodic boundary method	21
3.2	Schematic representation of two (de)protonation states	22
3.3	Schematic flowchart of the partial charges during (de)protonation	22
3.4	Schematic flowchart of the formation of input files for the (de)protonation events	23
3.5	Flowchart of the LAMMPS simulation	24
3.6	VMD snapshot of the initial configuration of the system. Atom representations: Si in yellow, O in red, H in white, Na ⁺ in blue, Cl ⁻ in cyan.	25
4.1	Density profile as function of z-position, of Na ⁺ for varying τ	30
4.2	Density profile as function of z-position, of Cl ⁻ for varying τ	30
4.3	Density profile as function of z-position, of H ₂ O for varying τ	31
4.4	Density profile as function of distance, of Na ⁺ for varying τ	32
4.5	Density profile as function of distance, of Cl ⁻ for varying τ	32
4.6	Screening function for varying τ	33
4.7	Water orientations for varying τ	34
4.8	Diffusion coefficient of Na ⁺ for varying τ	35
4.9	Diffusion coefficient of Cl ⁻ for varying τ	35
4.10	Diffusion coefficient of H ₂ O for varying τ	36
C.1	Average density profiles as function of z-position, before symmetrization	49
C.2	Density profiles of Na ⁺ as function of z-position, for individual simulations . .	50
C.3	Density profiles of Cl ⁻ as function of z-position, for individual simulations . .	51
C.4	Density profiles of H ₂ O as function of z-position, for individual simulations . .	52
C.5	Zoomed-out density profile as function of distance, of Na ⁺ for varying τ	53
C.6	Density profiles of Na ⁺ as function of distance, for individual simulations . . .	54
C.7	Density profiles of Cl ⁻ as function of distance, for individual simulations . . .	55
C.8	Water orientations for individual simulations	56
C.9	Visualization of bins used for MSD calculation	57

C.10 Average MSD for Na^+ , x,y-direction, $\tau = \infty$, using range γ	58
C.11 Average MSD plot at $\tau = \infty$	59
C.12 Average MSD plot at $\tau = 1000$	60
C.13 Average MSD plot at $\tau = 100$	61
C.14 Average MSD plot at $\tau = 10$	62
C.15 Average MSD plot at $\tau = 1$	63

List of Tables

3.1	Event frequency and average lifetime of protonated and deprotonated silanols for variable τ	26
3.2	Partial charges of silanol group atoms	26

List of Symbols

Latin symbols

A	Area	N	Number of simulations
c	Concentration	N_i	Number of particles of component i
D	Diffusion coefficient	pH	Measure of acidity
d	Distance	pK_a	Logarithmic acid dissociation constant
e	Elementary charge	Q	Surface charge
F	Force	q	Point charge
H	Height	R	Rate
J	Diffusive flux	r	Distance between particles
K	Equilibrium constant	r_c	Cut-off radius
k	Rate constant	T	Temperature
K_a	Acid dissociation constant	t	Time
k_B	Boltzmann constant	U	Potential energy
m	Mass	v	Velocity
MSD	Mean square displacement	x	Position
n_i	Number density of component i		
n_{dim}	Dimension		

Greek symbols

β	Thermal energy	μ	Mean
Γ	Screening function	ρ	Density
γ	Curve-fitting range for the MSD	σ	Standard deviation
Δt	Time step	σ_0	Surface charge density
ϵ_0	Permittivity of vacuum	σ_{LJ}	Pair coefficient: finite distance at which the inter-particle potential is zero
ϵ_{LJ}	Pair coefficient: depth of the potential well	τ	Period of (de)protonation events
$\cos\theta$	Water orientation angle with the surface normal	Ψ	Electric potential

List of Abbreviations

AFM	Atomic force microscopy
CP/MAS NMR	Cross polarization/magic angle spinning nuclear resonance spectroscopy
DS	Diffuse swarm
EDL	Electric double layer
IFF	Interface force field model (Emami <i>et al.</i> [5])
IHP	Inner Helmholtz plane
IR	Infrared spectroscopy
ISSC	Inner-sphere surface complex
JC	Joung and Cheatham model (Joung and Cheatham III [6])
LAMMPS	Large-scale atomic/molecular massively parallel simulator
LJ	Lennard-Jones
MD	Molecular dynamics
MSD	Mean square displacement
NMR	Nuclear magnetic resonance spectroscopy
NVT	Canonical ensemble, a statistical ensemble where number of particles (N), volume (V) and temperature (T) are constant
OHP	Outer Helmholtz plane
OSSC	Outer-sphere surface complex
PZC	Point of zero charge
SHG	Second harmonic generation spectroscopy
SPC/E	Extended simple point charge model (Berendsen <i>et al.</i> [7])
VMD	Visual molecular dynamics computer program
VSFS	Vibrational sum frequency spectroscopy

1

Introduction

In this chapter a brief introduction to the general area of interest of this thesis will be given. Additionally, the place of this research in the academic world as well as the context and relevance will be discussed. Finally, the research objective and research questions will be explained.

1.1. Social relevance

Silicon (Si) is one of the world's most common elements. According to the book "Essentials of Geology" by Frederick K. Lutgens and Edward J. Tarbuck [1], 27.7 percent of the mass of the earth's crust consists of silicon (see Figure 1.1).

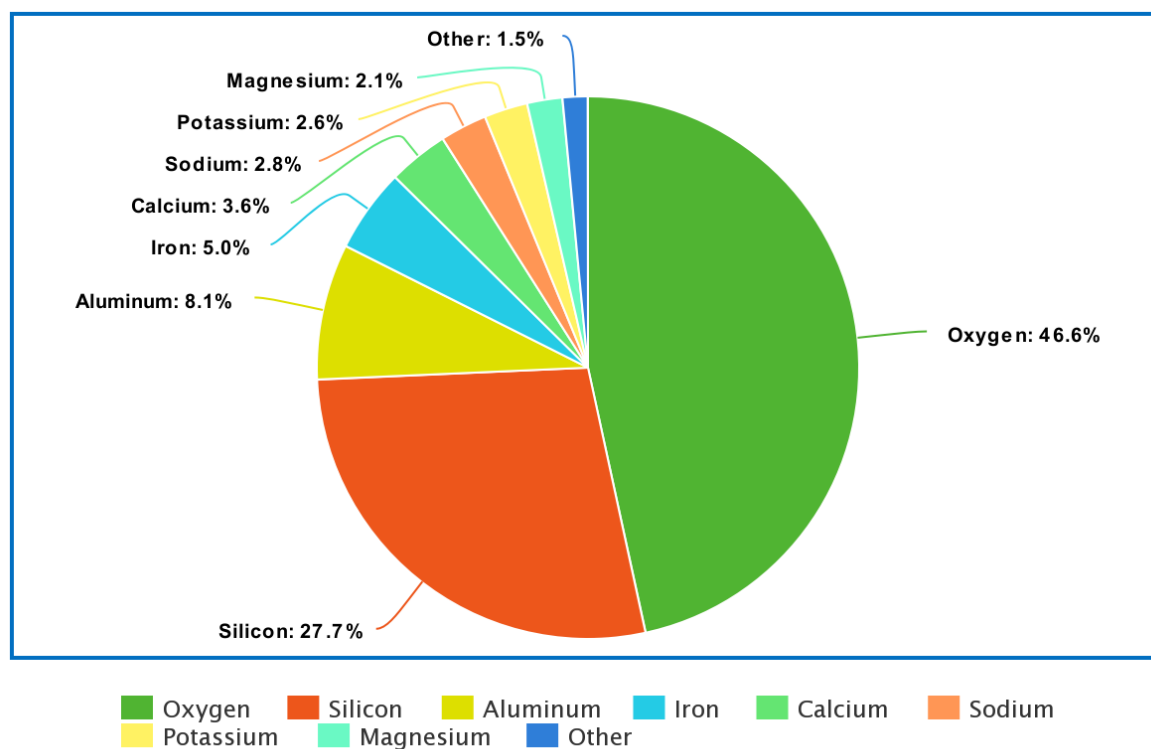


Figure 1.1: Composition of the earth's crust (Lutgens and Tarbuck [1])

Silicon is present in a variety of materials and minerals. The most common form is Silicon dioxide, or silica (SiO_2). Silica is the main component of sand and is used to make glass, crystals and aerogels. Silica exist in crystalline and amorphous form. The difference between these two is the structure. In crystalline silica, also called quartz, the Si and O-atoms are aligned in a neatly ordered grid. In amorphous (from the Greek word for shapeless) silica the atoms form no visible, repetitive structure.

Amorphous solids have the interesting property that their mechanical strength, refractive index, and electrical and thermal conductivity are the same in all directions. Amorphous silica is furthermore widely used in microelectronics as a semiconductor due to its insulating properties (Muller *et al.* [8]).

In recent years, the need for mechanically stable materials has grown tremendously. Think about uses in cation extraction from liquids such as desalination of sea water or the production of synthetic catalysts specifically engineered to improve reactions in various fields of industry. Other applications are found in electronics, ceramics, bioengineering and research equipment for chromatography. Researching the underlying kinetics of amorphous silica further would benefit these fields and applications. For example, by being able to make more accurate assumptions in calculations or developing new applications. Due to the developments in the field of nanotechnologies such as microfluidics [9], nanoelectronics [10] and use of nanoparticles in the medical field [11] the search for a better understanding of the characteristics of the solid-liquid interface of amorphous silica on a molecular level is growing in importance (Convery and Gadegaard [9], Ravindra *et al.* [10], Yang and Yu [11]).

1.2. Academic relevance

At the surface of an oxide in contact with a watery solution an acid-base equilibrium is formed. This equilibrium relates the concentrations of neutrally charged and negatively charged surface groups. Due to continuous protonation and deprotonation reactions, the local surface charge evolves over time while maintaining a constant surface charge.

The amount of experimental research on the influence of surface charge evolution on interfacial fluid properties is minimal due to the fact that available techniques are not sensitive enough to detect local changes at the surface on an atomic scale (Cruz-Chu *et al.* [12]). With the use of Molecular Dynamics (MD) simulations it is possible to build an atomic-scale solid-liquid interface and study intermolecular interactions in more detail. This can be used to gain a better understanding of the properties of amorphous silica and use this knowledge in the development of new applications. However, reactive simulations are computationally expensive, and explicit reactive force field parameters are limited. Consequently, the majority of MD simulations omit the acid-base equilibrium reaction and assume the surface charge distribution to be constant throughout the simulation (Lowe *et al.* [13]).

The assumption of a constant surface charge distribution overlooks the interactions the ions have with the locally changing charged surface. These interactions could influence the interfacial dynamics and structure of the electric double layer. Think of changes in diffusion near the surface and orientation of water molecules as well as overall changes in viscosity or electric permittivity. Modeling a dynamic surface charge distribution using MD simulation and studying its effects on the characteristics of the electric double layer has never been done before.

1.3. Scope of work

There are various pathways of (de)protonation of which the kinetics are relatively unknown (see Section 2.2.2). Incorporating all these pathways in a single simulation would be computationally very expensive. Simultaneously researching the effects of these phenomena would become too complex for a MSc thesis.

The goal of this thesis is to develop a method to mimic the acid-base equilibrium reaction in order to study the effect that the dynamic surface charge distribution has on the characteristics of the ionic solution, especially the electric double layer (EDL). This research is specifically focused on amorphous silica in contact with a solution of NaCl and water.

The initial method of mimicking (de)protonation by changing the partial charge of the hydrogen atom was devised by dr. R.M. Hartkamp. In this thesis the preliminary implementation was adjusted and developed further to fit this case. Furthermore, the initial conditions of the system (i.e. lammpsdata file, forcefield file) were made based on the works of M.F. Döpke.

1.4. Research question

The main research question of this thesis is:

What is the effect of introducing a dynamic surface charge distribution, in case of an ionic solution enclosed between two amorphous silica walls, on the electric double layer (EDL)?

In other words, what kind of effect would continuous protonation and deprotonation on the silica surface have on the characteristics of the adjacent fluid? To answer this, the question is divided into different sub-questions:

- **What is the typical protonation and deprotonation rate on a silica surface in contact with an aqueous solution?**

Acquiring a sufficient knowledge basis on the subject as well as the modeling technique is very important. This includes looking into the chemistry, reaction kinetics and possible usable experimental data. It is also relevant to discuss previous work to make accurate assumptions and fine-tune the scope of work. This entails a thorough literature study on the subject.

- **What properties are important in characterizing the effect of protonation and deprotonation?**

In other words, what kind of data is needed to answer the main research question? It is important to find these properties in order to produce useful data and meaningful results. These properties can be found by consulting previous research.

- **How can the occurrence of protonation and deprotonation be mimicked using MD simulation tools?**

Answering this question entails implementing the acquired knowledge of the literature review and creating a working model.

1.5. Hypothesis

The hypothesis of this thesis is that the evolution of the surface charge distribution influences the dynamics of the EDL in such a way that, under certain conditions, its effect cannot be ignored in MD simulation models. More specifically the occurrence of protonation and deprotonation will enhance the diffusivity of the ionic fluid near the silica wall.

1.6. Outline

The structure of this thesis is as follows. In the next chapter a thorough theoretical background will be given to form a basis for this MSc thesis. In Chapter 3, the used materials will be stated and the model will be explained. Chapter 4 will contain the results and the discussion, followed by the conclusion and recommendations.

2

Theoretical background

This chapter will provide the necessary background knowledge to fully understand the topic of this thesis. The silica-liquid interface will be explained, as well as the protonation and deprotonation events. Furthermore, a literature review on the equilibrium and rate constants will be given.

2.1. Silica-electrolyte interface

2.1.1. Amorphous silica

Amorphous silica is a material in which the SiO_2 building blocks are not present in a visually apparent structural pattern (Figure 2.1). The bulk of the material consists of silicon atoms that are each connected to four oxygen atoms. In the figure below Si is shown in yellow, O atoms in red.

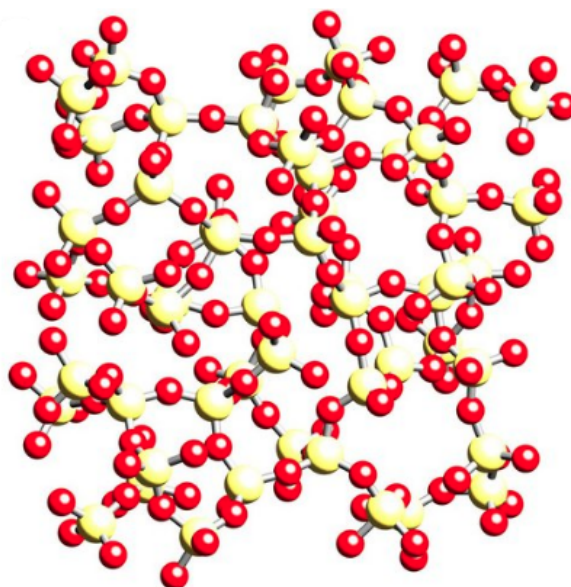


Figure 2.1: Visualization of the atomic structure of amorphous silica, from Lunt *et al.* [2]

2.1.2. Silanol groups

Besides bulk silicon atoms, there are also Si-atoms that have formed bonds with oxygen atoms outside the surface. The formed structure that is sticking out the surface is called an active group or silanol group (SiOH). This is shown in Figure 2.2.

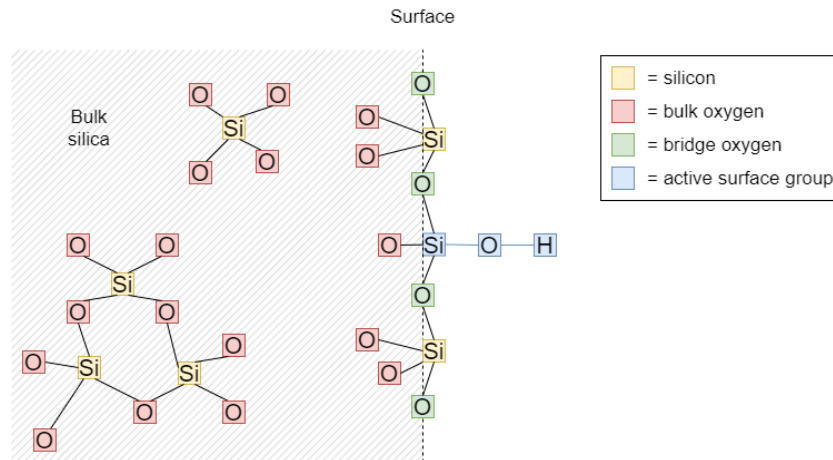


Figure 2.2: Visualization of the atomic structure of silica surface groups

Silanol groups were first discovered by Kiselev [14] in 1936. These active surface groups are able to interact with adjacent fluid particles. According to Yeon and van Duin [15], silanol formation on amorphous silica prefers high strain sites. Here the molecular bonds are stretched or compressed. This paper also suggests that the local density of silanol varies as a function of pretreatment temperature. Iler [16] confirmed this by finding silanol concentrations decrease with increasing temperature. Based on experiments by Cadogan and Sawyer [17] and Armistead *et al.* [18] the silanol concentration on the silica surface is thought to be around 4-5 groups nm^{-2} at temperatures around 400 K. In 1957 this was already theoretically calculated to be 4.55 nm^{-2} by de Boer *et al.* [19].

Silanol formation

The formation processes of silanol groups has also been researched. It was found that there are three main different pathways of silanol group formation by Yeon and van Duin [15]. The pathways of silanol formation are schematically visualized in Figure 2.3. These pathways are:

- H_3O^+ formation reaction

During the H_3O^+ formation reaction the oxygen atom of a water molecule attaches to a silicon atom in the surface. This water molecule then donates one of its hydrogen atoms to a passing water molecule. This leaves a SiOH-group attached to the surface.

- Deprotonation from H_3O^+

The pathway of deprotonation from H_3O^+ entails a passing H_3O^+ ion donating a hydrogen to an oxygen atom of the silica surface (a bridging oxygen/siloxane bridge). This bridge oxygen then breaks one of its bonds with the bulk silica wall and together with the remaining Si-bond and the adopted hydrogen forms a silanol group.

- H_2O dissociation

H_2O dissociation is a combination of the two before-mentioned pathways. A water molecule attaches itself to a Si-atom on the silica surface. One of the hydrogen atoms breaks from the water molecule leaving a newly formed silanol group and forms a bond with a nearby bridge oxygen. This bridge oxygen breaks one of its surface bonds and forms a second silanol group.

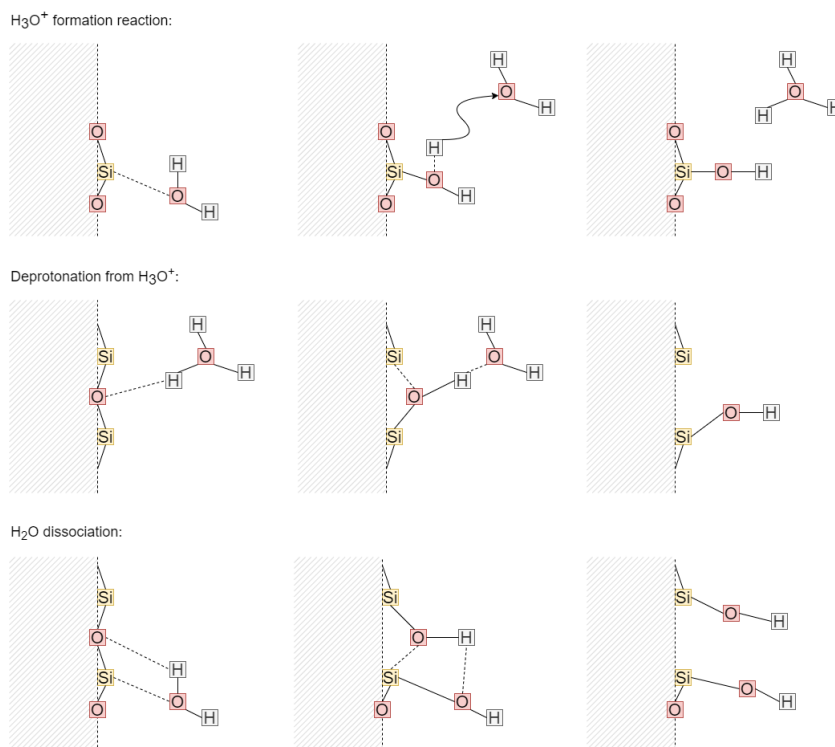


Figure 2.3: Schematic overview of three pathways of silica surface group formation

Different types of silanol groups

Between the silanol groups we can distinguish three main types: isolated, vicinal and geminal groups (Rosales-Landeros *et al.* [20]). The different types of silica active groups are visualized in Figure 2.4. Isolated silanols are so far away from other groups that they cannot form any hydrogen bonds with each other. When two groups are close enough to form an H-bond between them they are called vicinal, or bridged silanols. Geminal silanols involve Si-atoms that have bonded to two silanol groups. Zhuravlev [21] found a ratio between isolated, vicinal and geminal silanols of 26 : 61 : 13 at pretreatment temperatures of 180-200 K.

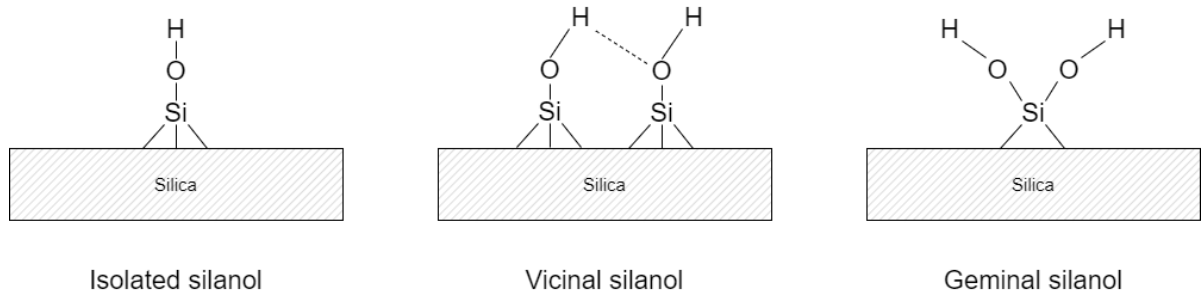


Figure 2.4: Visualization of different silanol groups, inspired by Jal *et al.* [3]

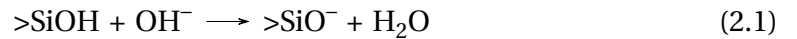
2.1.3. Surface charge density

Charge of an active surface group

There are three main forms in which active groups on silica exist: neutrally charged ($>\text{SiOH}$), negatively charged ($>\text{SiO}^-$) and positively charged ($>\text{SiOH}_2^+$) (Zhu *et al.* [22]). Here ">" represents the connection of the silanol group to the bulk silica.

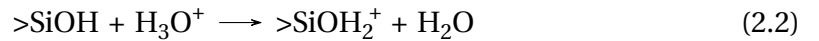
The appearance of $>\text{SiO}^-$ and $>\text{SiOH}_2^+$ is dependent on the acidity of the adjacent fluid. The formation of these different forms is explained using two acid-base reactions:

- $>\text{SiO}^-$ formation



Equation 2.1 shows that in a basic environment (or in the presence of hydroxide) the OH^- adopts a hydrogen from the neutrally charged silanol to form a negatively charged $>\text{SiO}^-$ -group.

- $>\text{SiOH}_2^+$ formation



In an acidic environment (or in the presence of a hydronium ion) the H_3O^+ donates a hydrogen to the neutrally charged silanol to form a positively charged $>\text{SiOH}_2^+$ -group (Equation 2.2).

Duval *et al.* [23] found that $>\text{SiOH}_2^+$ groups are only present at very low pH (for amorphous silica $\text{pH} \leq 2$). Therefore, Equation 2.2 does not appear in neutral conditions. In this thesis only neutrally and negatively charged silanol groups will be discussed.

Charge of an oxide surface

When silica comes in contact with fluid of a certain pH the silica surface adopts a surface charge through protonation and deprotonation reactions. The surface charge density can be measured by potentiometric acid-base titrations (Labbez *et al.* [24]) and visualized in a titration curve (see Figure 2.5). The surface charge is also dependent on the molarity of the electrolyte. As the molarity increases the titration curve becomes steeper. The surface becomes negatively charged at a pH greater than the point of zero charge (i.e. $\text{pH} > \text{PZC}$). For a fused (amorphous) silica surface this point lays around $\text{pH} = 2$ (Lian *et al.* [25]).

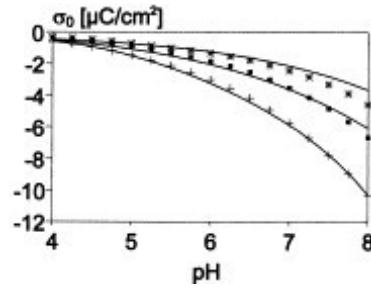


Figure 2.5: Titration curve for silica, from Sonnefeld *et al.* [4] (+: 0.1 M NaCl, ■: 0.01 M NaCl, ★: 0.001 M NaCl)

The surface charge is established by active surface groups. A percentage of these will become negatively charged to produce the value of the surface charge. Using the surface charge density found in the titration curve the number of deprotonated silanol groups in a system is calculated using Equation 2.3 (Campos *et al.* [26]).

$$\sigma_0 = -\frac{e}{A} N_{>\text{SiO}^-} \quad (2.3)$$

where:

- σ_0 = surface charge density
- e = elementary charge = $1.602 \cdot 10^{19}$ Coulomb
- A = area of the silica wall
- $N_{>\text{SiO}^-}$ = number of negatively charged silanol groups

2.1.4. Electric double layer

When an ionic solution comes into contact with a charged surface an electric double layer (EDL) is formed (Grahame [27]). A visual representation of the EDL is shown in Figure 2.6. When the surface charge of the silica wall is negative, cations will form a relatively immobile layer known as the Stern layer. This layer is followed by the diffuse layer. Here, the ions are not adsorbed to the wall, but the local charge of this layer is non-zero (Döpke *et al.* [28]). These two layers form the electric double layer. Outside the EDL is the bulk, where the ions are not influenced by the surface charge of the wall.

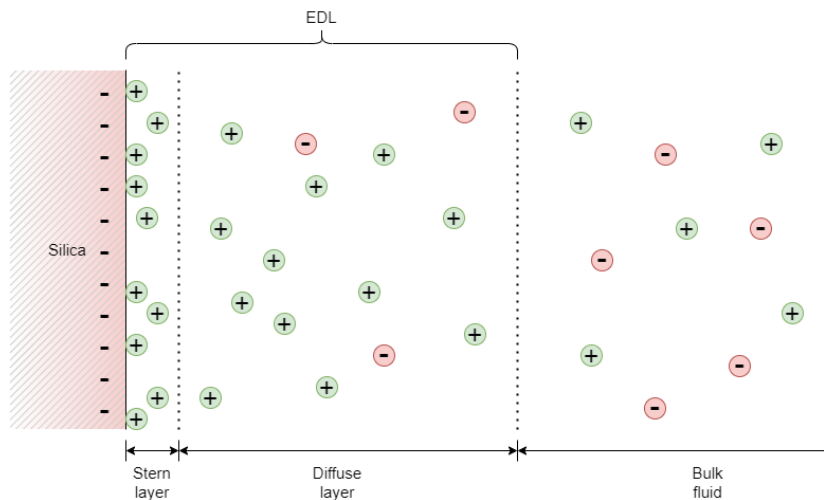


Figure 2.6: Visualization of the EDL model

2.2. Protonation and deprotonation

The process of the silanol group gaining or losing a hydrogen atom is called protonation and deprotonation respectively (see Figure 2.7).

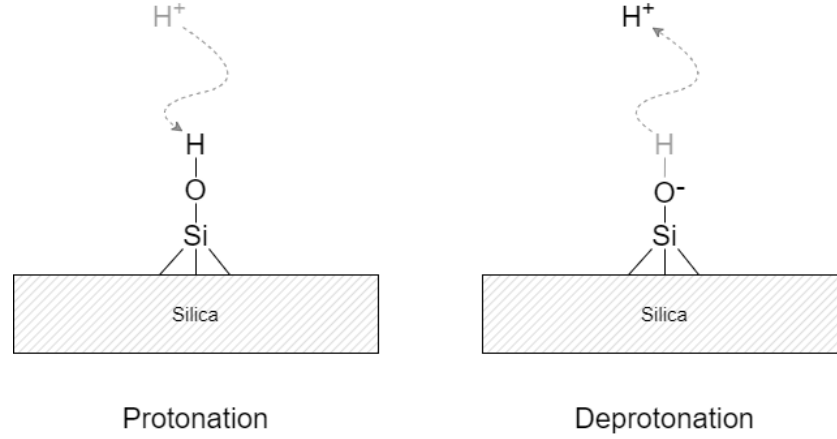


Figure 2.7: Schematic representation of protonation and deprotonation

In this work we only consider two possible status of active surface groups. Namely $>\text{SiOH}$ and $>\text{SiO}^-$. For each active surface group the equilibrium that is occurring can be written in the equilibrium reaction equation of Equation 2.4.



When the local pH (i.e. the concentration of H^+) is changed, the surface silanol groups "react" by losing or gaining a hydrogen from the fluid in order to reach the appropriate surface charge. Thus, with increasing pH the surface charge becomes more negative by deprotonation of neutral silanol groups and the equilibrium of the reaction of Equation 2.4 shifts to the right. The reverse is applicable with decreasing pH. Protonation and deprotonation reactions continuously occur while maintaining a constant overall surface charge. The resulting local change of surface charge could have an effect on the EDL (Figure 2.6). Sites on the silica wall that previously were neutrally charged could become negatively charged and thus attract positive ions. This could disturb the structure of the Stern layer. The changing local surface charge also affects the surface's hydrophilicity (Zhu *et al.* [22]).

2.2.1. Equilibrium constant

Equation 2.4 is an equilibrium reaction. When the system is in equilibrium the rate of the forward reaction is equal to the rate of the backward reaction, thus the net concentrations of the reactants and the products are constant. The ratio between these concentrations is called the equilibrium constant. For acid-base reactions the equilibrium constant K is called the acid dissociation constant K_a .

The formula for the acid dissociation constant for the (de)protonation reaction is given in Equation 2.5.

$$K_a = \frac{[>\text{SiO}^-][\text{H}^+]_0}{[>\text{SiOH}]} \quad (2.5)$$

where:

K_a = acid dissociation constant

$[>\text{SiO}^-]$ = concentration of deprotonated (negatively charged) silanol groups

$[\text{H}^+]_0$ = concentration of H^+ -atoms near the surface

$[>\text{SiOH}]$ = concentration of protonated (neutrally charged) silanol groups

In practice the logarithmic constant pK_a is used more frequently (see Equation 2.6).

$$\begin{aligned} K_a &= 10^{-pK_a} \\ pK_a &= -\log_{10} K_a \end{aligned} \quad (2.6)$$

In 1992, Ong *et al.* [29] used surface second harmonic generation experiments to find the pK_a -values of silica. In their experiments two types of silanol groups at a ratio of 81:19 were ascertained that had pK_a -values of 8.5 and 4.9 respectively. A potentiometric titration study by Allen *et al.* [30] similarly found the ratio of 85:15 with pK_a -values of 9.0 and 5.5 respectively. They both hypothesized that the high valued sites were silanol groups that were somehow connected through hydrogen bonds or a bridge water molecule. The sites with lower pK_a -values were believed to be isolated silanols. This was argued by the notion that lower pK_a -values represent a stronger acid, or a stronger tendency to deprotonate. Thus, sites that are very close and/or hydrogen bonded to each other (vicinal and geminal silanols) would have a higher tendency to stay protonated.

Contrary to this, in 2017, vibrational sum frequency spectroscopy (VSFS) was used to assign pK_a -values as high as 10.5 to isolated silanol groups (Dalstein *et al.* [31]). They state that the earlier mentioned pK_a -values of around 8.5 and 4.5 cannot be assigned to isolated silanols, because while decreasing the pH of the solution, they reported no significant changes in the amplitude of the peak assigned to the isolated silanol groups. Furthermore, they concluded that sample preparation technique has a large influence on silanol type ratios. This could explain the differences in research data.

2.2.2. (De)protonation rate constant

How often these local protonation and deprotonation events happen is expressed by the rate constant. The rate constant of a reaction is described using the rate law (see Equation 2.7).

$$R = k \cdot c \quad (2.7)$$

where:

R = rate

k = rate constant

c = concentration

Given that the rates of Equation 2.4 in both direction are the same in equilibrium a relationship between rate constants and the concentrations is formulated (see Equation 2.8). Using the pK_a -values for the different types of silanol groups, the ratio of the rate constants is known.

$$\frac{k^+}{k^-} = \frac{[>\text{SiO}^-][\text{H}^+]_0}{[>\text{SiOH}]} = K_a \quad (2.8)$$

where:

- k^+, k^- = rate constant in forward and backward direction respectively
- $[>\text{SiO}^-]$ = concentration of deprotonated (negatively charged) silanol groups
- $[\text{H}^+]_0$ = concentration of H^+ -atoms at the surface
- $[>\text{SiOH}]$ = concentration of protonated (neutrally charged) silanol groups
- K_a = acid dissociation constant

There is much debate about the actual values and rate limiting factors of the protonation and deprotonation rate constants (k^+ and k^-). In the following subsections an overview of literature research is provided.

Dependence on pH

In 1986, Fleming [32] stated that the deprotonation rate must be high because there was found to be no change in pH during a silica polymerization reaction without pH buffers. He concluded the rate constant is dependent on ionic strength, but not on pH.

In contrast, Lowe *et al.* [13] found protonation in the presence of H_3O^+ and deprotonation in the presence of OH^- are exothermic and fast reactions without activation energy. They described a (de)protonation pathway where the H^+ -atom can be transported from a H_3O^+ to a deprotonated site, or from a protonated site to a OH^- from a distance up to four water molecules away. This phenomenon is called a water bridge of proton holes. The H^+ -atom in a sense skips from water molecule to water molecule until it reaches its destination. When a H_3O^+ or OH^- comes close enough to the silanol group, the (de)protonation will occur without an activation barrier. This would mean the rate constants are dependent on the presence of H^+ or OH^- ions and thus would be dependent on pH.

Different pathways of proton movement

There are multiple ways in which a H^+ -atom could reach a SiO^- site to protonate and can explain the proton transport phenomena in wet amorphous silica. The before-mentioned pathway of proton hopping along a water bridge is one. Additionally, Mahadevan and Garofalini [33] among others confirmed there is an excess H_3O^+ at the silica/water interface. The local presence of H^+ -ions at the interface would result in the immediate protonation reaction of the backward reaction of Equation 2.4. Finally, Lockwood and Garofalini [34] stated there are also other transport mechanisms such as surface and subsurface proton transfer that account for enhanced proton conduction.

Stability of silanol groups

Lockwood and Garofalini [34] found that the lifetime of hydronium ions is shorter near the silica/water-interface than in bulk water. Which could mean that deprotonated sites of $>\text{SiO}^-$ are highly unstable and once formed would almost immediately receive a donor hydrogen from a nearby H_3O^+ . Considering that the total number of deprotonated sites

at any given moment remains the same (as does the surface charge), it can be concluded that the rate constants must be high. Additionally, Lockwood and Garofalini [34] found that only 14.3% of the silanol groups deprotonate during the production step of their simulation of 1.0 ns. This also is corroborated by Dalstein *et al.* [31]. In their vibrational sum frequency spectroscopy (VSFS) experiments they found that a percentage of less than 25% of all active surface groups deprotonate even at a pH as high as 10. In general, they state, >SiOH is very stable. This can be explained by the difference in pK_a -values in silanol types.

Quantitative value

The only research that has a quantitative estimate of the rate constant is Lian *et al.* [25]. They formulated a relation between pH and the surface charge and found rates of $k^+ = 5 \cdot 10^{-12} \text{s}^{-1}$ and $k^- = 2.2 \cdot 10^{-4} \text{s}^{-1} \text{M}^{-1}$. Where k^+ and k^- are the rate constants of the forward (deprotonation) and backward (protonation) reaction of Equation 2.4 respectively. The rate constants were found by fitting Equation 2.9 for different pH and surface charge.

$$Q = -eN_{total} \frac{k^+ \cdot 10^{-pH} \exp(-\beta e \Psi_0)}{k^+ + k^- \cdot 10^{-pH} \exp(-\beta e \Psi_0)} \quad (2.9)$$

where:

- Q = surface charge
- e = elementary charge = $1.602 \cdot 10^{19}$ Coulomb
- N_{total} = total number of silanol sites
- k^+, k^- = rate constants of the forward and backward reaction respectively
- pH = measure of acidity = $-\log_{10}[\text{H}^+]$
- $\beta = k_B T$ = thermal energy (Boltzmann constant and temperature)
- Ψ_0 = surface electrical potential

Lian *et al.* [25] imposed the rate relation $K = k^+ / k^-$ on Equation 2.9 to eliminate k^+ as a variable to form Equation 2.10 and find k^- .

$$Q = -eN_{total} \frac{K \cdot k^- \cdot 10^{-pH} \exp(-\beta e \Psi_0)}{K \cdot k^- + k^- \cdot 10^{-pH} \exp(-\beta e \Psi_0)} \quad (2.10)$$

However, this approach is illegitimate because in Equation 2.10 the fraction is independent of backward rate constant k^- . Other than this, the derivation for Lian's equation (Equation 2.9) is faulty. The explanation for this statement can be found in Appendix A.1.

Dissolution of silica

The (de)protonation kinetics clearly deviate from other formation or breaking of bonds, for which the reaction kinetics is determined by the activation barrier (Karlsson *et al.* [35]). The dissolution rates of silica have been thoroughly researched. Here, by dissolution is meant the breaking of the Si–O bonds of the material and the formation of silicic acid (Si(OH)_4). Even though the occurrence of this phenomenon is not within the topic of this thesis, the order of magnitude could be of use. These rates range from $10^{-10} \text{ mol/m}^2/\text{s}$ to $10^{-8} \text{ mol/m}^2/\text{s}$ for silica glass, depending on the pH value of the fluid (Crundwell [36]). For quartz Nangia and Garrison [37] reported rates in the order of $10^{-11} \text{ mol/m}^2/\text{s}$ and $10^{-13} \text{ mol/m}^2/\text{s}$. Obviously, protonation and deprotonation rates would have to be fast compared to surface dissolution rates (Dove and Elston [38]).

Relevance

It is important to repeat that amorphous silica is just an example material chosen as a basis for this thesis. Protonation and deprotonation events are occurring in many more materials, like aluminum oxide (Al_2O_3), titanium oxide (TiO_2) and zirconium oxide (ZrO_2). Even if the physical rate constants for amorphous silica turn out to be relatively low under ambient conditions, there will also be conditions under which the rate will be elevated (e.g. extreme pH or temperatures). Finding relations between the rate constants and its effects on the characteristics of the EDL would be very valuable.

2.3. Properties of the EDL

While researching the effects of the evolution of the surface charge distribution on the characteristics of the electric double layer it is interesting to look at a number of properties.

2.3.1. Structure of the EDL

It is interesting to figure out how protonation and deprotonation events influence the structure of the electric double layer. The ion distribution and the width of the Stern layer are good indicators of the robustness of the EDL. The smaller the width, the closer the cations are to each other and thus the more immobile the Stern layer is.

2.3.2. Adsorption type

In an ionic solution, water molecules orient themselves around charged ions and form so-called hydration shells. Hydration shells play a role in the type of adsorption of ions to a surface (Bourg and Sposito [39]). When one of the water molecules in the first hydration shell is swapped for a surface atom, this is called an inner-sphere surface complex (ISSC). Outer-sphere surface complexes (OSSC) have a first hydration shell that is intact. Ions that are on the edge of the diffuse layer form the diffuse swarm (DS). The different adsorption types are visualized in Figure 2.8.

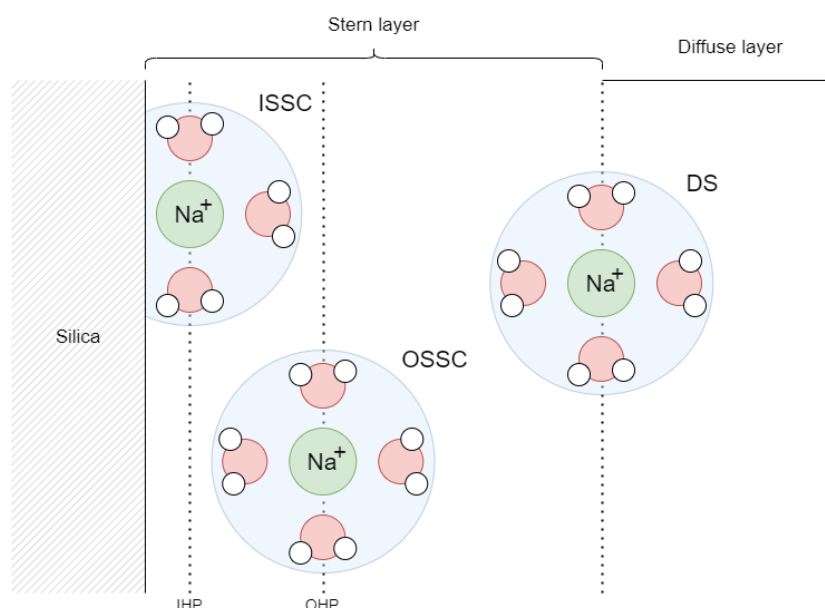


Figure 2.8: Visualization of different adsorption types

The plane that passes through ISSC ions is called the inner Helmholtz plane (IHP) and the plane through OSSC ions is called the outer Helmholtz plane (OHP). The exact definition of the Stern layer varies. Some use the OHP as the outer boundary of the Stern layer (Döpke *et al.* [28]) where others use the plane that passes through the DS ions (Bourg and Sposito [39]).

2.3.3. Electrostatic screening

Electrostatic screening is a phenomenon where charged particles influence the effective surface charge. The surface charge at a certain distance is perceived to be less negative due to the "screening" of positive ions in front of the surface. The screening effect could be influenced by increase of protonation and deprotonation events as it influences the positions of the charged particles.

2.3.4. Water orientation

Water molecules are polar. The oxygen of a water molecule is negatively charged and the hydrogen atoms are positively charged. Changes in local surface charge directly influence the orientation of water molecules. Furthermore, the orientation of water molecules in a fluid is influenced by the presence of charged particles. The negative side will orient itself toward the positive Na^+ ions and away from the negative Cl^- ions.

2.3.5. Diffusion

The diffusion coefficient is an important transport property. Fick's law of diffusion relates the diffusion coefficient to the movement of the atoms. (Equation 2.11).

$$J = -D \frac{\partial \rho}{\partial x} \quad (2.11)$$

where:

J = diffusive flux

D = diffusion coefficient

ρ = concentration

x = position

This equation relates the diffusive flux to the change in concentration. In other words, when there is a concentration gradient (i.e. local concentration differences within the system) matter will move from high to low concentrated areas until equilibrium is established. The diffusion coefficient thus represents a measure of how fast this concentration gradient is balanced.

Deprotonation of an active surface group will force nearby ions to move away from or towards the negative site. Calculating the diffusion coefficient both perpendicular and parallel to the surface will give an idea of what direction the ions move in.

2.4. Experimental methods

Experimental research on surface charge evolution and its effects on interfacial fluid properties is minimal due to the fact that available techniques are not sensitive enough to detect local changes at the surface on an atomic scale (Cruz-Chu *et al.* [12]). However, there are several experimental methods that give information about the structural, thermodynamic or chemical properties of the system. Unfortunately, there is no method that can paint a full picture and the interpretation of data remains a debated topic. In this section, some experimental techniques are explained.

2.4.1. Direct imaging

It is possible to produce a direct image of the surface using atomic force microscopy (AFM). This technique involves a small probe that scans the atomic landscape of the surface. However, even though this can be used to distinguish between different silanol types, this technique cannot be used to differentiate between protonated or deprotonated silanol groups due to the hydrogen atom's small size (Jal *et al.* [3]). Furthermore, AFM is a perturbative method. The measuring itself could disturb the collected data. It deserves to be said that AFM is generally called a direct imaging technique, but post-processing models are needed to produce the comprehensible results. This again involves a measure of interpretation of the system (i.e. the pK_a -value).

2.4.2. Indirect measurement

Infrared spectroscopy

Infrared spectroscopy (IR) has been used to characterize the presence of different silanol groups. This is mostly a form of qualitative measuring so no conclusions can be made about the amount silanol groups present, but it is possible to assign ratios. Again, it is not possible to make a distinction between deprotonated and protonated silanol groups. Furthermore, there is still no unanimous agreement about the physical meaning of peaks in the output of the measurements. In 1972, Van Cauwelaert *et al.* [40] reasoned that the 3745 cm^{-1} peak should be assigned to isolated and geminal silanols. In 1987, Hoffmann and Knözinger [41] identified the frequency to only geminal silanol groups and in 1992, Morrow and McFarlan [42] identified the same frequency (3743 cm^{-1}) as vicinal silanol groups that were not hydrogen bonded. Apparently, the absorption, emission, or reflection properties of these different types of silanol groups are too similar for IR spectroscopy to distinguish properly. The "true" frequencies are most likely too close together to be able to form separate peaks.

Nuclear magnetic resonance spectroscopy

Other than IR, nuclear magnetic resonance spectroscopy (NMR) is also used to identify silanol groups. In 1988, Bronnimann *et al.* [43] found it is impossible to differentiate between isolated and geminal groups using proton-NMR (H-NMR). Using Si-NMR, Sindorf and Maciel [44] identified -92 ppm to represent geminal silanol groups and -100 ppm isolated and vicinal silanol groups. However, these statements are all based on personal interpretation. All known possible silanol types at the time were used to form a credible assumption. As time progresses, for example two forms of geminal silanols were identified (Pfeiffer-Laplaud *et al.* [45]). In convex and concave geminals the hydrogens are either facing each other or facing away from each other. It is safe to say that these two forms could

have very different IR or NMR outputs. This is substantiated by the research of Ogenko [46]. He states that the peaks in IR and NMR spectroscopy previously thought to belong to geminals could also indicate electronic interactions and differences in the orientation of the active surface groups.

Second harmonic generation spectroscopy

Using second harmonic generation spectroscopy (SHG) alongside other methods, it is possible to produce an indication of which pK_a -values are present in what magnitudes on the silica surface (Fisk *et al.* [47]). However, it has not yet been qualitatively proven to which silanol groups these values belong. More on this technique can be found in Section 2.2.1.

Cross polarization/magic angle spinning nuclear magnetic resonance spectroscopy

Finding out whether a silanol group has formed hydrogen bonds can be done using cross polarization spin dynamics (CP/MAS NMR). For example, Chuang and Maciel [48] found in 1997 that 60% of isolated active groups were not hydrogen bonded. They also found that 50% of geminal silanol groups were hydrogen bonded. This is an interesting technique to be used in researching why some silanol groups deprotonate more than others. Being able to further differentiate between active surface groups can also be used in the assigning of pK_a -values.

2.5. Conclusion

The kinetics of protonation and deprotonation events is a topic that is definitely up for debate. Currently, there is no decisive research available that provide actual values for the rate constants of amorphous silica or other oxide materials. Literature also does not provide useful methods to obtain these rate constants. The paper by Lian *et al.* [25] giving an exact value appears to be mistaken. Nonetheless, it is known that protonation and deprotonation events do happen. There are different pathways explained that make proton movement possible. This is a good incentive to dive further into researching its effects. The goal is to answer the question:

What are the effects of varying the (de)protonation rate constants on the electric double layer?

Answering this question would bring us a step further in substantiating or disproving the assumption of static surface charge distribution in simulation models.

3

Methodology

In this chapter the model is explained in detail. Furthermore, the materials, assumptions, and input variables are given. Lastly, it is explained which methods were used to process the raw data to produce usable results.

3.1. Molecular dynamics simulation

The modeling technique used in this thesis is called molecular dynamics simulation (MD simulation). Molecular simulation is a method to mimic events without doing physical experiments. MD simulations can provide information of a molecular level that is impossible to obtain experimentally. It can also be used to research extreme conditions or dangerous materials. MD simulation is therefore considerably cheaper than physical experimentation. It is being used in a broad spectrum of areas ranging from protein folding to desalination of sea water.

MD simulations use the current positions and velocities of atoms to calculate the future positions of the atoms. MD solves Newton's second law of motion by integrating over discrete time steps. Interactions between atoms are calculated with multiple types of potentials. These are bonds, angles and two nonbonded potentials: the Lennard-Jones potential and the Coulomb potential. Lastly, MD simulation uses periodic boundary conditions to mimic an infinitely large system with a finite number of particles. The potentials, integration scheme and periodic boundary conditions are explained in the next sections.

3.1.1. Potentials

Lennard-Jones potential

All atoms experience an attraction to each other when they are within a certain range. This is called van der Waals attraction. However, as the atoms move closer together the negatively charged electron clouds will overlap and start to repel. This is called Pauli repulsion.

The Lennard-Jones potential (LJ-potential) combines van der Waals attraction and Pauli repulsion into Equation 3.1.

$$U_{LJ}(r) = 4\epsilon_{LJ} \left[\left(\frac{\sigma_{LJ}}{r} \right)^{12} - \left(\frac{\sigma_{LJ}}{r} \right)^6 \right] \quad (3.1)$$

where:

U_{LJ} = Lennard-Jones potential

ϵ_{LJ} = Pair coefficient: depth of the potential well

σ_{LJ} = Pair coefficient: finite distance at which the interparticle potential is zero

r = distance between particles

Coulomb potential

Positively charged atoms are attracted to negatively charged atoms, and vice-versa. Atoms of equal sign experience a repulsive interatomic force. The electrostatic potential, also called Coulomb potential is stated in Equation 3.2.

$$U_{el}(r) = \frac{1}{4\pi\epsilon_0} \frac{q_i q_j}{r} \quad (3.2)$$

where:

U_{el} = electrostatic potential

ϵ_0 = permittivity of vacuum

q = point charge

r = distance between particles

Bonds and angles

Atoms that are bonded to each other (e.g. oxygen and hydrogen in water molecules) are fixed together using harmonic bond potentials. These are harmonic bonds that prevent the atoms from moving further away from each other than the characteristic equilibrium length. A stiffness parameter is stated as a measure of damping. Similarly, when an atom has molecular bonds with two other atoms, they form an angle that is characterized by an equilibrium angle and a stiffness factor stated in the angle potential.

3.1.2. Velocity-Verlet integration

Velocity-Verlet integration is an algorithm used to calculate the positions and velocities of the next discrete time step. The interaction potentials with all surrounding atoms together with the kinetic energy of the atoms form the total energy. To save computer power not every interaction with every atom in the system was calculated. For this, cut-off criteria were put into place. The method is explained using the following equations.

$$\mathbf{x}(t + \Delta t) = \mathbf{x}(t) + \mathbf{v}(t) \cdot \Delta t + \frac{1}{2} \frac{\mathbf{F}(t)}{m} \cdot (\Delta t)^2 \quad (3.3)$$

$$\mathbf{F}(t + \Delta t) = -\nabla U_{total}(\mathbf{x}(t + \Delta t)) \quad (3.4)$$

$$\mathbf{v}(t + \Delta t) = \mathbf{v}(t) + \frac{1}{2} \left(\frac{\mathbf{F}(t)}{m} + \frac{\mathbf{F}(t + \Delta t)}{m} \right) \cdot \Delta t \quad (3.5)$$

In Equation 3.3 a second degree Taylor polynomial is used to acquire the position of the next time step, using only the positions, velocities and forces of the current time step. Then, the forces of the next step $\mathbf{F}(t + \Delta t)$ are calculated using the interaction potentials and the new positions $\mathbf{x}(t + \Delta t)$ (see Equation 3.4). Lastly, the velocities of the next step are calculated using Equation 3.5.

3.1.3. Periodic boundary conditions

Periodic boundary conditions were applied to simulate an infinite system while accounting for limited computer power. This method models a smaller box that holds a limited number of atoms. When an atom leaves the box on one side, it appears again on the direct opposite side. The area around an atom in which it interacts with other atoms is indicated by the cut-off radius (r_c). The cut-off radius used in this thesis among other simulation conditions can be found in Section 3.3.1. A visual representation of periodic boundary conditions is shown in Figure 3.1. While calculating the pairwise interaction between atoms only the closest mirror image of an atom is used. This means that the absolute minimum of the distance between two atoms is used. This way, the atom interactions are calculated mimicking a very large system with infinite boundaries, while only calculating (and storing) properties of a limited number of atoms.

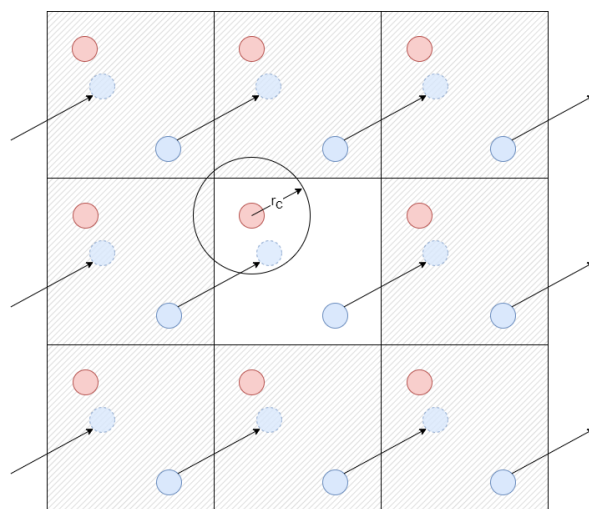


Figure 3.1: Visualization of the periodic boundary method

3.2. Protonation and deprotonation model

In this thesis a model was made to mimic the events of protonation and deprotonation without simulating the actual proton movement. This has made the model considerably faster computational wise.

3.2.1. Overview

During the simulation of protonation and deprotonation events the hydrogen remained attached to the silanol ($>\text{SiOH}$). In order to simulate a deprotonation event, the hydrogen's partial charge was brought to zero. A schematic view of the two silanol states in the simulation is shown in Figure 3.2. During an event, the partial charges of the oxygen and silicon atoms also changed, but the sign remained the same. For clarity, the change in partial

charge of the silicon atoms is not shown in the figure.

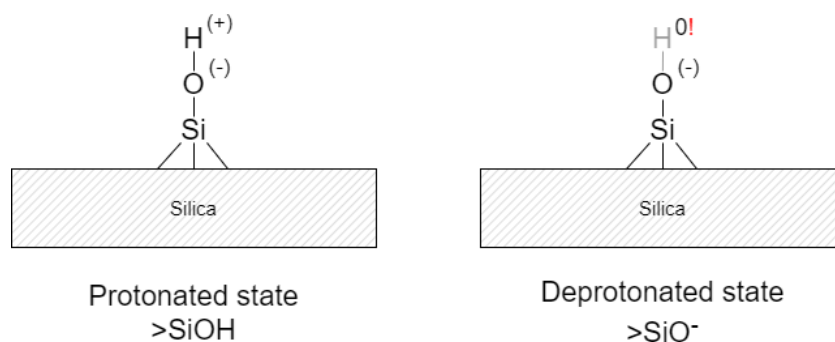


Figure 3.2: Schematic representation of two (de)protonation states

The Lennard-Jones parameter ϵ was set to zero so essentially the hydrogen atom was only active in electrostatic interactions. This was done under the assumption that dispersion interaction of hydrogen is considered to be small and most likely does not influence the results. When the atom was neutrally charged, neighboring molecules and ions did not "feel" its presence and the silanol was deprotonated ($>\text{SiO}^-$). It was then possible, for example, for a Na^+ ion to take its place. A protonation event was simulated similarly by changing the partial charge from zero to the protonated value.

Every couple of time steps (depending on the rate constant), a (de)protonation event was simulated. The partial charges were ramped up or down over a period called the transit time. This was needed to ensure system stability by eliminate overlap of possible ions or water molecules with the "reappearing" hydrogen. Protonation and deprotonation happened simultaneously to maintain a constant surface charge and neutral system charge. A schematic view of the evolution of the charges of a silanol group during deprotonation and protonation is shown in Figure 3.3.

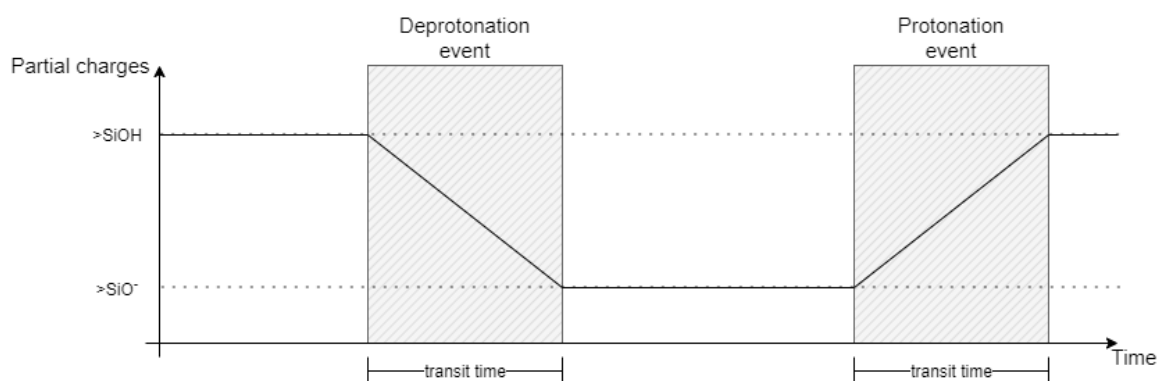


Figure 3.3: Schematic flowchart of the partial charges during (de)protonation

3.2.2. Selection of random silanols

Python was used to provide the model with information on which silanol to protonate or deprotonate. The python scripts can be found in Appendix E. For every event, a random silanol was chosen from the protonated list, as well as a random silanol from the deprotonated list. The atom numbers of the involved Si, O and H atoms were stored in files. Then

the protonating and deprotonating silanols were removed from their respective lists and put in the other list. A flowchart of the process is given in Figure 3.4.

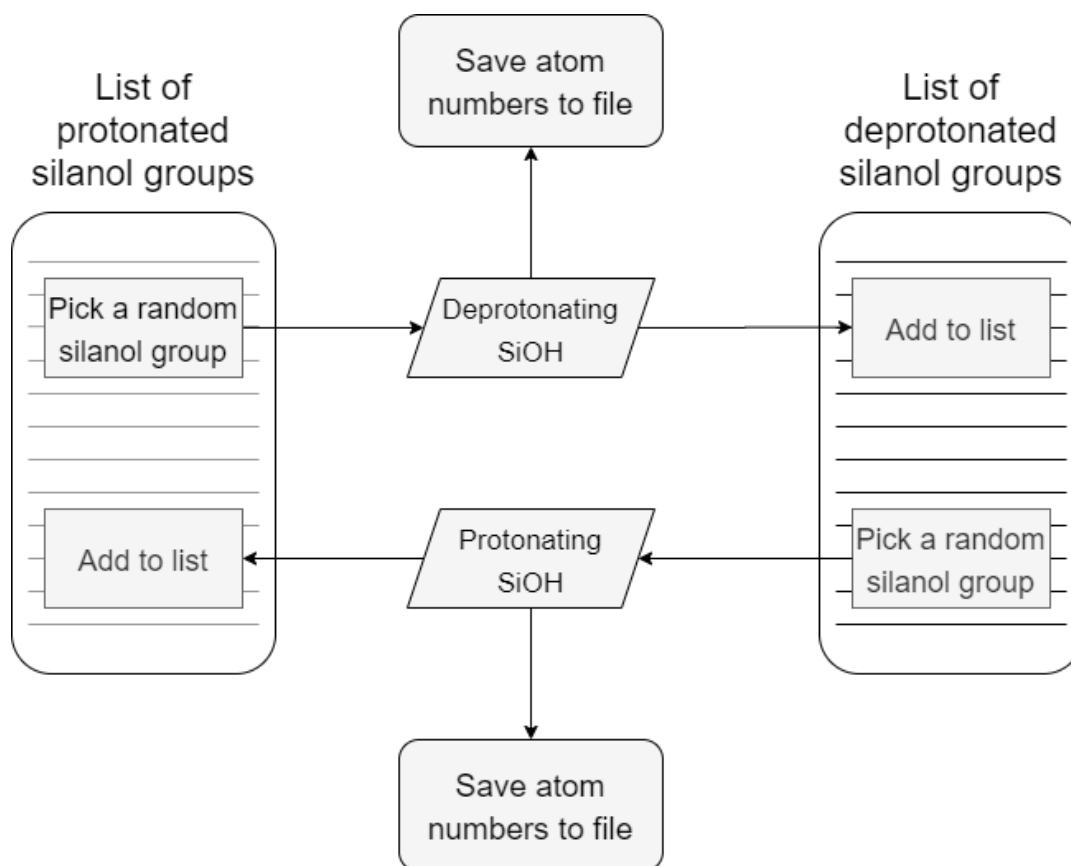


Figure 3.4: Schematic flowchart of the formation of input files for the (de)protonation events

As mentioned in Section 2.2.2 different type of silanols likely have different probabilities to deprotonate. This phenomenon has been implemented in the python script. In this thesis isolated, vicinal and geminal silanols had a probability ratio of deprotonating of 1:1:1, because no acceptable assumptions could be made. This means isolated silanols were just as likely to deprotonate as geminal or vicinal silanols.

3.3. Simulation protocol

LAMMPS (Large-scale Atomic/Molecular Massively Parallel Simulator) is a popular open-source computer program that implements the Molecular Dynamics Simulation technique and is the simulation tool that was used in this thesis. The simulation is visualized in the form of a flowchart in Figure 3.5.

The force field parameters, initial positions and the simulation conditions form the input for LAMMPS. The input is explained in detail in the next sections. After the simulation finished running, the output data was generated. The output analysis is discussed further in Section 3.4.

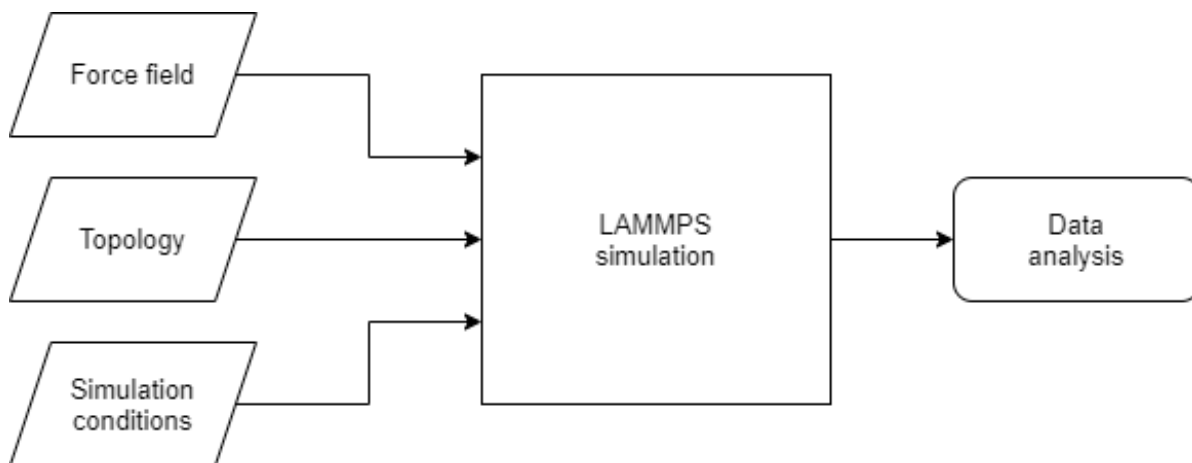


Figure 3.5: Flowchart of the LAMMPS simulation

3.3.1. Force field

The force field includes the parameters that provide information about the behavior of the atoms. Of each atom type, the mass was given, as well as the pair coefficients ϵ_{LJ} and σ_{LJ} needed to calculate the Lennard-Jones potential. The atom coefficients in this thesis were based on the SPC/E [7] water model, the JC [6] ion model and the IFF [5] SiO-interface model (Berendsen *et al.* [7], Joung and Cheatham III [6], Emami *et al.* [5]). Additionally, the file provides bond coefficients, angle coefficients and the charge of different atom types. In this thesis the ϵ value of the hydrogen atoms that were part of the active surface groups was assumed to be zero. This was done to eliminate any Lennard-Jones interactions with the hydrogen atoms attached to deprotonated silanol groups. Furthermore, the cut-off length of both the LJ and the electrostatic potential was 12 Å. Lastly, the accuracy of the K-space solver used to calculate the long-range Coulombic interactions was chosen to be 10^{-4} . The force field input file can be found in Appendix D.1.

3.3.2. Topology

The topology input provides the LAMMPS program with the initial conditions of the system. It includes the type and position of each atom, as well as the type of bond each atom has with other atoms. The system was periodic in x,y-direction. In the z-direction a vacuum was introduced following the implementation of Yeh and Berkowitz [49]. In this thesis the box size was 35Å x 35Å x 80 Å. Figure 3.6 contains a snapshot of the initial configuration.

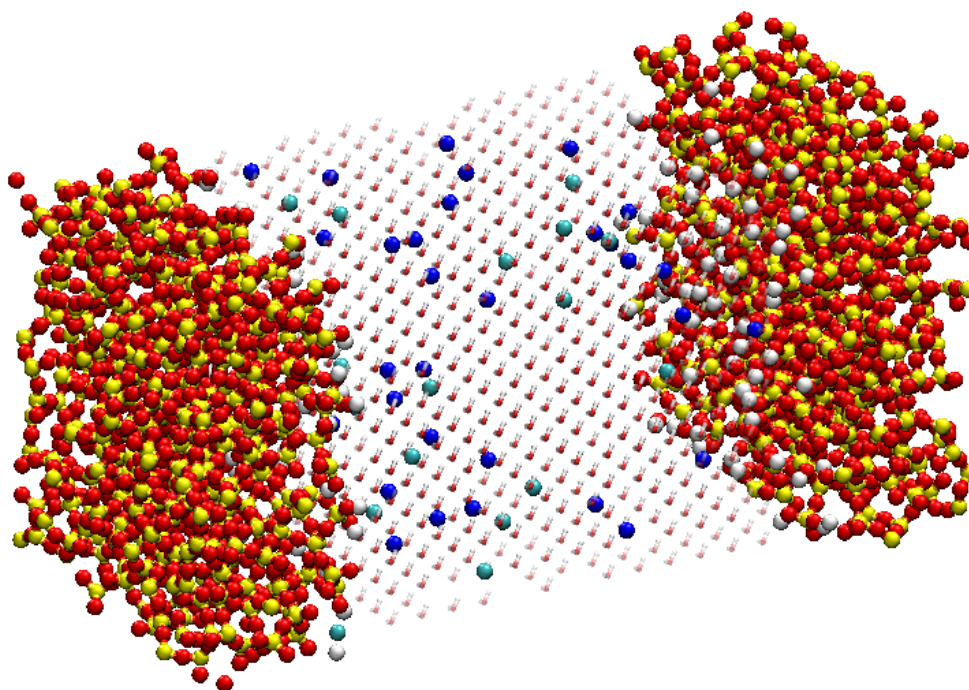


Figure 3.6: VMD snapshot of the initial configuration of the system. Atom representations: Si in yellow, O in red, H in white, Na^+ in blue, Cl^- in cyan.

Creating the initial topology was done using the scripts and geometry from Döpke *et al.* [28]. This silica model is proved to be in accordance with known properties for amorphous silica such as silanol density. Two of these silica walls were separated by 40 Å. The resulting space was filled with water molecules with a density of 1 g/cm³. To simulate salty water 18 Na^+ and 18 Cl^- ions were added (0.6 M NaCl). The surface charge of -100 mC/m² was modeled by deprotonating 16 randomly chosen silanols (8 on each wall). This surface charge is within the range that represents a pH of 7-8 at a concentration of 0.6 M NaCl (Karlsson *et al.* [35]). Due to the LAMMPS requirement of maintaining a neutrally charged system, an additional 16 Na^+ ions were added to the water to counter the negative surface charge. The calculation of the number of ions and the surface charge is given in Appendix B.1 and B.2 respectively.

3.3.3. Simulation conditions

The simulation conditions include the parameters and commands needed to run the simulation. This input was made up of two parts: initialization and production.

Initialization

During the initialization stage, the system is brought to equilibrium. The initialization phase introduced a force that is equivalent to a pressure of 1 atm with which the walls push on the water. These walls were then fixed in space. The system was coupled to a Nosé–Hoover thermostat to keep the temperature at a constant 298 K with a damping factor of 100 fs. Lastly, when atoms partly overlap in the initial configuration and the time step is too large, the interaction potentials can make atoms move further than a full box length in a single time step and the system would crash. To avoid this, an energy minimization was performed and the time step was slowly ramped up to 1 fs.

Production

All simulations had a running time of 10 ns after equilibrium. At a time step of 1 fs this equals to 10 million time steps. Every 1000 time steps (1 ps) thermodynamic system data was stored in an output file. At a varying event period τ one protonation and deprotonation event was simulated. The transit time was set to 1000 fs. An overview the variable event periods τ that were used related to event frequency and protonation and deprotonation lifetime can be found in Table 3.1. Every simulation has been run 5 times with different random seed numbers to achieve higher statistical relevance. The simulation input files can be found in Appendix D.

Table 3.1: Event frequency and average lifetime of protonated and deprotonated silanols for variable τ

τ	Event frequency	Average lifetime	
		Protonated silanol	Deprotonated silanol
1	10^{12} /s	50 ps	8 ps
10	10^{11} /s	500 ps	80 ps
100	10^{10} /s	5000 ps	800 ps
1000	10^9 /s	50000 ps	8000 ps
∞	never	∞	∞

At the moment of an event, the required atom numbers were read from the files made using the Python scheme that was explained in Section 3.2.2. In Table 3.2 the partial charges of the different atoms are shown in the two different states of silanol groups.

Table 3.2: Partial charges of silanol group atoms

Element	Partial Charges	
	Protonated >SiOH	Deprotonated >SiO ⁻
Si	1.1	0.725 (0.35) ¹
O	-0.675	-0.9
H	0.4	0

¹ In case of doubly deprotonated geminal silanol groups

3.4. Data analysis

LAMMPS produces data in the form of trajectory files. These files contain the positions of all the atoms at different time intervals (i.e. frames). This data was analyzed using Python in combination with the MDAnalysis and Maicos-Delft packages (in-house post processing tool). All results were made by combining the 5 simulations, symmetrizing and averaging. The post-processing of the raw data was done in the following ways.

3.4.1. Density profile as function of z-position

A density or concentration profile relates the number of atoms to the z-position normal to the wall. This tool is used to visualize the structure of the electric double layer. The density profiles in this thesis were produced using the average position of each atom. The molarity in mol/L was plotted against z-position in nm.

3.4.2. Density profile as function of distance

In order to define the adsorption type of ions the distance of the ions to the surface is needed. The conventional density profiles plotted against z-position do not account for surface roughness (Döpke *et al.* [28]). To get a better view of the exact distance of ions to the closest point on the surface a density profile as function of the closest distance to the wall, d was used. The molarity in mol/L was plotted against distance in nm.

3.4.3. Screening function

The screening function is calculated using Equation 3.6. The symmetrized average densities were used and the resulting screening function in mC/m² was plotted against z-position in nm.

$$\Gamma = \sigma_0 + \int_0^H e(n_{\text{Na}^+} - n_{\text{Cl}^-}) \cdot dz \quad (3.6)$$

where:

Γ = screening function

σ_0 = surface charge density

H = channel height

e = elementary charge = $1.602 \cdot 10^{19}$ Coulomb

n = number density of ions

dz = position in z-direction

3.4.4. Water orientation

The positions of both the oxygen and hydrogen atoms were used to calculate the angle the water molecules make with the surface normal. In a water orientation plot the preferred orientation ($\cos\theta$) is plotted against the z-position in nm.

3.4.5. Diffusion coefficient

The diffusion coefficient gives information about the movement of the particles in the system. The diffusion coefficient in m²/s both parallel and perpendicular to the wall was plotted against z-position in nm. In order to distinguish between diffusion in the Stern layer of the EDL, the diffuse layer and the bulk, varying bin sizes were implemented. For every bin, the diffusion coefficient was calculated. The bin sizes were chosen, with the use of density profiles, in such a way that the Stern layer was in a single bin. The bins used in this thesis are visualized with the density profiles in Appendix C.4.1.

First, the mean square displacement (MSD) was calculated. The MSD is a measure for average displacement of an atom over time in the system. The expression for the MSD in a certain direction is shown in Equation 3.7.

$$MSD = \langle |x(t) - x_0|^2 \rangle = \frac{1}{N} \sum_{i=1}^N |x^{(i)}(t) - x^{(i)}(0)|^2 \quad (3.7)$$

where:

MSD = mean square displacement in a certain direction

x = positions of the atoms

t = time

N = number of total atoms in the system

The principle of sliding origins was used to gain more statistics. Instead of just one calculation of the MSD from $t = 0 \rightarrow t = \text{end}$, the MSD was calculated multiple times from $t = i \rightarrow t = \text{end}$ with i ranging from 0 to $\text{end}-1$. These results were combined and averaged to produce a statistically more robust result. Additionally, as the system is symmetrical the data was symmetrized to add statistics.

Second, the diffusion coefficient is related to the MSD as stated in Equation 3.8.

$$MSD = 2n_{dim}Dt \quad (3.8)$$

where:

MSD = mean square displacement

n_{dim} = dimension of the MSD

D = diffusion coefficient

t = time

The diffusion coefficient in z-direction is thus equal to half the slope of the MSD graph in z-direction. For diffusion along the wall (x,y-direction) the average of the MSD_x and MSD_y was used. Only a small time frame was used to place a linear fit to the MSD curve. The range used in this thesis was $1 \text{ ps} < \gamma < 10 \text{ ps}$. Data points at times shorter than 1 ps fall into the "ballistic regime" and only represent particle movement due to Brownian motion. Longer times consisted of too little statistics due to particles leaving the bins. In Figure C.10 in Appendix C.4 shows an example plot of a MSD on this range.

4

Results and discussion

Introducing a dynamic surface charge distribution for varying τ resulted in several changes in the electric double layer (EDL). A change was visible in the structure of the EDL, the diffusion coefficient, screening function, adsorption type and water orientation. These changes in the EDL are substantiated in the following sections.

The shaded area around the curves in all figures represent the 68% confidence interval ($\mu \pm \sigma$), based on five simulations ($N = 5$) unless otherwise specified.

4.1. Structure of the EDL

The density profiles as a function of z-position for both Na^+ and Cl^- are given in Figures 4.1 and 4.2 respectively. At decreasing event period τ , both profiles show a clear trend of decreasing molar concentration close to the surface. As ions move further away from the surface, the molarity in the bulk is slightly increased for decreasing τ . The density profile of water is shown in Figure 4.3 and showed no significant changes.

The structure of the electric double layer changes with varying τ . The Stern layer is hard to define in terms of physical boundaries. The peak around 2.4 nm in Figure 4.1 represents a high density of ions and can be used to represent the Stern layer. At decreasing τ the peak shifted further away from the surface and decreased in magnitude. As this peak is flattened out, the cations are less closely packed together and the Stern layer is less well defined. As a consequence, the anion layer that follows the Stern layer (the peak at 2.9 nm in Figure 4.2) also becomes less apparent for decreasing τ .

The density profiles for the individual simulations and the average before symmetrization can be found in Appendix C.1.

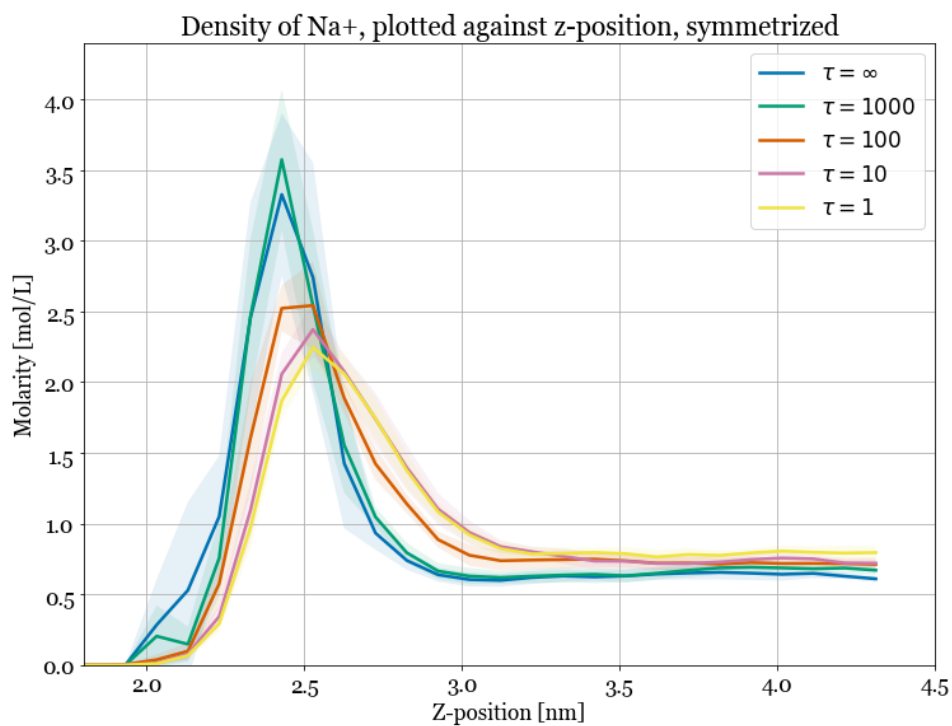


Figure 4.1: Density profile as function of z-position, of Na⁺ for varying τ

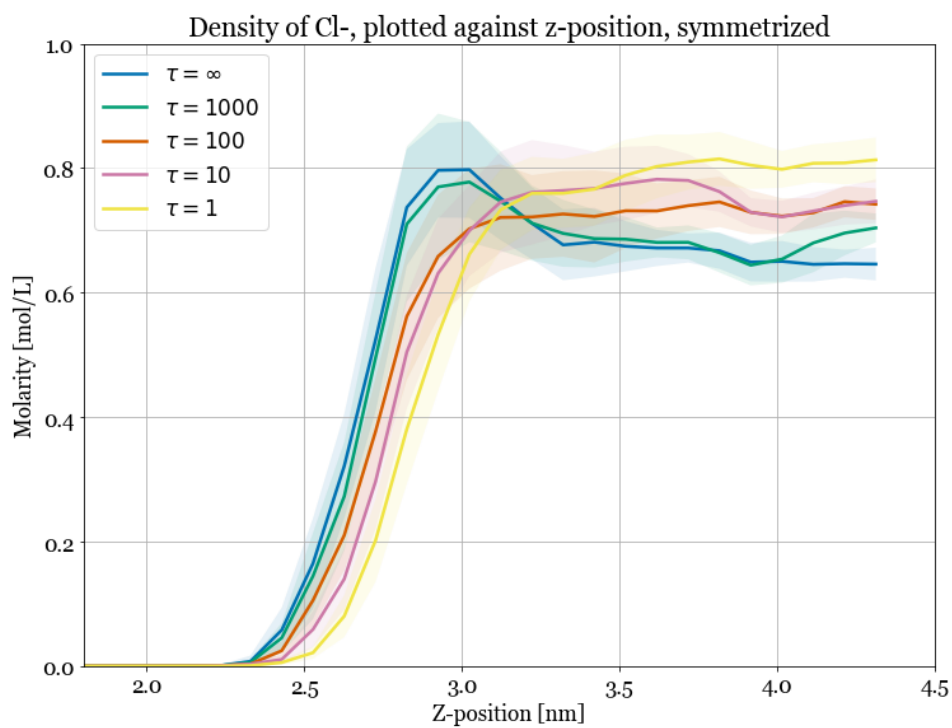


Figure 4.2: Density profile as function of z-position, of Cl⁻ for varying τ

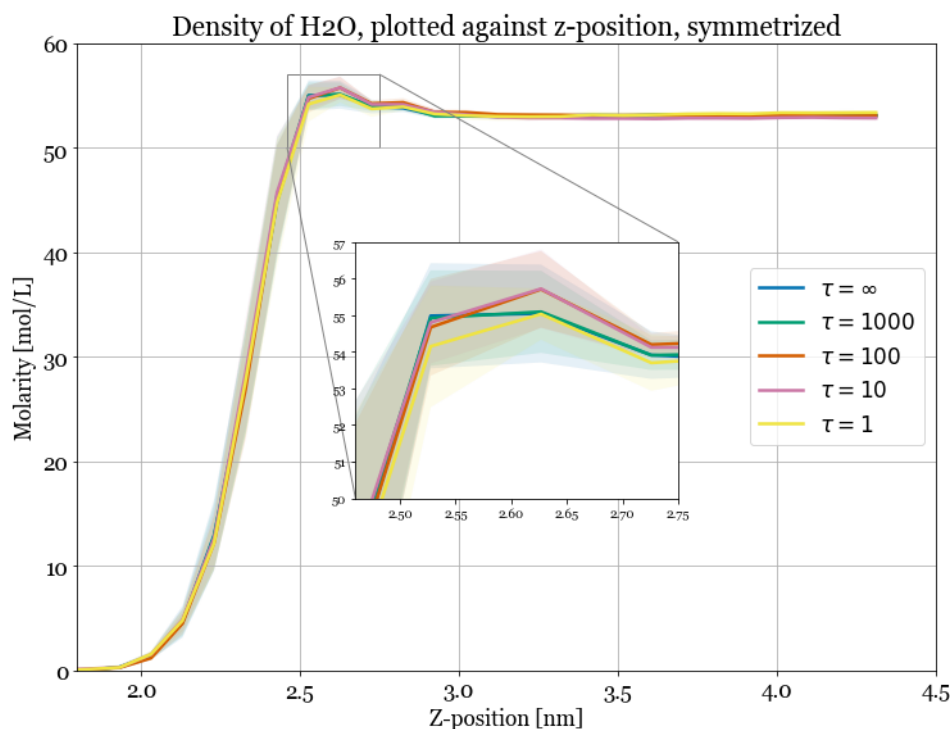


Figure 4.3: Density profile as function of z-position, of H₂O for varying τ

4.2. Adsorption type

Figure 4.4 and 4.5 give the density profiles as function of distance for both Na⁺ and Cl⁻ ions. These figures show the changes in adsorption type for varying τ . The plot for Na⁺ has been zoomed in for a clearer view of the peaks. The full plot can be found in Appendix C.2. The plots for each individual simulation are given in Appendix C.2.

Ions are found to adsorb less close to the surface for decreasing τ . A decrease can be found in inner-sphere surface complexes for Na⁺ (peak at 0.16 nm in Figure 4.4) and outer-sphere surface complexes for both Na⁺ and Cl⁻ (peaks at 0.23 nm in Figure 4.4 and 0.245 nm in Figure 4.5). At decreasing τ the diffuse swarm (DS) adsorption increased for Na⁺ (peak at 0.43 nm in Figure 4.4) and decreased for Cl⁻ (peaks at 0.45 nm and 0.65 nm in Figure 4.5). As ions are adsorbed less closely to the wall for lower values of τ their mobility increases. In case of an imposed pressure gradient or electric field the ions will be able to move more which will result in an increased current.

The flattening of the distinct peaks in adsorption of Na⁺ at decreasing τ explains the widening of the Stern layer in the density plot in Figure 4.1. An important discussion point here is that the decrease in adsorption close to the surface could be an overestimation because protonation events occurred randomly. The probability of protonation was equal for all >SiO⁻ regardless of adsorption of Na⁺. However, it is expected that at decreasing τ the decrease in adsorption close to the surface is also caused by interactions with nearby deprotonating silanol groups.

Even at low τ , Na⁺ adsorption of all three types is present and consequently the Stern layer is visible in Figure 4.1. For Cl⁻ however, the DS adsorption (peaks at 0.45 nm and 0.65 nm) are notably less visible at low τ . This is corroborated by the absence of a distinct anion layer in the density profile of Cl⁻ (the peak at 2.9 nm in Figure 4.2).

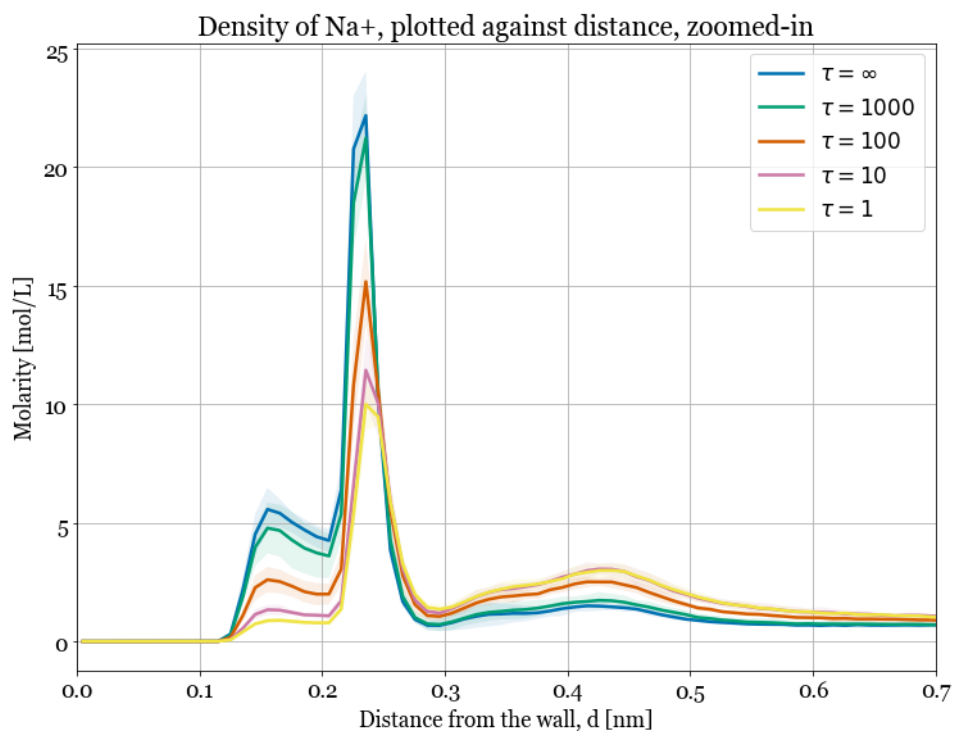


Figure 4.4: Density profile as function of distance, of Na⁺ for varying τ

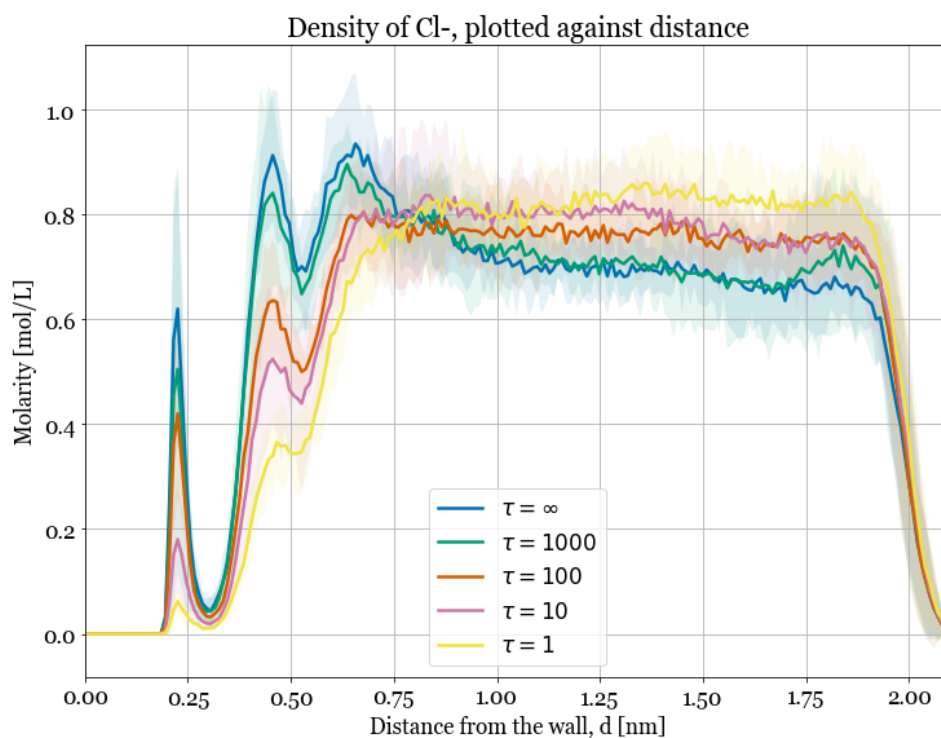


Figure 4.5: Density profile as function of distance, of Cl⁻ for varying τ

4.3. Electrostatic screening

Figure 4.6 shows the screening function for the system. Starting from the wall surface (around 2 nm) the Na^+ start to counteract the surface charge. It can happen that the Na^+ ions overcompensate for the negative surface charge. At this distance, the surface will "appear" to be positively charged. This phenomenon is called charge inversion. At event periods $\tau = \infty$ and $\tau = 1000$ at z-coordinates of around 2.7 nm charge inversion is present. At lower τ the effect of charge inversion is decreasing. At lower τ the Stern layer is therefore wider and the Na^+ ions are less closely packed together. The surface charge is screened more gradually and charge inversion is less likely. The absence of charge inversion explains the absence of a distinct anion layer (2.9 nm in Figure 4.2).

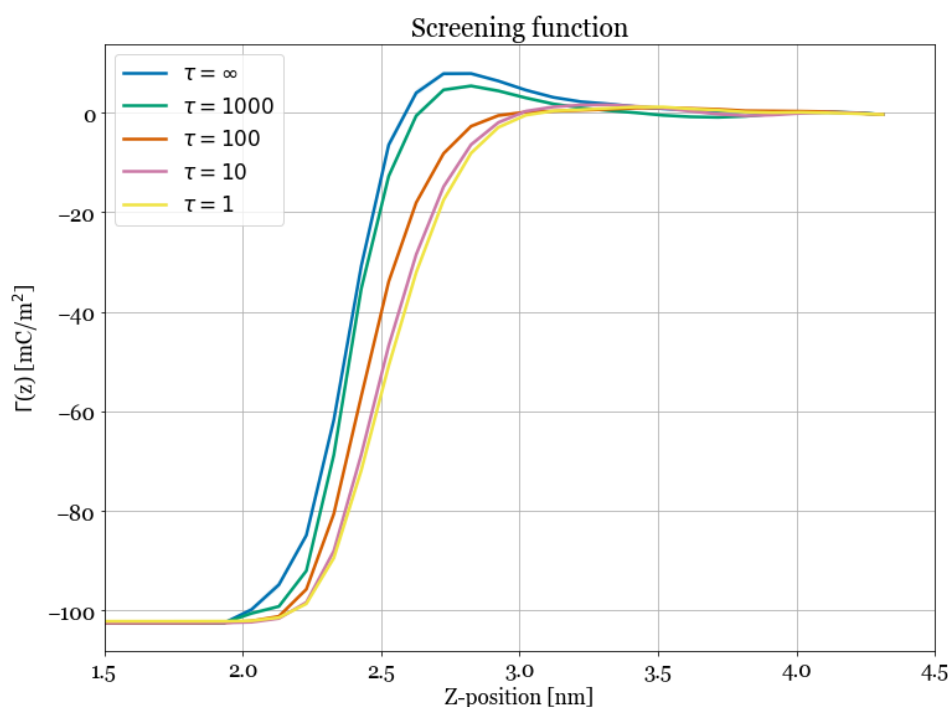


Figure 4.6: Screening function for varying τ

4.4. Water orientation

The water orientations for varying τ are shown in Figure 4.7. Negative $\cos\theta$ represent the positive side of water molecules turning toward the negatively charged surface. The baseline ($\tau = \infty$) is comparable to literature (Dewan *et al.* [50]). For high τ (the blue and green curve) the orientations flip slightly from negative to positive around 2.7 nm. This corroborates with the charge inversion in Figure 4.6. Furthermore, it is found that widening of the negative peak (i.e. the z-positions at which $\cos\theta < 0$) matches the widening of the Stern layer in Figure 4.1. In other words, the water molecules "feel" the surface charge at larger distances from the surface due to the decrease in screening of Na^+ ions in the Stern layer at lower values of τ .

The increase of the magnitude of the peak at 2 nm at decreasing τ could represent an increasing degree of structure in water molecules close to the surface. This might be due to the fact that there are less ions close to the surface that can disturb the orientation of the

water molecules. However, the uncertainty of this trend should be considered.

The plots for each individual simulation are given in Appendix C.3.

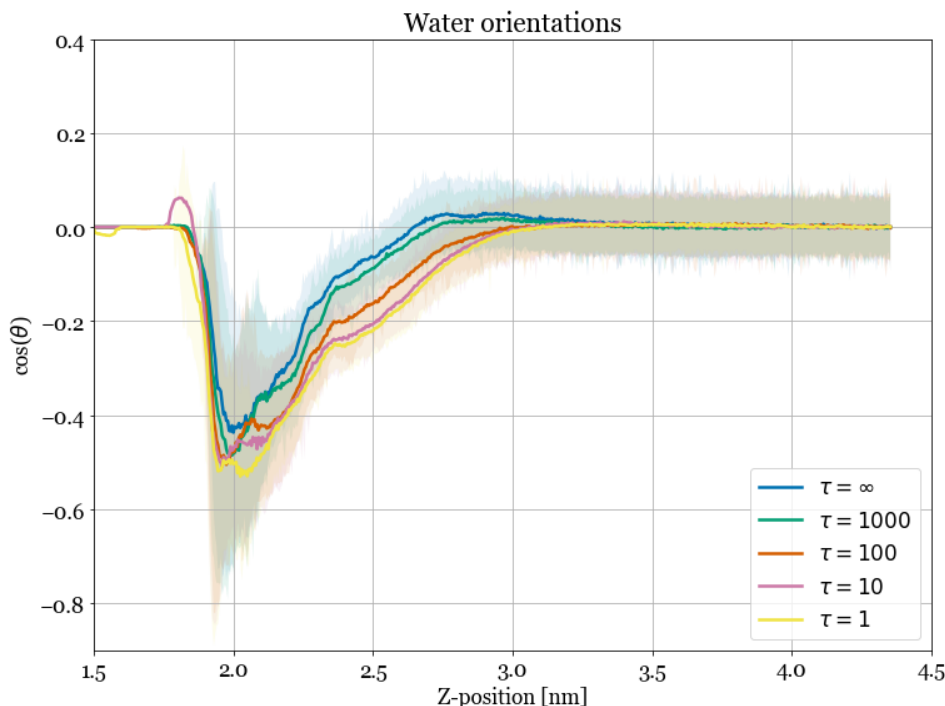


Figure 4.7: Water orientations for varying τ

4.5. Diffusion coefficient

Figures 4.8-4.10 show the diffusion coefficients both parallel to the wall and perpendicular to the wall for Na^+ ions, Cl^- ions and water molecules respectively. The average uncertainty is $\pm 0.72 \cdot 10^{-9} \text{ m}^2/\text{s}$. The MSD plots that were used to calculate the diffusion coefficient can be found in Appendix C.4.

The increase in diffusion at decreasing τ for Na^+ and water close to the surface is explained by the fact that higher (de)protonation frequency will increasingly force the ions and water molecules to move toward and away from deprotonated sites. The decreasing degree of structure in of the Stern layer can be a consequence of this increase in diffusion close to the surface. At $\tau = 1$ the most change in diffusion coefficient is found. It is hypothesized that, as τ comes closer to the time scale of the dynamics of the particles, the effect of τ on the diffusion is maximized. Following this theory, extremely low τ values ($\tau \ll 1$) would have less effect on the movement of particles as they can no longer "keep up" with the change in local surface charge and would perceive the surface charge to be more evenly distributed over all silanol groups. The diffusion coefficient of Cl^- ions in z-direction shows a considerably smaller increase close to the surface compared to x,y-direction (see Figure 4.9b). This is thought to be because Cl^- ions are further away from the surface and are forced to mostly move parallel to the surface due to the increased density in the bulk. However, this could also be explained by the uncertainty of the diffusion coefficients.

At decreasing τ the diffusion coefficients in the bulk decreased. It is expected that this decrease is due to the increase in density in the bulk (see Figures 4.1 and 4.2). It must be noted that the dynamics of the bulk fluid are influenced by the conditions of the surface as the diffusion coefficients do not match with known bulk values in literature ($2.49 \cdot 10^{-9} \text{ m}^2/\text{s}$ for SPC/E water (van der Spoel *et al.* [51]), $1.34 \cdot 10^{-9} \text{ m}^2/\text{s}$ for JC Na^+ and $1.66 \cdot 10^{-9} \text{ m}^2/\text{s}$ for JC Cl^- (Joung and Cheatham III [52])).

Lastly, the different pathways of how protonation and deprotonation occur are not taken into account in this model. It is important to understand that this can influence the results. In this work it is possible for a deprotonated silanol to randomly protonate even if a Na^+ ion is adsorbed. It is unlikely this silanol would protonate while being in this state. Ignoring this results in an overestimation of the increase of diffusion close to the surface.

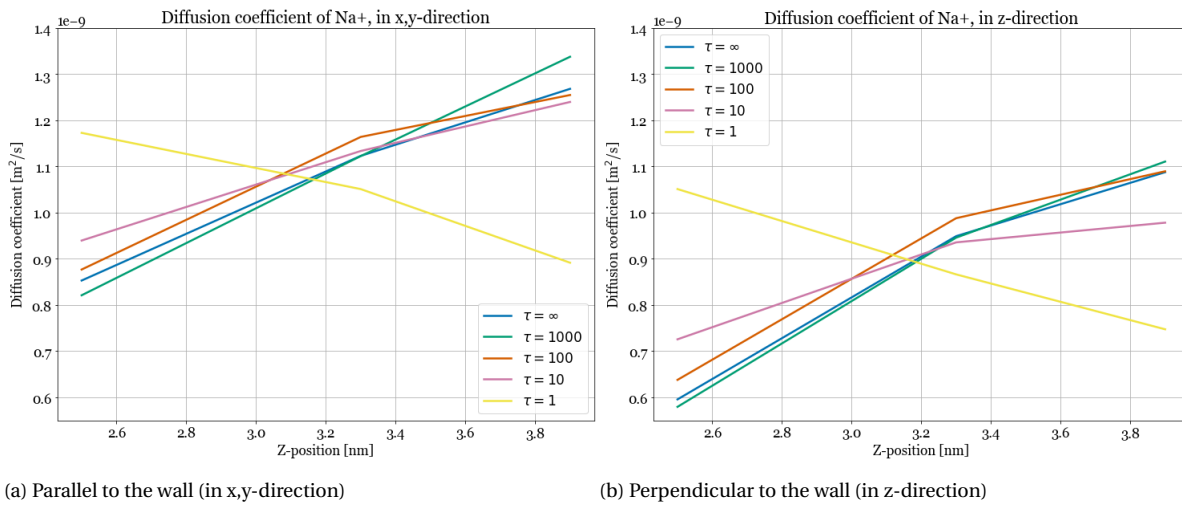


Figure 4.8: Diffusion coefficient of Na^+ for varying τ

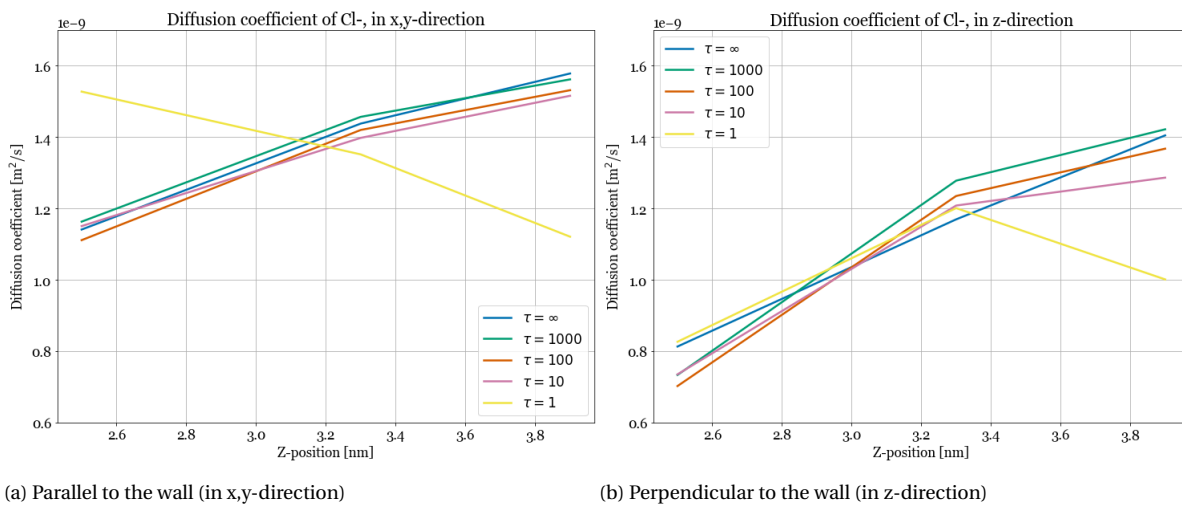


Figure 4.9: Diffusion coefficient of Cl^- for varying τ

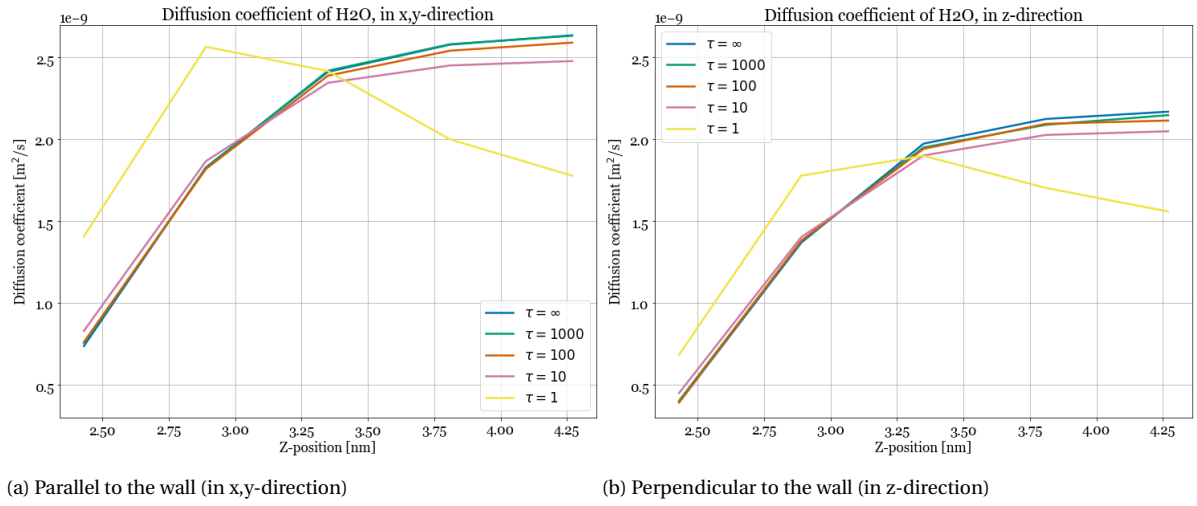


Figure 4.10: Diffusion coefficient of H₂O for varying τ

5

Conclusion

Due to the limited capabilities of measuring techniques that operate on an atomic scale, no exact values for the rate constants of the solid-liquid interfacial acid-base equilibrium reaction are currently known. Nevertheless, literature review indicated that protonation and deprotonation events do happen and that several pathways make proton movement possible.

In this thesis a MD simulation model was developed that incorporates protonation and deprotonation events at a variable period τ to research its effect on the characteristics of the electric double layer (EDL). Decreasing τ resulted in increasing diffusion coefficients close to the surface. This increase is explained by the fact that the ions and water molecules will be forced to move toward or away from deprotonated sites more frequently at lower values of τ . The Stern layer will thus become less immobile and increase in thickness. The change in diffusion has a significant influence on other characteristics of the EDL. At decreasing τ ions moved further away from the surface, adsorbing more in the diffuse swarm (DS) and less in the inner- and outer-sphere surface complexes (ISSC and OSSC). This brought about a decrease in the occurrence of charge inversion.

As a whole, dynamic surface charge distribution has a considerable impact on the characteristics of the electric double layer depending on τ and should be considered in future MD simulations.

6

Recommendations

This chapter provides a few of recommendations for future research. These are ideas that could further improve, validate or expand on this work.

6.1. Event periods

The most important flaw of this thesis is the lack of a quantitative value of the rate constant. Knowing these values would transform this work into a tool that can validate a simulation approach. If the true event period is low enough to have effects on the characteristics of the EDL, the dynamic surface charges cannot be ignored in simulations. If a method is developed to closely measure local fluctuations in surface charge one can use this experimental data to improve the relevance of the model.

6.2. Adsorption times

The diffusion coefficients have a high uncertainty which puts the found relations and trends up for debate. Calculating ion adsorption types can provide confirmation of the trend in dynamics. Due to the time limitations of this thesis the adsorption times of Na^+ ions were not investigated. A decrease in average adsorption times with decreasing τ is expected to be a result of increased ion movement close to the surface.

6.3. Effect of (de)protonation frequency on flow profiles

The model that was developed can be expanded further to include a channel flow (both by pressure gradient of electric field). One can imagine that when the structure of the Stern layer changes, the effective cross-sectional area of a nano tube would vary as a result. Second to this, when ions are less strongly absorbed to the wall and move more freely this will also influence the current flow.

6.4. Protonation probability of silanols

In the model of this thesis all silanols had the same the probability to protonate or deprotonate. The model can be improved by implementing a protocol for choosing silanols to protonate and deprotonate based on their physical conditions. Physically there are several scenarios that can influence this probability. For example, if the hydrogen is attracted

to a nearby deprotonated silanol it would already be stretching its OH-bond and be more likely to break that bond. Furthermore, a deprotonated silanol is expected to be less likely to protonate if a cation is adsorbed close by. MD simulation can be used to find a relation between vibration frequencies of the silanols and the likelihood of protonation and deprotonation. Higher vibration frequencies can indicate a nearby attraction and a weaker bond. Silanols vibrating on higher frequencies would have a higher probability to deprotonate.

Bibliography

- [1] F. K. Lutgens and E. J. Tarbuck, *Essentials of geology*, 7th ed. (Upper Saddle River, NJ : Prentice Hall, 2000).
- [2] A. J. Lunt, P. Chater, and A. M. Korsunsky, *On the origins of strain inhomogeneity in amorphous materials*, Scientific reports **8**, 1 (2018).
- [3] P. K. Jal, S. Patel, and B. K. Mishra, *Chemical modification of silica surface by immobilization of functional groups for extractive concentration of metal ions*, Talanta **62**, 1005 (2004).
- [4] J. Sonnefeld, M. Löbbus, and W. Vogelsberger, *Determination of electric double layer parameters for spherical silica particles under application of the triple layer model using surface charge density data and results of electrokinetic sonic amplitude measurements*, Colloids and Surfaces A: Physicochemical and Engineering Aspects **195**, 215 (2001).
- [5] F. S. Emami, V. Puddu, R. J. Berry, V. Varshney, S. V. Patwardhan, C. C. Perry, and H. Heinz, *Force field and a surface model database for silica to simulate interfacial properties in atomic resolution*, Chemistry of Materials **26**, 2647 (2014).
- [6] I. S. Joung and T. E. Cheatham III, *Determination of alkali and halide monovalent ion parameters for use in explicitly solvated biomolecular simulations*, The journal of physical chemistry B **112**, 9020 (2008).
- [7] H. Berendsen, J. Grigera, and T. Straatsma, *The missing term in effective pair potentials*, Journal of Physical Chemistry **91**, 6269 (1987).
- [8] D. A. Muller, T. Sorsch, S. Moccio, F. Baumann, K. Evans-Lutterodt, and G. Timp, *The electronic structure at the atomic scale of ultrathin gate oxides*, Nature **399**, 758 (1999).
- [9] N. Convery and N. Gadegaard, *30 years of microfluidics*, Micro and Nano Engineering (2019).
- [10] N. Ravindra, V. R. Mehta, and S. Shet, *Silicon nanoelectronics and beyond: An overview and recent developments*, JOM **57**, 16 (2005).
- [11] Y. Yang and C. Yu, *Advances in silica based nanoparticles for targeted cancer therapy*, Nanomedicine: Nanotechnology, Biology and Medicine **12**, 317 (2016).
- [12] E. R. Cruz-Chu, A. Aksimentiev, and K. Schulten, *Water- silica force field for simulating nanodevices*, The Journal of Physical Chemistry B **110**, 21497 (2006).
- [13] B. M. Lowe, C.-K. Skylaris, and N. G. Green, *Acid-base dissociation mechanisms and energetics at the silica–water interface: An activationless process*, Journal of colloid and interface science **451**, 231 (2015).

- [14] A. Kiselev, *The structure of silicic acid gels*, Kolloidn. Zh **2**, 17 (1936).
- [15] J. Yeon and A. C. van Duin, *Reaxff molecular dynamics simulations of hydroxylation kinetics for amorphous and nano-silica structure, and its relations with atomic strain energy*, The Journal of Physical Chemistry C **120**, 305 (2016).
- [16] R. K. Iler, *The chemistry of silica*, Solubility, polymerization, colloid and surface properties and biochemistry of silica (1979).
- [17] D. F. Cadogan and D. T. Sawyer, *Gas-solid chromatography using various thermally activated and chemically modified silicas*, Analytical Chemistry **42**, 190 (1970).
- [18] C. Armistead, A. Tyler, F. Hambleton, S. Mitchell, and J. A. Hockey, *Surface hydroxylation of silica*, The Journal of Physical Chemistry **73**, 3947 (1969).
- [19] J. de Boer, M. Hermans, and J. Vleeskens, *The chemisorption and physical adsorption of water on silica. i*, Proceedings of the Koninklijke Academie van Wetenschappen. Series B, Physical Sciences **60**, 45 (1957).
- [20] C. Rosales-Landeros, C. E. Barrera-Díaz, B. Bilyeu, V. V. Guerrero, F. Ure, *et al.*, *A review on $cr(vi)$ adsorption using inorganic materials*, American Journal of Analytical Chemistry **4**, 8 (2013).
- [21] L. Zhuravlev, *The surface chemistry of amorphous silica. zhuravlev model*, Colloids and Surfaces A: Physicochemical and Engineering Aspects **173**, 1 (2000).
- [22] J. Zhu, C. Tang, J. Wei, Z. Li, M. Laipan, H. He, X. Liang, Q. Tao, and L. Cai, *Structural effects on dissolution of silica polymorphs in various solutions*, Inorganica Chimica Acta **471**, 57 (2018).
- [23] Y. Duval, J. Mielczarski, O. Pokrovsky, E. Mielczarski, and J. Ehrhardt, *Evidence of the existence of three types of species at the quartz- aqueous solution interface at ph 0- 10: Xps surface group quantification and surface complexation modeling*, The Journal of Physical Chemistry B **106**, 2937 (2002).
- [24] C. Labbez, A. Nonat, I. Pochard, and B. Jönsson, *Experimental and theoretical evidence of overcharging of calcium silicate hydrate*, Journal of Colloid and Interface Science **309**, 303 (2007).
- [25] C. Lian, X. Kong, H. Liu, and J. Wu, *Flow effects on silicate dissolution and ion transport at an aqueous interface*, Physical Chemistry Chemical Physics **21**, 6970 (2019).
- [26] A. F. C. Campos, W. Costa de Medeiros, R. Aquino, and J. Depeyrot, *Surface charge density determination in water based magnetic colloids: A comparative study*, Materials Research **20**, 1729 (2017).
- [27] D. C. Grahame, *The electrical double layer and the theory of electrocapillarity*. Chemical reviews **41**, 441 (1947).
- [28] M. F. Döpke, J. Lutzenkirchen, O. A. Moulton, B. Siboulet, J.-F. Dufrêche, J. T. Padding, and R. Hartkamp, *Preferential adsorption in mixed electrolytes confined by charged amorphous silica*, The Journal of Physical Chemistry C **123**, 16711 (2019).

- [29] S. Ong, X. Zhao, and K. B. Eisenthal, *Polarization of water molecules at a charged interface: second harmonic studies of the silica/water interface*, Chemical Physics Letters **191**, 327 (1992).
- [30] L. H. Allen, E. Matijević, and L. Meites, *Exchange of Na^+ for the silanolic protons of silica*, Journal of Inorganic and Nuclear Chemistry **33**, 1293 (1971).
- [31] L. Dalstein, E. Potapova, and E. Tyrode, *The elusive silica/water interface: Isolated silanols under water as revealed by vibrational sum frequency spectroscopy*, Physical Chemistry Chemical Physics **19**, 10343 (2017).
- [32] B. A. Fleming, *Kinetics of reaction between silicic acid and amorphous silica surfaces in NaCl solutions*, Journal of Colloid and Interface Science **110**, 40 (1986).
- [33] T. Mahadevan and S. Garofalini, *Dissociative chemisorption of water onto silica surfaces and formation of hydronium ions*, The Journal of Physical Chemistry C **112**, 1507 (2008).
- [34] G. K. Lockwood and S. H. Garofalini, *Proton dynamics at the water-silica interface via dissociative molecular dynamics*, The Journal of Physical Chemistry C **118**, 29750 (2014).
- [35] M. Karlsson, C. Craven, P. M. Dove, and W. H. Casey, *Surface charge concentrations on silica in different 1.0 M metal-chloride background electrolytes and implications for dissolution rates*, Aquatic Geochemistry **7**, 13 (2001).
- [36] F. K. Crundwell, *On the mechanism of the dissolution of quartz and silica in aqueous solutions*, ACS omega **2**, 1116 (2017).
- [37] S. Nangia and B. J. Garrison, *Reaction rates and dissolution mechanisms of quartz as a function of pH*, The Journal of Physical Chemistry A **112**, 2027 (2008).
- [38] P. M. Dove and S. F. Elston, *Dissolution kinetics of quartz in sodium chloride solutions: Analysis of existing data and a rate model for 25 °C*, Geochimica et Cosmochimica Acta **56**, 4147 (1992).
- [39] I. C. Bourg and G. Sposito, *Molecular dynamics simulations of the electrical double layer on smectite surfaces contacting concentrated mixed electrolyte (NaCl-CaCl₂) solutions*, Journal of colloid and interface science **360**, 701 (2011).
- [40] F. Van Cauwelaert, P. Jacobs, and J. Uytterhoeven, *Identification of the α-type hydroxyls on silica surfaces*, The Journal of Physical Chemistry **76**, 1434 (1972).
- [41] P. Hoffmann and E. Knözinger, *Novel aspects of mid and far IR Fourier spectroscopy applied to surface and adsorption studies on SiO₂*, Surface science **188**, 181 (1987).
- [42] B. Morrow and A. McFarlan, *Surface vibrational modes of silanol groups on silica*, The Journal of Physical Chemistry **96**, 1395 (1992).
- [43] C. E. Bronnimann, R. C. Zeigler, and G. E. Maciel, *Proton NMR study of dehydration of the silica gel surface*, Journal of the American Chemical Society **110**, 2023 (1988).

- [44] D. W. Sindorf and G. E. Maciel, *Silicon-29 nmr study of dehydrated/rehydrated silica gel using cross polarization and magic-angle spinning*, Journal of the American Chemical Society **105**, 1487 (1983).
- [45] M. Pfeiffer-Laplaud, D. Costa, F. Tielens, M.-P. Gageot, and M. Sulpizi, *Bimodal acidity at the amorphous silica/water interface*, The Journal of Physical Chemistry C **119**, 27354 (2015).
- [46] V. Ogenko, *Chemical physics of dispersed material surfaces*, Reaction Kinetics and Catalysis Letters **50**, 103 (1993).
- [47] J. D. Fisk, R. Batten, G. Jones, J. P. O'Reill, and A. M. Shaw, *ph dependence of the crystal violet adsorption isotherm at the silica- water interface*, The Journal of Physical Chemistry B **109**, 14475 (2005).
- [48] I.-S. Chuang and G. E. Maciel, *A detailed model of local structure and silanol hydrogen bonding of silica gel surfaces*, The Journal of Physical Chemistry B **101**, 3052 (1997).
- [49] I.-C. Yeh and M. L. Berkowitz, *Ewald summation for systems with slab geometry*, The Journal of chemical physics **111**, 3155 (1999).
- [50] S. Dewan, V. Carnevale, A. Bankura, A. Eftekhari-Bafrooei, G. Fiorin, M. L. Klein, and E. Borguet, *Structure of water at charged interfaces: A molecular dynamics study*, Langmuir **30**, 8056 (2014).
- [51] D. van der Spoel, P. J. Van Maaren, and H. J. Berendsen, *A systematic study of water models for molecular simulation: derivation of water models optimized for use with a reaction field*, The Journal of chemical physics **108**, 10220 (1998).
- [52] I. S. Joung and T. E. Cheatham III, *Molecular dynamics simulations of the dynamic and energetic properties of alkali and halide ions using water-model-specific ion parameters*, The Journal of Physical Chemistry B **113**, 13279 (2009).
- [53] S. H. Behrens and D. G. Grier, *The charge of glass and silica surfaces*, The Journal of Chemical Physics **115**, 6716 (2001).

A

Derivations

A.1. Equation 2.9

This section contains the explanation of the error of the derivation for the formula relating rate constants to surface charge and pH by Lian *et al.* [25] (Equation A.1).

$$Q = -eN_{total} \frac{k^+ \cdot 10^{-pH} \exp(-\beta e \Psi_0)}{k^+ + k^- \cdot 10^{-pH} \exp(-\beta e \Psi_0)} \quad (\text{A.1})$$

where:

- Q = surface charge
- e = magnitude of the charge of an electron = $1.602 \cdot 10^{19}$ Coulomb
- N_{total} = total number of silanol sites
- k^+, k^- = rate constants of the forward and backward reaction respectively
- pH = pH value of the fluid
- $\beta = k_B T$ = thermal energy (Boltzmann constant and temperature)
- Ψ_0 = surface electrical potential

According to Behrens and Grier [53] we can obtain the value of the concentration of H^+ -atoms near the surface using Equation A.2.

$$\begin{aligned} [H^+]_0 &= [H^+]_b \exp(-\beta e \psi_0) \\ [H^+]_0 &= 10^{-pH} \exp(-\beta e \psi_0) \end{aligned} \quad (\text{A.2})$$

where:

- $[H^+]_0$ = concentration of H^+ -atoms near the surface
- $[H^+]_b$ = concentration of H^+ -atoms of the bulk = 10^{-pH}
- β^{-1} = thermal energy = $k_B T$
- e = magnitude of the charge of an electron = $1.602 \cdot 10^{19}$ Coulomb
- ψ_0 = electrostatic potential of the surface

Combining Equations A.1 and A.2 reduces Lian's equation to:

$$Q = -eN_{total} \frac{k^+ \cdot [H^+]_0}{k^+ + k^- \cdot [H^+]_0} \quad (\text{A.3})$$

Applying the condition $K_a = k^+ / k^-$:

$$Q = -eN_{total} \frac{K_a \cdot k^- \cdot [H^+]_0}{K_a \cdot k^- + k^- \cdot [H^+]_0} \quad (A.4)$$

$$Q = -eN_{total} \frac{K_a \cdot [H^+]_0}{K_a + [H^+]_0} \quad (A.5)$$

Known is the equation for the acid dissociation constant (Equation A.6):

$$\frac{k^+}{k^-} = \frac{[>SiO^-][H^+]}{[>SiOH]} = K_a \quad (A.6)$$

Here $[H^+]$ is the concentration of hydrogen ions near the wall, $[H^+] = [H^+]_0$. Imposing this equation on Lian's formula leads to:

$$Q = -eN_{total} \frac{\frac{[>SiO^-][H^+]_0}{[>SiOH]} \cdot [H^+]_0}{\frac{[>SiO^-][H^+]_0}{[>SiOH]} + [H^+]_0} \quad (A.7)$$

$$Q = -eN_{total} \frac{\frac{[>SiO^-][H^+]_0}{[>SiOH]}}{\frac{[>SiO^-]}{[>SiOH]} + 1} \quad (A.8)$$

$$Q = -eN_{total} \frac{[>SiO^-][H^+]_0}{[>SiO^-] + [>SiOH]} \quad (A.9)$$

$$Q = -eN_{total} \frac{[>SiO^-][H^+]_0}{N_{total}} \quad (A.10)$$

$$Q = -e[>SiO^-][H^+]_0 \quad (A.11)$$

However, the known expression for surface charge is as Equation A.12:

$$Q = -e[>SiO^-] \quad (A.12)$$

As, $[H^+]_0 \neq 0$, Lian *et al.*'s formulation of the relationship between the rate constants and the surface charge is concluded to be invalid ([25]). Fitting a titration curve cannot be used to find rate constants as it does not hold information on kinetics.

B

Calculations

B.1. Number of ions in seawater

- Salinity of seawater = 34.7 g/kg
34.7 g NaCl : 1 kg seawater
34.7 g NaCl : 965.3 g H₂O
- $M_{\text{NaCl}} = 58.44 \text{ g/mol}$
 $M_{\text{H}_2\text{O}} = 18.02 \text{ g/mol}$
- $n = m / M$
 $n_{\text{NaCl}} = 0.59 \text{ mol}$
 $n_{\text{H}_2\text{O}} = 53.57 \text{ mol}$
- Atom ratio NaCl:H₂O = 1:91
1650 H₂O molecules in box : 18 NaCl molecules

The salinity of seawater in this thesis is 34.7 g/kg. This means there is 34.7 g of salt in 1 kg of seawater. Then, in 1 kg of seawater there is 34.7 g of salt and $1000 - 34.7 = 965.3 \text{ g}$ of pure water. The molar mass of NaCl is 58.44 g/mol and that of water is 18.02 g/mol. This gives $34.7/58.44 = 0.59 \text{ mol}$ of NaCl and $965.3/18.02 = 53.57 \text{ mol}$ of H₂O. This is a ratio of NaCl:H₂O of 1:91. In the simulation box there are 1638 water molecules. $1638/91 = 18$ salt molecules.

B.2. Number of deprotonated sites due to surface charge

- Surface charge density = -100 mC/m^2
- $1 \text{ mC} = 6.2415 \cdot 10^{15} \text{ e}$
- $1 \text{ m}^2 = 10^{20} \text{ \AA}^2$
- Surface charge density = $0.0062415 \text{ e/\AA}^2$
- Area of one wall = $35^2 \text{ \AA}^2 = 1225 \text{ \AA}^2$
- Number of deprotonated sites per wall = $7.6458375 \approx 8$

C

Additional results

C.1. Density profiles as function of z-position

C.1.1. Average density profiles before symmetrization

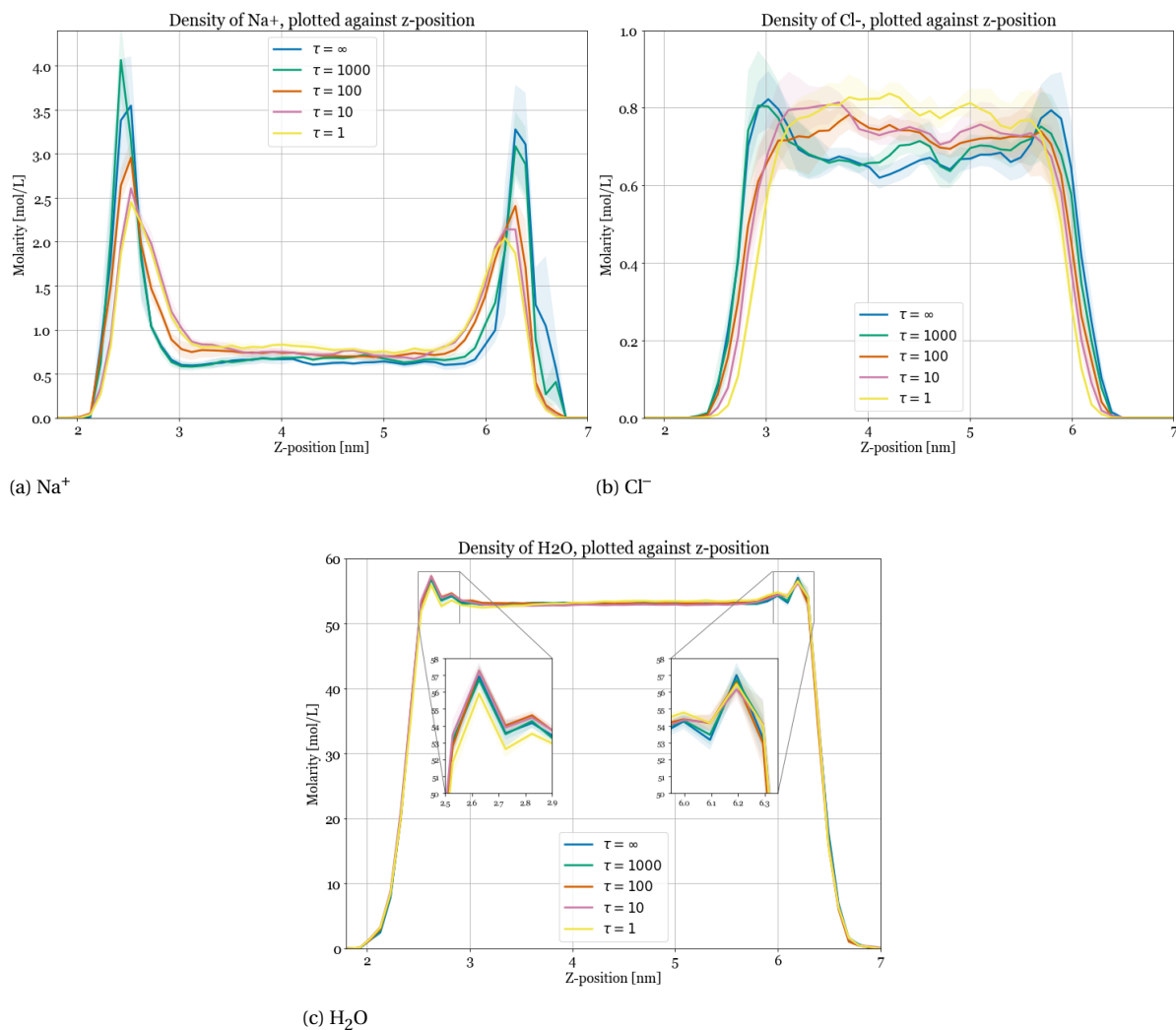


Figure C.1: Average density profiles as function of z-position, before symmetrization

C.1.2. Density profiles for individual simulations

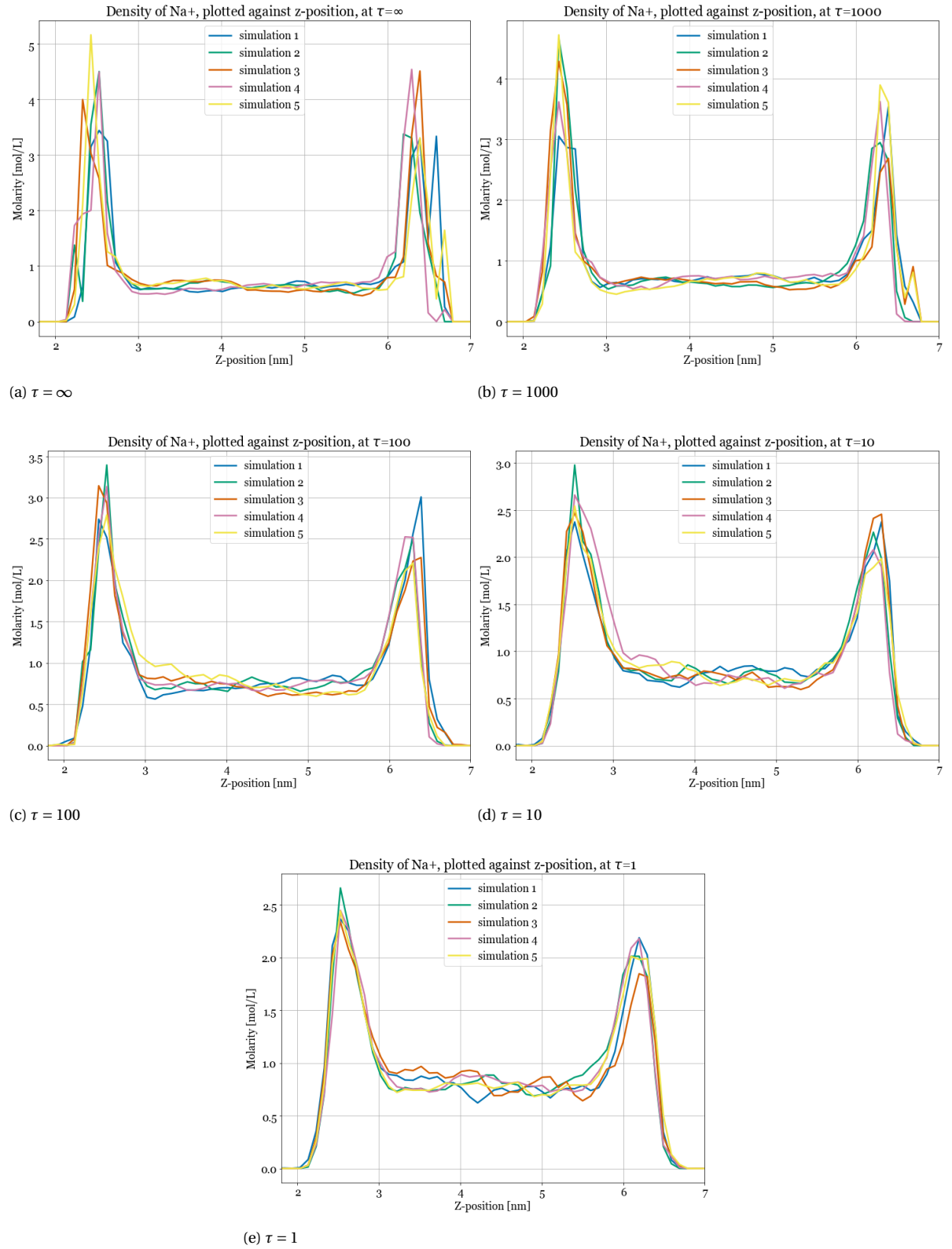
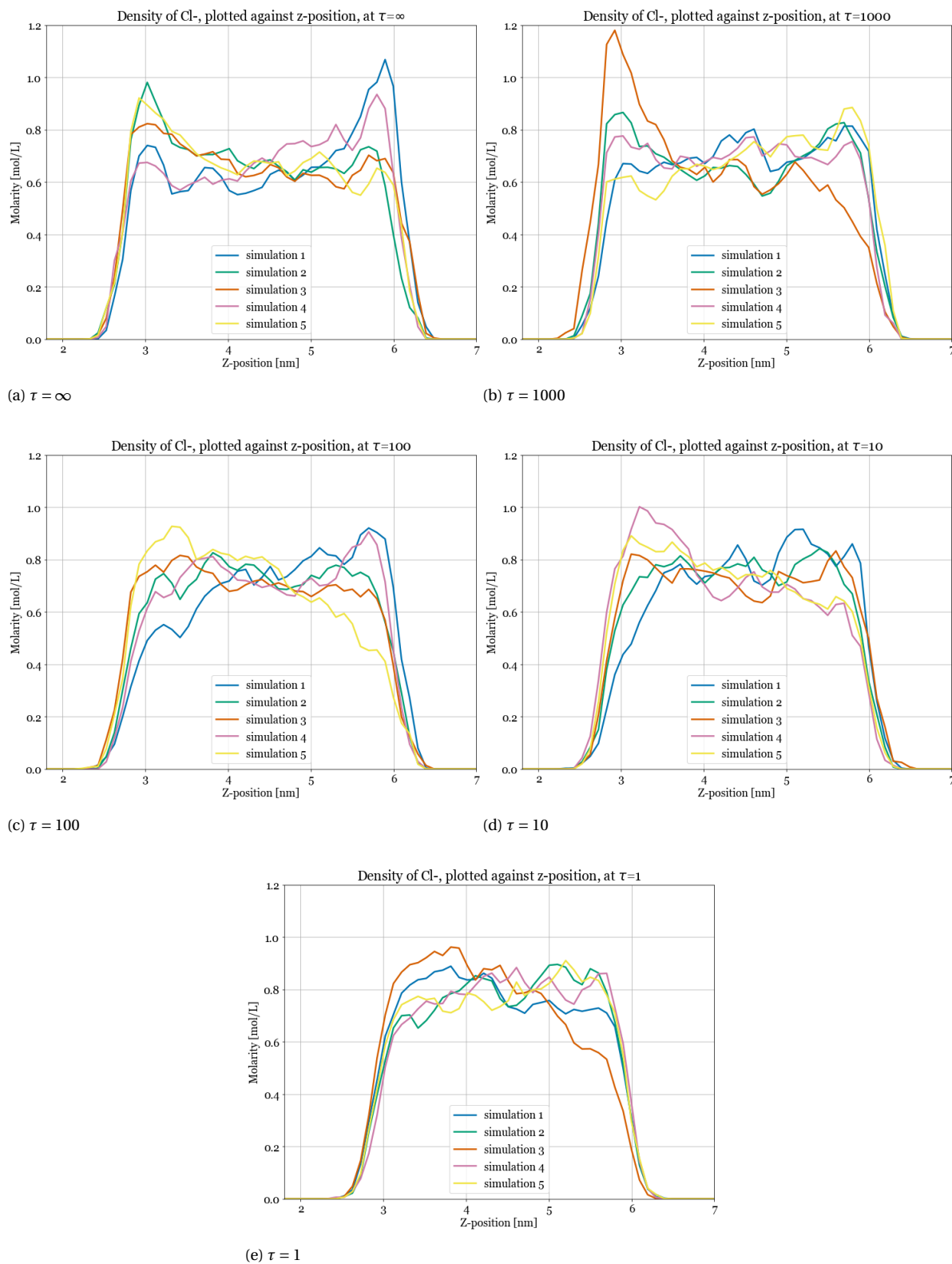


Figure C.2: Density profiles of Na^+ as function of z-position, for individual simulations

Figure C.3: Density profiles of Cl^- as function of z-position, for individual simulations

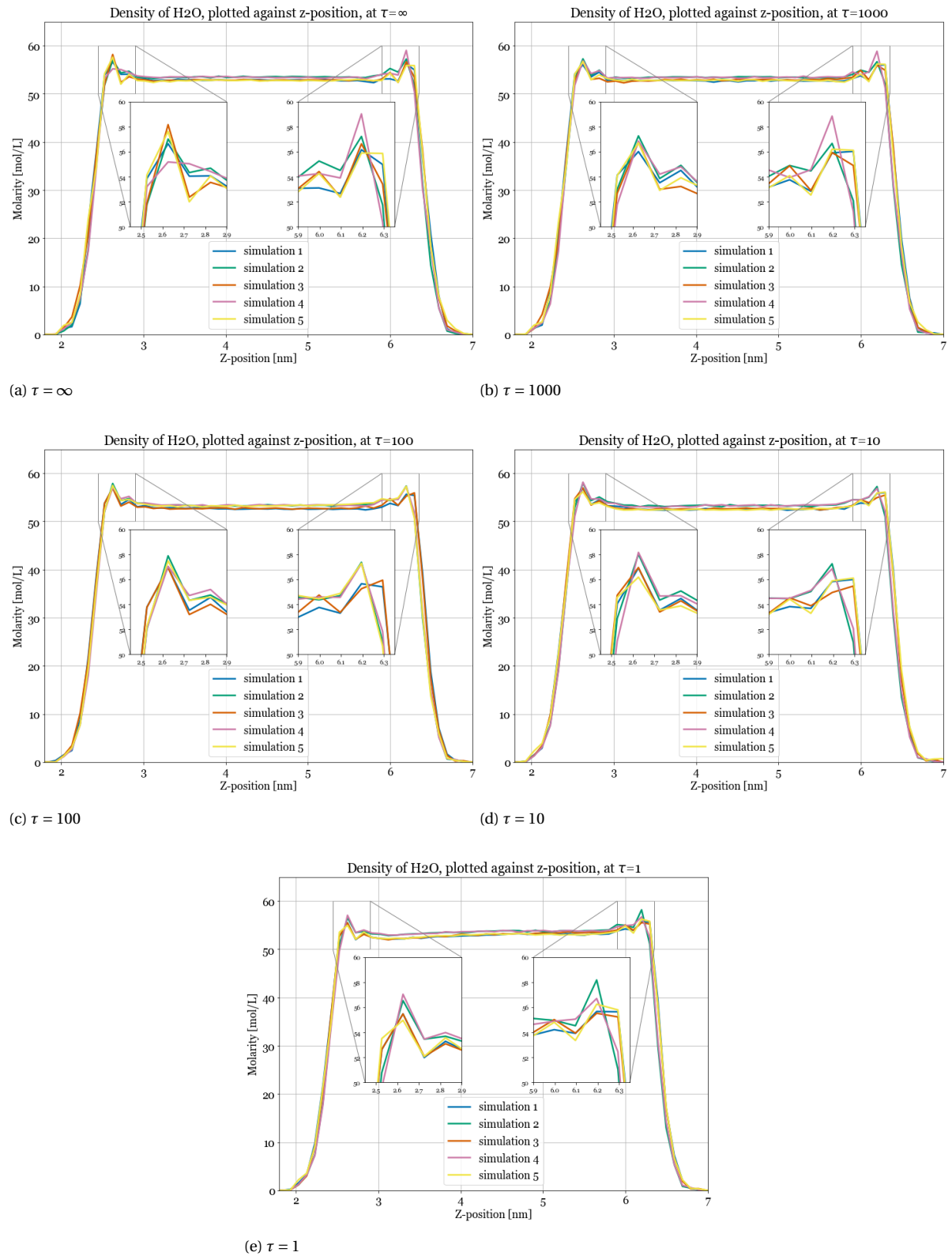


Figure C.4: Density profiles of H₂O as function of z-position, for individual simulations

C.2. Density profiles as function of distance

C.2.1. Zoomed-out density profile of Na^+

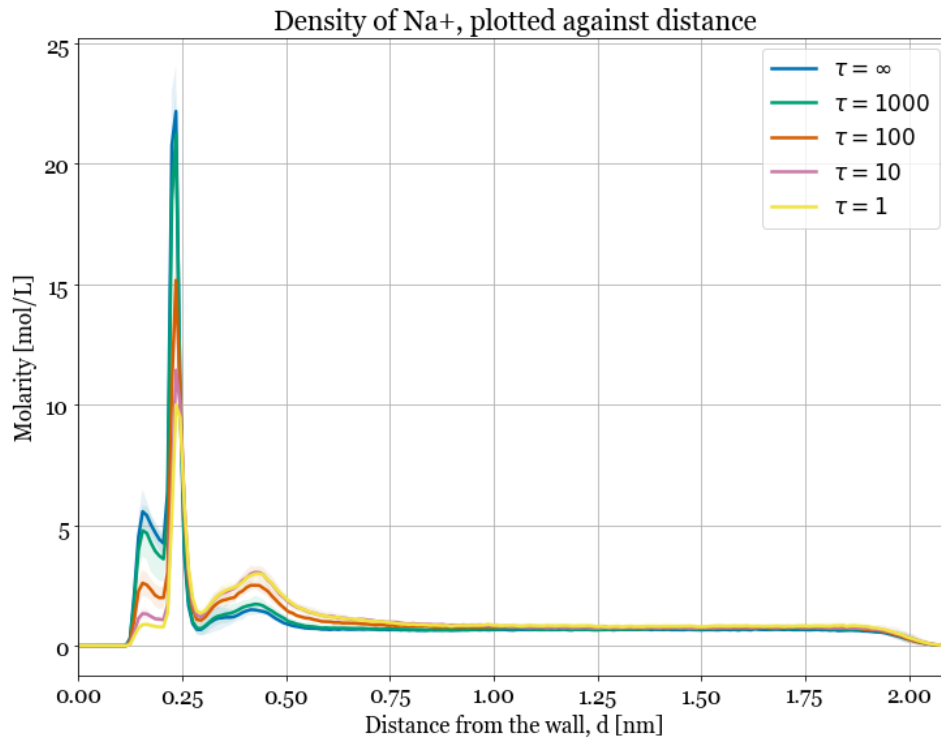


Figure C.5: Zoomed-out density profile as function of distance, of Na^+ for varying τ

C.2.2. Density profiles for individual simulations

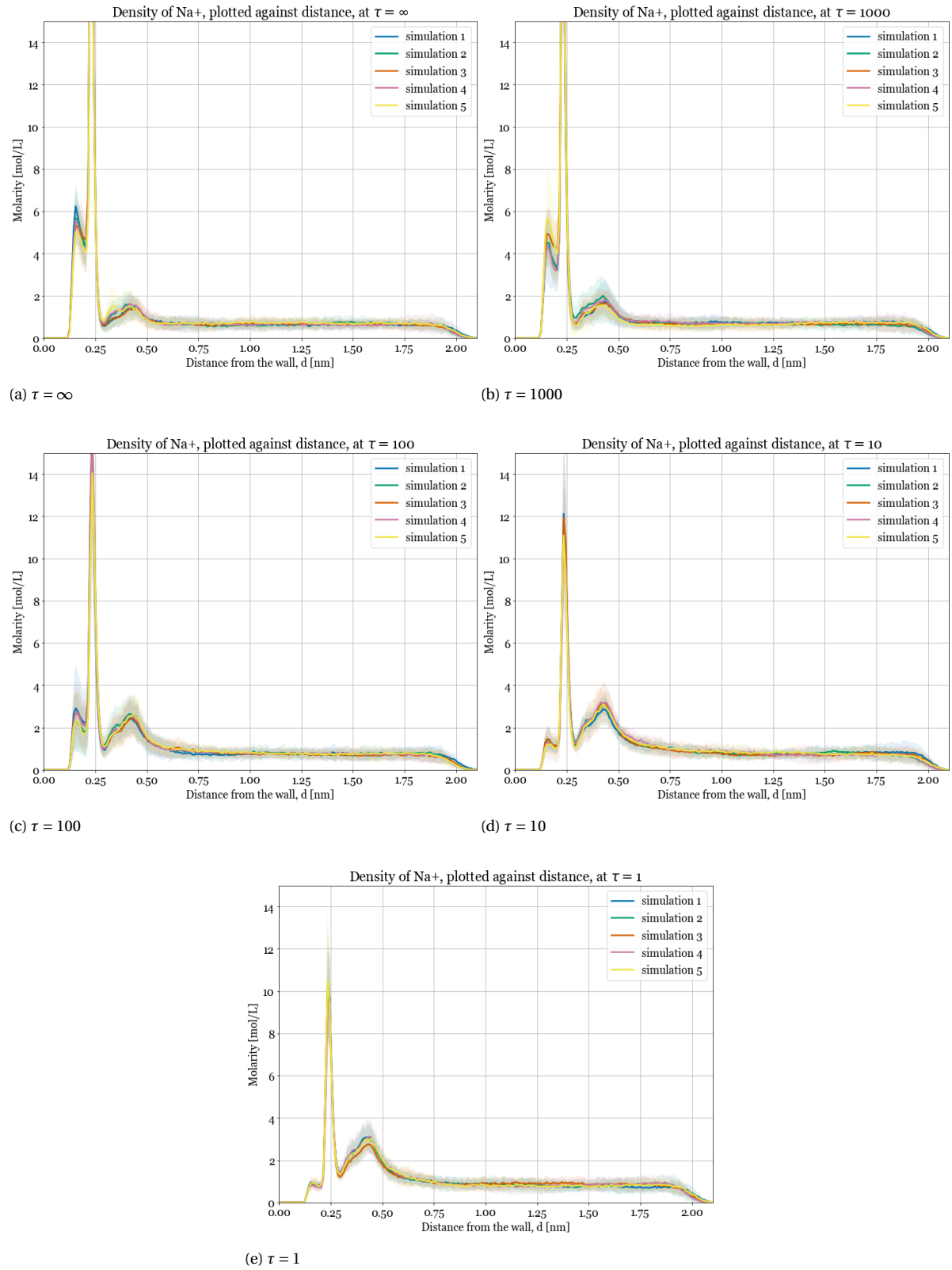
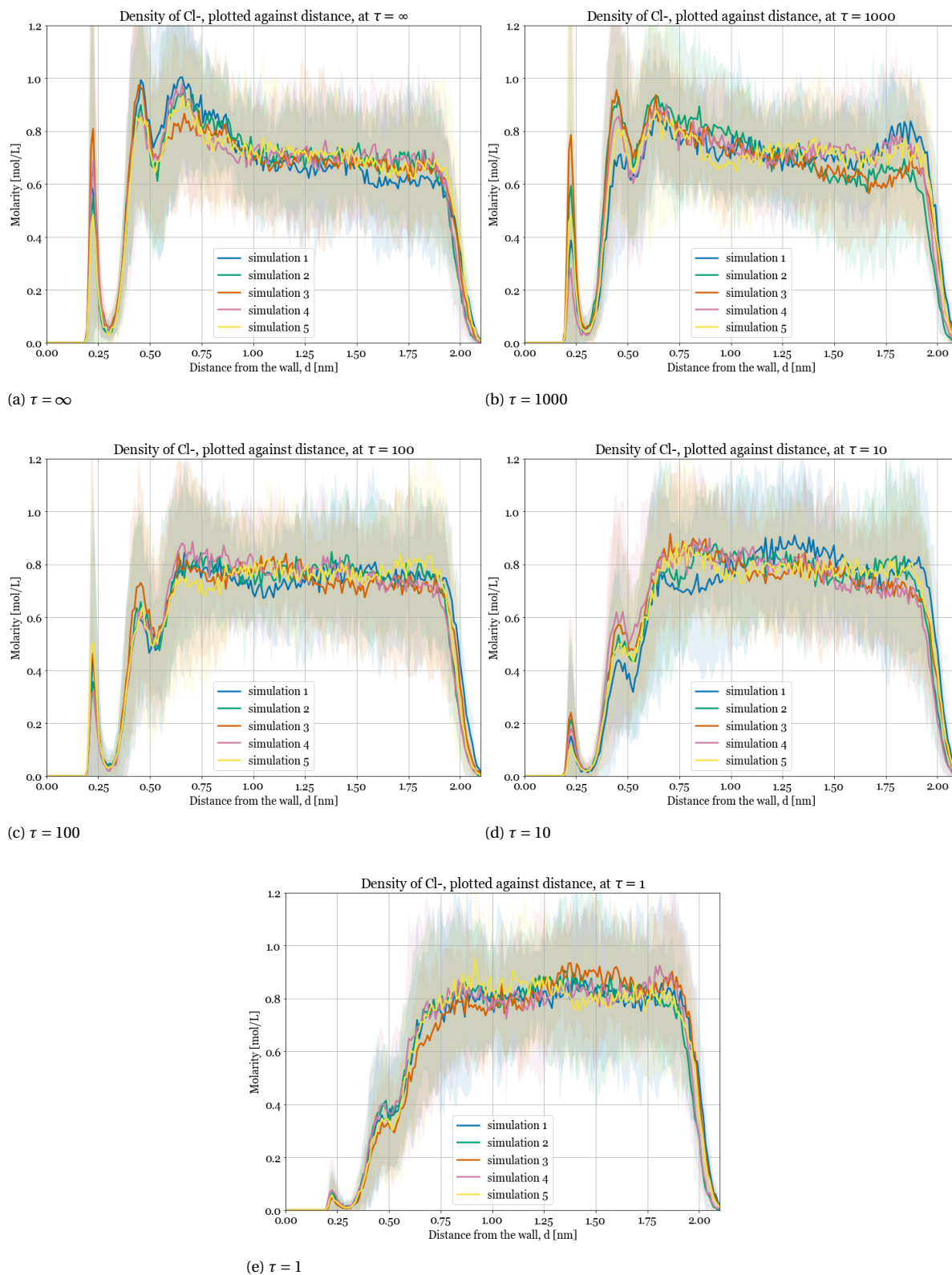


Figure C.6: Density profiles of Na^+ as function of distance, for individual simulations

Figure C.7: Density profiles of Cl^- as function of distance, for individual simulations

C.3. Water orientation plots

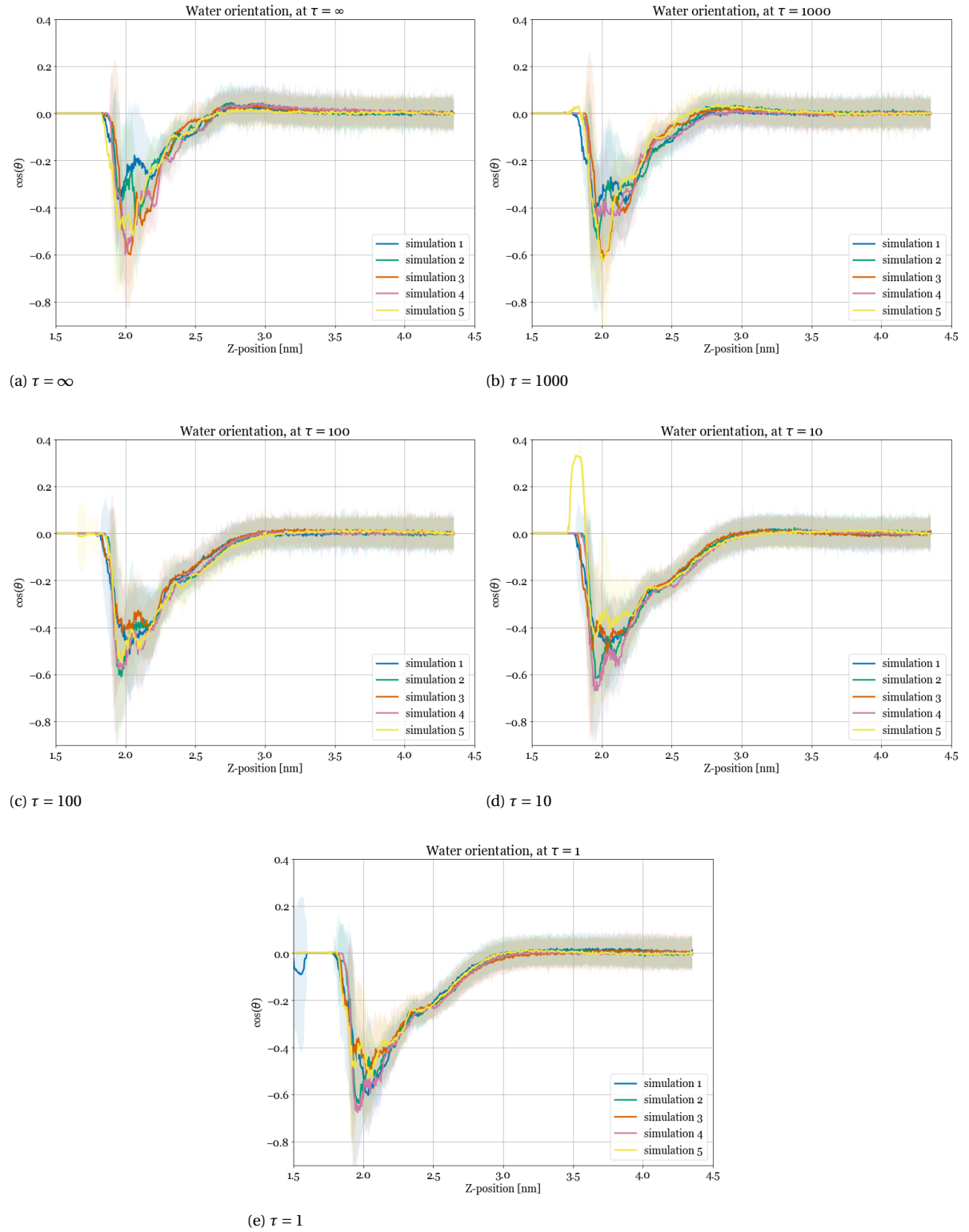


Figure C.8: Water orientations for individual simulations

C.4. MSD plots

C.4.1. Visualization of bin sizes used for MSD calculation

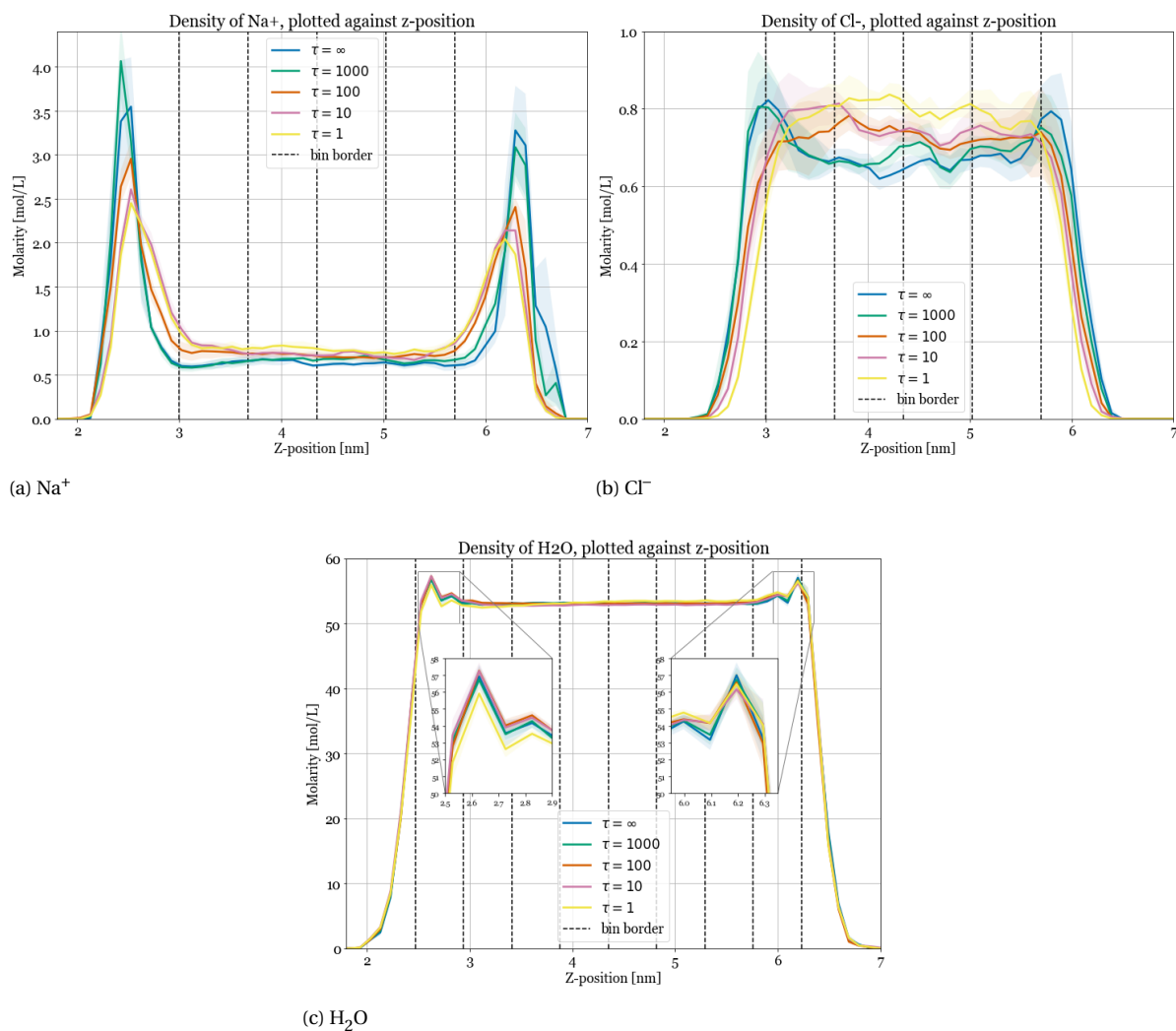


Figure C.9: Visualization of bins used for MSD calculation

C.4.2. Visualization of the curve-fitting range γ

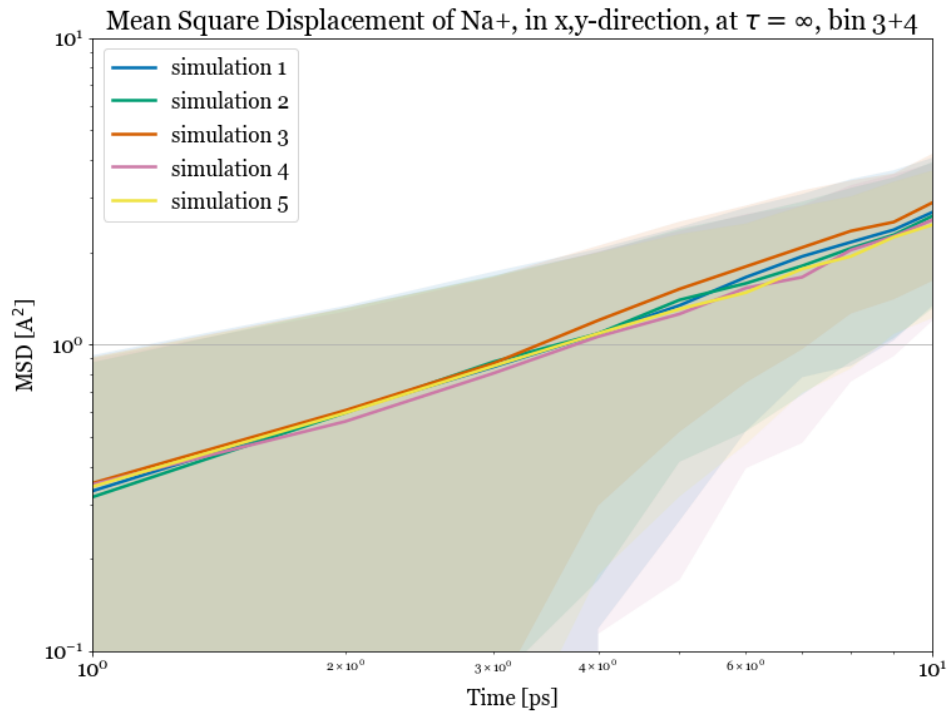
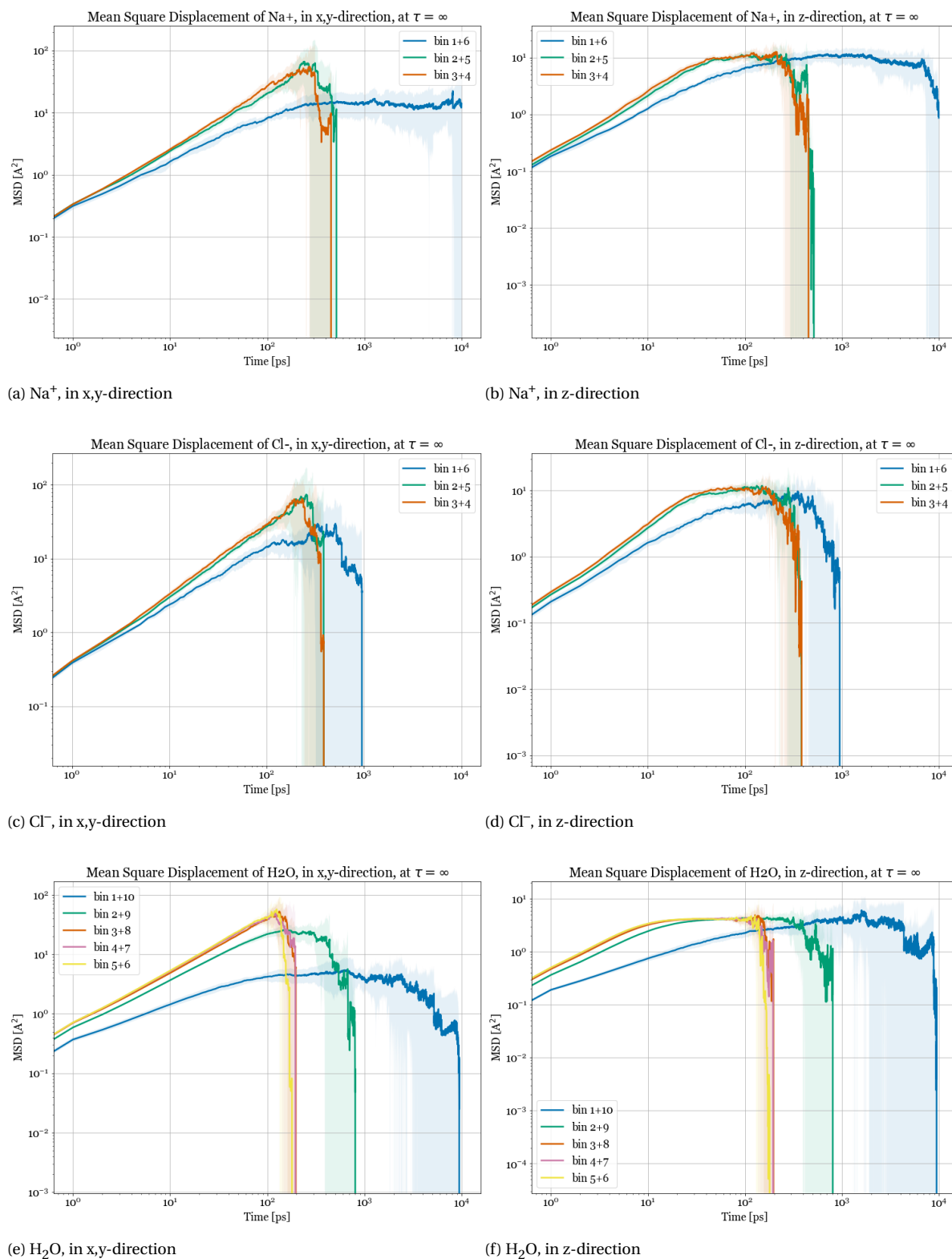
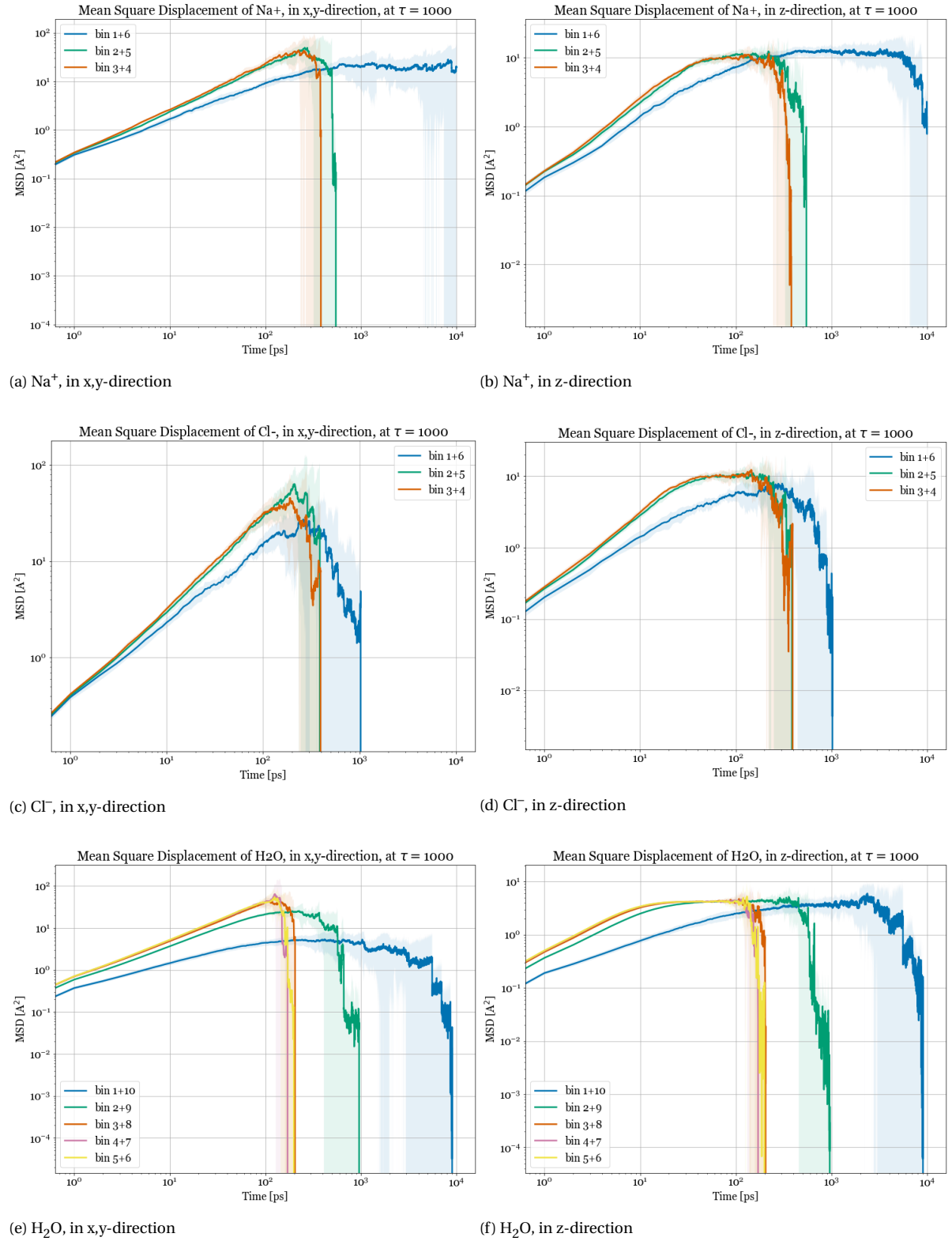
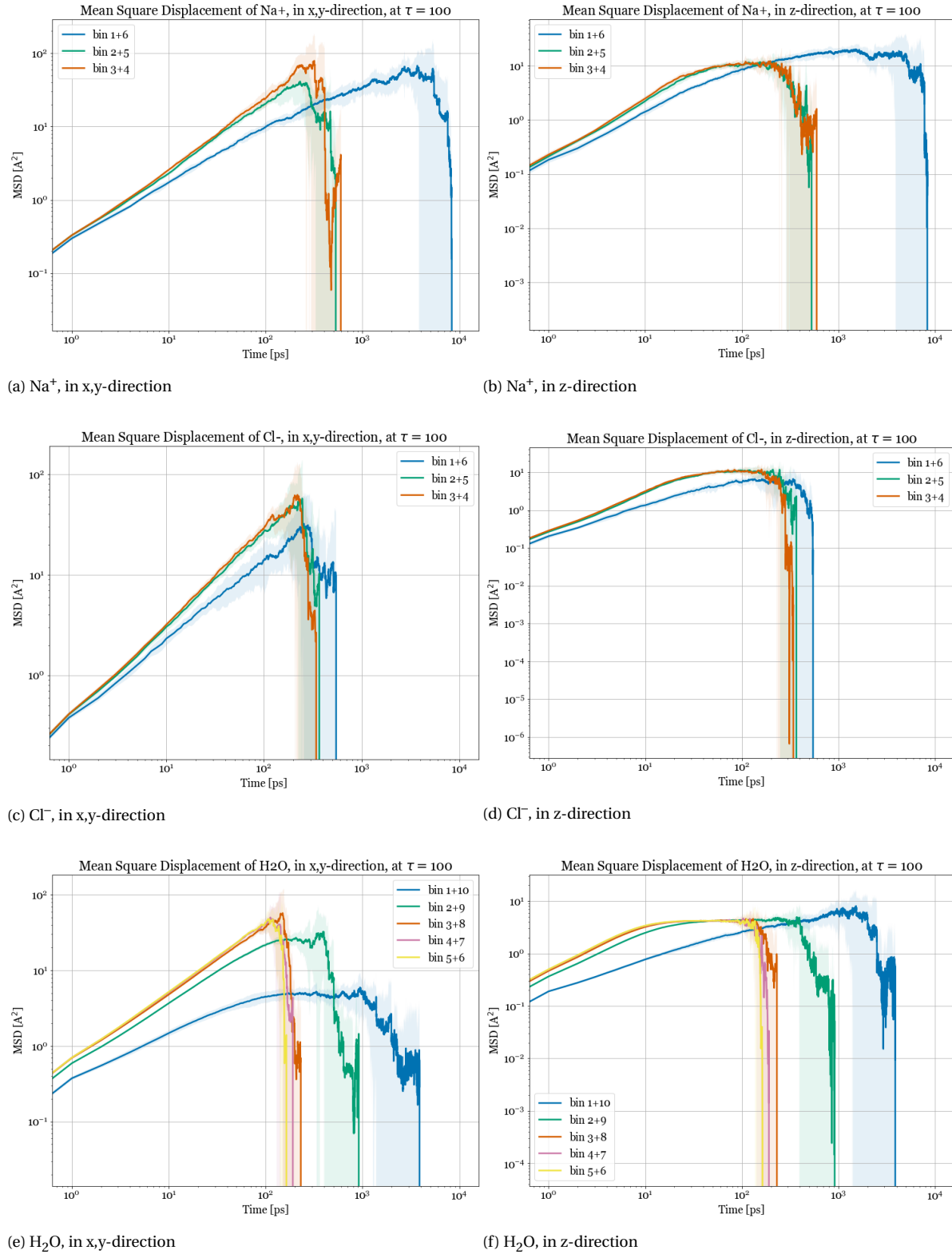


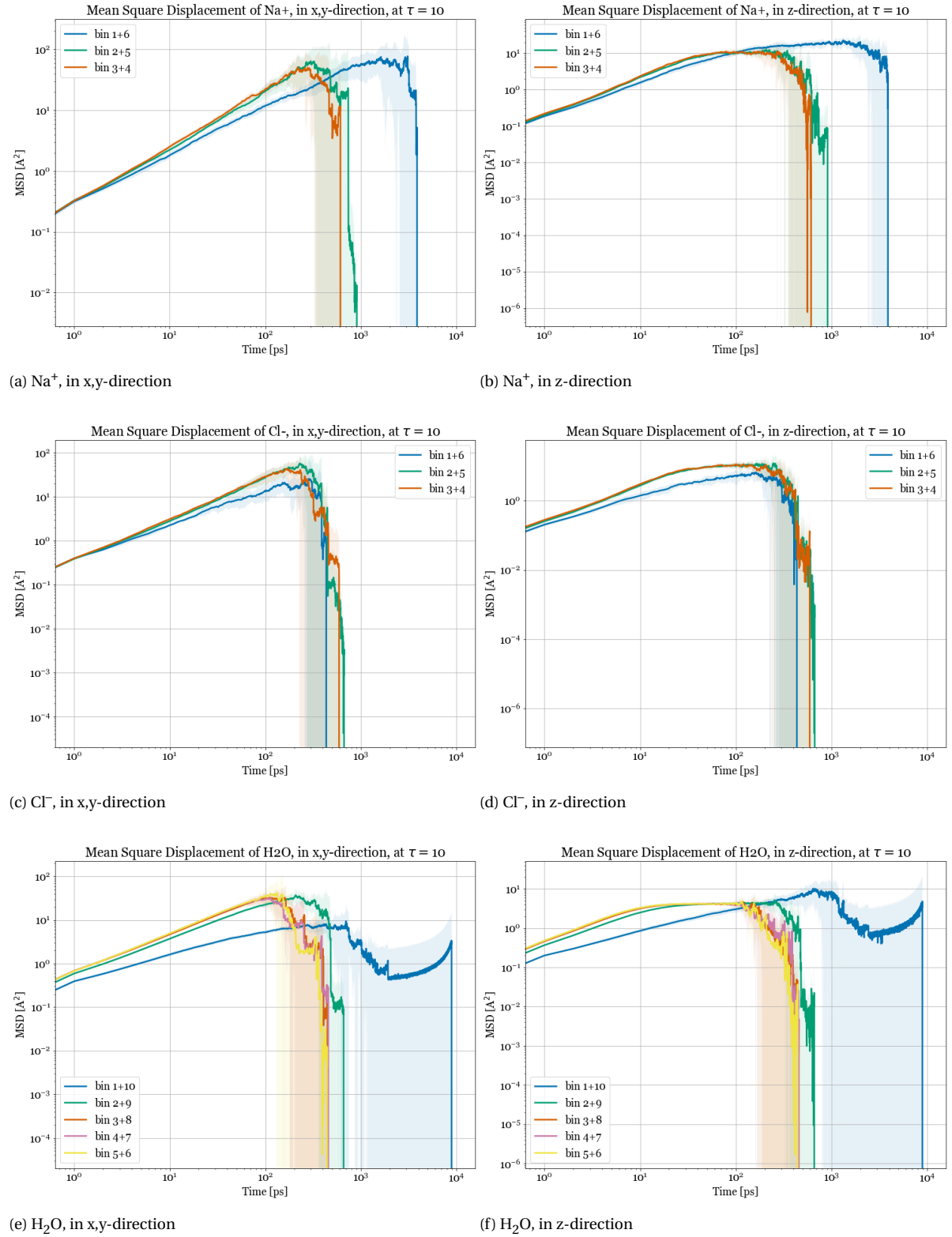
Figure C.10: Average MSD for Na⁺, x,y-direction, $\tau = \infty$, using range γ

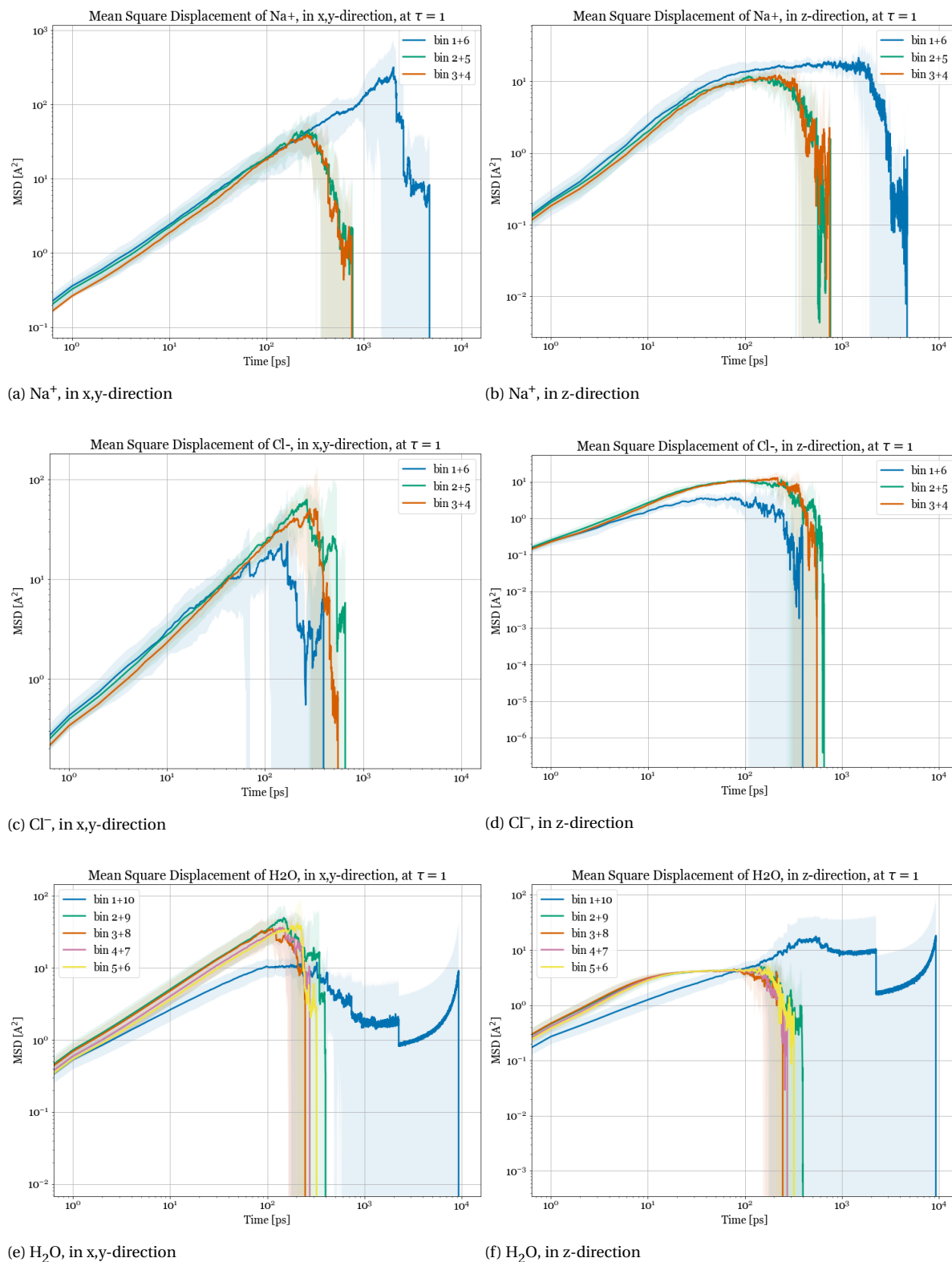
C.4.3. Average MSD plots

Figure C.11: Average MSD plot at $\tau = \infty$

Figure C.12: Average MSD plot at $\tau = 1000$

Figure C.13: Average MSD plot at $\tau = 100$

Figure C.14: Average MSD plot at $\tau = 10$

Figure C.15: Average MSD plot at $\tau = 1$

D

LAMMPS scripts

D.1. in.forcefield

```
##### FORCE FIELDS #####

pair_style lj/cut/coul/long 12.0 12.0

pair_modify mix arithmetic # tail yes # ATC + Lorentz-Berthelot
kspace_style ppm 1e-4
kspace_modify slab 3.0
bond_style harmonic
angle_style harmonic
dihedral_style none
improper_style none

special_bonds lj 0.0 0.0 1.0 coul 0.0 0.0 1.0 dihedral no

# Masses
#
mass 1 15.999000 # Ow
mass 2 1.008000 # Hw
mass 3 15.999000 # Ob
mass 4 28.085000 # Sib
mass 5 15.999000 # Od
mass 6 28.085000 # Sid
mass 7 28.085000 # Sidd
mass 8 15.999000 # Os
mass 9 28.085000 # Sis
mass 10 28.085000 # Siss
mass 11 1.008000 # Hs
mass 12 22.990000 # Na
mass 13 35.450000 # Cl

# Pair Coeffs
# epsilon, sigma
pair_coeff 1 1 0.155354 3.166000 # Ow Ow
pair_coeff 1 2 0.000000 2.083000 # Ow Hw
pair_coeff 1 3 0.091592 3.128700 # Ow Ob
pair_coeff 1 4 0.120199 3.431600 # Ow Sib
pair_coeff 1 5 0.137670 3.128700 # Ow Od
pair_coeff 1 6 0.120199 3.431600 # Ow Sid
pair_coeff 1 7 0.120199 3.431600 # Ow Sidd
pair_coeff 1 8 0.137670 3.128700 # Ow Os
pair_coeff 1 9 0.120199 3.431600 # Ow Sis
pair_coeff 1 10 0.120199 3.431600 # Ow Siss
pair_coeff 1 11 0.000000 2.066300 # Ow Hs
pair_coeff 1 12 0.234060 2.662769 # Ow Na
pair_coeff 1 13 0.044567 3.998226 # Ow Cl
pair_coeff 2 2 0.000000 1.000000 # Hw Hw
pair_coeff 2 3 0.000000 2.045700 # Hw Ob
pair_coeff 2 4 0.000000 2.348600 # Hw Sib
pair_coeff 2 5 0.000000 2.045700 # Hw Od
pair_coeff 2 6 0.000000 2.348600 # Hw Sid
pair_coeff 2 7 0.000000 2.348600 # Hw Sidd
pair_coeff 2 8 0.000000 2.045700 # Hw Os
pair_coeff 2 9 0.000000 2.348600 # Hw Sis
pair_coeff 2 10 0.000000 2.348600 # Hw Siss
pair_coeff 2 11 0.000000 0.983300 # Hw Hs
pair_coeff 2 12 0.000000 1.579769 # Hw Na
pair_coeff 2 13 0.000000 2.915226 # Hw Cl
pair_coeff 3 3 0.054000 3.091400 # Ob Ob
pair_coeff 3 4 0.070866 3.394300 # Ob Sib
pair_coeff 3 5 0.081166 3.091400 # Ob Od
pair_coeff 3 6 0.070866 3.394300 # Ob Sid
pair_coeff 3 7 0.070866 3.394300 # Ob Sidd
pair_coeff 3 8 0.081166 3.091400 # Ob Os
pair_coeff 3 9 0.070866 3.394300 # Ob Sis
pair_coeff 3 10 0.070866 3.394300 # Ob Siss
pair_coeff 3 11 0.000000 2.029000 # Ob Hs
pair_coeff 3 12 0.137995 2.625469 # Ob Na
pair_coeff 3 13 0.026275 3.960926 # Ob Cl
pair_coeff 4 4 0.093000 3.697200 # Sib Sib
pair_coeff 4 5 0.106518 3.394300 # Sib Od
pair_coeff 4 6 0.093000 3.697200 # Sib Sid
pair_coeff 4 7 0.093000 3.697200 # Sib Sidd
pair_coeff 4 8 0.106518 3.394300 # Sib Os
pair_coeff 4 9 0.093000 3.697200 # Sib Sis
pair_coeff 4 10 0.093000 3.697200 # Sib Siss
pair_coeff 4 11 0.000000 2.331900 # Sib Hs
pair_coeff 4 12 0.181096 2.928369 # Sib Na
pair_coeff 4 13 0.034482 4.263826 # Sib Cl
pair_coeff 5 5 0.122000 3.091400 # Od Od
pair_coeff 5 6 0.106518 3.394300 # Od Sid
pair_coeff 5 7 0.106518 3.394300 # Od Sidd
pair_coeff 5 8 0.122000 3.091400 # Od Os
pair_coeff 5 9 0.106518 3.394300 # Od Sis
pair_coeff 5 10 0.106518 3.394300 # Od Siss
pair_coeff 5 11 0.000000 2.029000 # Od Hs
pair_coeff 5 12 0.207418 2.625469 # Od Na
pair_coeff 5 13 0.039494 3.960926 # Od Cl
pair_coeff 6 6 0.093000 3.697200 # Sid Sid
pair_coeff 6 7 0.093000 3.697200 # Sid Sidd
pair_coeff 6 8 0.106518 3.394300 # Sid Os
pair_coeff 6 9 0.093000 3.697200 # Sid Sis
pair_coeff 6 10 0.093000 3.697200 # Sid Siss
pair_coeff 6 11 0.000000 2.331900 # Sid Hs
pair_coeff 6 12 0.181096 2.928369 # Sid Na
pair_coeff 6 13 0.034482 4.263826 # Sid Cl
pair_coeff 7 7 0.093000 3.697200 # Sidd Sidd
pair_coeff 7 8 0.106518 3.394300 # Sidd Os
pair_coeff 7 9 0.093000 3.697200 # Sidd Sis
pair_coeff 7 10 0.093000 3.697200 # Sidd Siss
pair_coeff 7 11 0.000000 2.331900 # Sidd Hs
pair_coeff 7 12 0.181096 2.928369 # Sidd Na
pair_coeff 7 13 0.034482 4.263826 # Sidd Cl
pair_coeff 8 8 0.122000 3.091400 # Os Os
pair_coeff 8 9 0.106518 3.394300 # Os Sis
pair_coeff 8 10 0.106518 3.394300 # Os Siss
pair_coeff 8 11 0.000000 2.029000 # Os Hs
pair_coeff 8 12 0.207418 2.625469 # Os Na
pair_coeff 8 13 0.039494 3.960926 # Os Cl
pair_coeff 9 9 0.093000 3.697200 # Sis Sis
pair_coeff 9 10 0.093000 3.697200 # Sis Siss
pair_coeff 9 11 0.000000 2.331900 # Sis Hs
pair_coeff 9 12 0.181096 2.928369 # Sis Na
pair_coeff 9 13 0.034482 4.263826 # Sis Cl
pair_coeff 10 10 0.093000 3.697200 # Siss Siss
pair_coeff 10 11 0.000000 2.331900 # Siss Hs
pair_coeff 10 12 0.181096 2.928369 # Siss Na
pair_coeff 10 13 0.034482 4.263826 # Siss Cl
pair_coeff 11 11 0.000000 0.966600 # Hs Hs
pair_coeff 11 12 0.000000 1.563069 # Hs Na
pair_coeff 11 13 0.000000 2.898526 # Hs Cl
pair_coeff 12 12 0.352642 2.159538 # Na Na
pair_coeff 12 13 0.067146 3.494996 # Na Cl
```

```

pair_coeff 13 13 0.012785 4.830453 # Cl Cl

# Bond Coeffs
#
bond_coeff 1 1000.000000 1.000000 # O-Hw
bond_coeff 2 285.000000 1.680000 # SiO
bond_coeff 3 1000 0.945000 # OH #stiffness changed from 495.000000

# Angle Coeffs
#
angle_coeff 1 1000.000000 109.470000 # HwOwHw
angle_coeff 2 100.000000 149.000000 # SiOSi
angle_coeff 3 100.000000 109.500000 # OSiO
angle_coeff 4 50.000000 115.000000 # SiOH

```

```
# Charges of the atoms
```

```

set type 1 charge -0.847600 # Ow
set type 2 charge 0.423800 # Hw
set type 3 charge -0.550000 # Ob
set type 4 charge 1.100000 # Sib
set type 5 charge -0.900000 # Od
set type 6 charge 0.725000 # Sid
set type 7 charge 0.350000 # Sids
set type 8 charge -0.675000 # Os
set type 9 charge 1.100000 # Sis
set type 10 charge 1.100000 # Siss
set type 11 charge 0.400000 # Hs
set type 12 charge 1.000000 # Na
set type 13 charge -1.000000 # Cl

```

D.2. in.simulation

D.2.1. Initialization

```

shell mkdir outputs
log outputs/out1.log
shell rm log.lammps
#####
# initialization
##### SETTING UP #####

units real
dimension 3
newton on
boundary p p f
atom_style full

#-----INPUT-----#
read_data inputs/in.lammpsdata
include inputs/in.forcefield
#-----#

variable Temp equal 298      # Temperature in K
variable Pres equal 1.0      # Pressure in atm.
variable timestep equal 1.0  # fs

run_style verlet

neighbor 2.0 bin
neigh_modify every 1 delay 0 check yes # rebuilt list every step,
do not delay, rebuilt if atom has moved half the skin distance or more

variable Nthermo equal 1000  # every 1 ps give themodata
thermo_style one
thermo ${Nthermo}

variable Ndump equal 1000 # every 1 ps dump trj
dump trj all dcd ${Ndump} outputs/out.dcd
dump_modify trj unwrap yes

#dump trj all custom ${Ndump} outputs/out.lammpstrj id type xu yu zu
#dump_modify trj sort 1
#dump_modify trj append yes
#dump_modify trj format line "%8d %5d %.3f %.3f %.3f %.3f"

##### INITIALIZATION #####

print ""
print "SURFACE CHARGE"
print ""

variable numSC loop 16      # Number of deprotonated sites
variable qHd equal 0
variable qOd equal -0.9
variable qSid equal 0.725
variable Hsc file inputs/H_surfacecharge.dat # files of atom IDs
variable Osc file inputs/O_surfacecharge.dat
variable Sisc file inputs/Si_surfacecharge.dat
#LOOP
label loop1
set atom ${Hsc} charge ${qHd} # set atom charges to deprotonated
set atom ${Osc} charge ${qOd}
set atom ${Sisc} charge ${qSid}
next numSC # take next deprotonated site number
next Hsc Osc Sisc
jump in.simulation loop1 #jump back up to start loop again

print ""
print "FIXES"
print ""

group SHAKE type 1 2 8 11

```

```

region BLOCK1 block -1000 1000 -1000 1000 -1000 -35
region BLOCK2 block -1000 1000 -1000 1000 35 1000
group REGION1 region BLOCK1
group REGION2 region BLOCK2
group RIGID type 3 4
group RIGID1 intersect RIGID REGION1
group RIGID2 intersect RIGID REGION2
group ALL type 1 2 3 4 5 6 7 8 9 10 11 12 13

```

```

variable n1 equal count(RIGID1) # pressure through walls
variable n2 equal count(RIGID2)
variable area equal (1.0*(yhi-ylo)*(xhi-xlo))
variable pressure equal 0.101325*${Pres} # in MPa
variable force1 equal v_pressure*0.00014393*v_area/v_n1
# 69.4786 pN = 1 Kcal/mol-Angstrom
variable force2 equal -v_pressure*0.00014393*v_area/v_n2
# 1MPa = 0.00014393 Kcal/mol-Angstrom^3

```

```

fix 0 SHAKE shake 1.0e-6 1000 0 b 1 3 a 1
fix 1 RIGID1 aveforce NULL NULL v_force1
fix 2 RIGID2 aveforce NULL NULL v_force2
fix 3 RIGID momentum 1 linear 0 0 1
fix 4 RIGID1 momentum 1 linear 1 1 0
fix 5 RIGID2 momentum 1 linear 1 1 0

```

```

print ""
print "ELIMINATING OVERLAP"
print ""

```

```

variable Ninit equal 1000000
variable Nequi equal 1000000 # 1 ns

```

```

timestep ${0.0001*v_timestep}
fix 6 ALL nvt temp ${Temp} ${Temp} $(1000000*dt)
run ${Ninit}
unfix 6

```

```

timestep ${0.001*v_timestep}
fix 6 ALL nvt temp ${Temp} ${Temp} $(100000*dt)
run ${Ninit}
unfix 6

```

```

timestep ${0.01*v_timestep}
fix 6 ALL nvt temp ${Temp} ${Temp} $(10000*dt)
run ${Ninit}
unfix 6

```

```

timestep ${0.1*v_timestep}
fix 6 ALL nvt temp ${Temp} ${Temp} $(1000*dt)
run ${Ninit}
unfix 6

```

```

timestep ${0.2*v_timestep}
fix 6 ALL nvt temp ${Temp} ${Temp} $(100*dt)
run ${Ninit}
unfix 6

```

```

timestep ${0.4*v_timestep}
fix 6 ALL nvt temp ${Temp} ${Temp} $(100*dt)
run ${Ninit}
unfix 6

```

```

timestep ${0.6*v_timestep}
fix 6 ALL nvt temp ${Temp} ${Temp} $(100*dt)
run ${Ninit}
unfix 6

```

```
timestep ${0.8*v_timestep}
```

```
fix 6 ALL nvt temp ${Temp} ${Temp} $(100*dt)
run ${Ninit}
unfix 6

timestep ${tstep}
fix 6 ALL nvt temp ${Temp} ${Temp} $(100*dt)
```

D.2.2. Production

```
shell mkdir outputs
log outputs/out1.log
shell rm log.lammps
#####
# production k=1000 (every 1000 ps = 1 ns)
##### SETTING UP #####

units real
dimension 3
newton on
boundary p p f
atom_style full

#-----INPUT-----#
read_data inputs/min.lammpsdata
include inputs/in.forcefield

reset_timestep 0 # set timestep counter to x

variable Nprod equal 10000000 # 10 ns
variable reacttime equal 1000000
# react every 1000000 timesteps = 1000 ps = 1 ns
# !CAN NEVER BE SMALLER THAN TRANSITTIME!
#-----#

variable Temp equal 298 # Temperature in K
variable Pres equal 1.0 # Pressure in atm.
variable tstep equal 1.0 # ifs

run_style verlet

neighbor 2.0 bin
neigh_modify every 1 delay 0 check yes # rebuilt list every step,
do not delay, rebuilt if atom has moved half the skin distance or more

variable Nthermo equal 1000 # every 1 ps give themodata
thermo_style one
thermo ${Nthermo}

variable Ndump equal 1000 # every 1 ps dump trj
dump VMD all dcd ${Ndump} outputs/out.dcd
dump_modify VMD unwrap yes

variable Niondump equal 50 # every 50 fs dump Ow, Na, Cl
group ION type 1 12 13
dump ions ION dcd ${Niondump} outputs/ions.dcd
dump_modify ions unwrap yes

##### INITIALIZATION #####

print ""
print "FIXES"
print ""

group SHAKE type 1 2 8 11
region BLOCK1 block -1000 1000 -1000 1000 -1000 -32
region BLOCK2 block -1000 1000 -1000 1000 32 1000
group REGION1 region BLOCK1
group REGION2 region BLOCK2
group RIGID type 3 4
group RIGID1 intersect RIGID REGION1
group RIGID2 intersect RIGID REGION2
group ALL type 1 2 3 4 5 6 7 8 9 10 11 12 13
group SIM subtract ALL RIGID1 RIGID2

timestep ${tstep}

fix 0 SHAKE shake 1.0e-6 1000 0 b 1 3 a 1
fix 1 SIM nvt temp ${Temp} ${Temp} $(100*dt)

##### SIMULATION #####

print ""
print "SETTING VARIABLES"
print ""

variable transittime equal 1000
variable statictime equal ${reacttime}-${transittime}
variable numreactionsint equal ceil(${Nprod}/${reacttime})
```

```
run ${Ninit}

run ${Nequi}

write_data outputs/min.lammpsdata nocoeff

quit

variable numreactions loop ${numreactionsint}

variable qHp equal 0.4 # partrial charges
variable qHd equal 0
variable qOp equal -0.675
variable qOd equal -0.9
variable qSip equal 1.1
variable qSid equal 0.725
variable qSidd equal 0.35

variable Hpl file inputs/which_H_protonates.left
variable Opl file inputs/which_O_protonates.left
variable Sipl file inputs/which_Si_protonates.left
variable Cpl file inputs/charge_of_protonating_Si.left
variable Hdl file inputs/which_H_deprotonates.left
variable Odl file inputs/which_O_deprotonates.left
variable Sidl file inputs/which_Si_deprotonates.left
variable Cdl file inputs/charge_of_deprotonating_Si.left
variable Hpr file inputs/which_H_protonates.right
variable Opr file inputs/which_O_protonates.right
variable Sipr file inputs/which_Si_protonates.right
variable Cpr file inputs/charge_of_protonating_Si.right
variable Hdr file inputs/which_H_deprotonates.right
variable Odr file inputs/which_O_deprotonates.right
variable Sidr file inputs/which_Si_deprotonates.right
variable Cdr file inputs/charge_of_deprotonating_Si.right

log outputs/out2.log

print ""
print "PRODUCTION"
print ""

#LOOP
label loop2
print "numreactions="
print ${numreactions}

timestep ${tstep}
run ${statictime}
#run with current static surface configuration

variable startstep equal step
# set transition variables for H and O for this loop
variable Htp atom ${qHd}+(${qHp}-${qHd})*(step-${startstep})/
${transittime}
variable Otp atom ${qOd}+(${qOp}-${qOd})*(step-${startstep})/
${transittime}
variable Htd atom ${qHp}+(${qHd}-${qHp})*(step-${startstep})/
${transittime}
variable Otd atom ${qOp}+(${qOd}-${qOp})*(step-${startstep})/
${transittime}
# set charge variables for Si for this loop
if "${Cpl}" == "${qSip}" then &
"variable Sitpl atom ${qSid}+(${qSip}-${qSid})
*(step-${startstep})/${transittime}" &
elif "${Cpl}" == "${qSid}" &
"variable Sitpl atom ${qSidd}+(${qSid}-${qSidd})
*(step-${startstep})/${transittime}" &
if "${Cdl}" == "${qSid}" then &
"variable Sitdl atom ${qSip}+(${qSid}-${qSip})
*(step-${startstep})/${transittime}" &
elif "${Cdl}" == "${qSidd}" &
"variable Sitdl atom ${qSid}+(${qSidd}-${qSid})
*(step-${startstep})/${transittime}" &
if "${Cpr}" == "${qSip}" then &
"variable Sitpr atom ${qSid}+(${qSip}-${qSid})
*(step-${startstep})/${transittime}" &
elif "${Cpr}" == "${qSid}" &
"variable Sitpr atom ${qSidd}+(${qSid}-${qSidd})
*(step-${startstep})/${transittime}" &
if "${Cdr}" == "${qSid}" then &
"variable Sitdr atom ${qSip}+(${qSid}-${qSip})
*(step-${startstep})/${transittime}" &
elif "${Cdr}" == "${qSidd}" &
"variable Sitdr atom ${qSid}+(${qSidd}-${qSid})
*(step-${startstep})/${transittime}" &
set atom ${Hpl} charge v_Htp
set atom ${Opl} charge v_Otp
set atom ${Hdl} charge v_Htd
```

```

set atom ${Odl} charge v_Otd
set atom ${Hpr} charge v_Htp
set atom ${Opr} charge v_Otp
set atom ${Hdr} charge v_Htd
set atom ${Odr} charge v_Otd
set atom ${Sipl} charge v_Sitpl
set atom ${Sidl} charge v_Sitdl
set atom ${Sipr} charge v_Sitpr
set atom ${Sidr} charge v_Sitdr

run ${transittime} pre no post no
# run for transittime to ramp up/down charges

set atom ${Hpl} charge ${qHp} # set charges to static values
set atom ${Opl} charge ${qOp}
set atom ${Sipl} charge ${qCpl}
set atom ${Hdl} charge ${qHd}
set atom ${Odl} charge ${qOd}
set atom ${Sidl} charge ${qCdl}
set atom ${Hpr} charge ${qHp}

```

```

set atom ${Opr} charge ${qOp}
set atom ${Sipr} charge ${qCpr}
set atom ${Hdr} charge ${qHd}
set atom ${Odr} charge ${qOd}
set atom ${Sidr} charge ${qCdr}

variable startstep delete
next numreactions
# take next atoms that react from lists + next reaction number
next Hpl Opl Sipl Hdl Odl Sidl Hpr
Opr Sipr Hdr Odr Sipr Cpl Cdl Cpr Cdr

jump in.simulation loop2 # jump back up to start loop again

print ""
print "OUTPUT"
print ""

write_data outputs/out.lammpsdata nocoeff

quit

```




Python scripts

E.1. Creating initialization input files

```
#!/usr/bin/env

import numpy
from PyMD.IO import write_lammpsdata, read_lammpsdata
from PyMD.functions import add_water
from PyMD.System import System, Box
import argparse
from random import randint, seed

if __name__ == '__main__':

    parser = argparse.ArgumentParser()

    parser.add_argument('--fin', type=str)
    parser.add_argument('--charge', type=str)
    parser.add_argument('--seed', type=str)
    parser.add_argument('--style', type=str)

    args = parser.parse_args()

    if args.style == None:
        args.style = 'default'

    ##% uncomment for parser arguments
    # system = read_lammpsdata(args.fin, style=args.style) # read file
    # C = int(args.charge)
    # randseed = args.seed

    ##% uncomment for manual input arguments
    system = read_lammpsdata("outputs\\in.lammpsdata", style='default')
    C = -100 # charge density mC/m^2
    randseed = 1238

    ##% setting up the surface charge
    area = system.box.lengths[0]*system.box.lengths[1]
    # area of one wall in A^2
    area_conversion = 10**(-20)
    # (1 m^-2 = 10^-20 A^-2)
    electron_conversion = 6.24150975*10**18
    # (1 C = 6.24150975*10^18 e)
    charge = C*10**(-3)*area_conversion*electron_conversion # in e/A^2
    n_deprotonated = round(-charge*area)
    # rounded number of deprotonated sites per wall

    print(int(n_deprotonated), "deprotonated sites per wall needed")
    if -charge*area % 1 < 0.5:
        print("Number of deprotonated sites rounded down,
        surface charge is less negative than", C, "mC/m^2, pH is lower")
    elif -charge*area % 1 > 0.5:
        print("Number of deprotonated sites rounded up,
        surface charge is more negative than", C, "mC/m^2, pH is higher")
    left = numpy.where(system.pos[:, 2] < 0)[0]+1 # all left atoms
    right = numpy.where(system.pos[:, 2] > 0)[0]+1 # all right atoms
    Hs = numpy.where(system.types == 11)[0]+1 # all atoms of type 11=Hs

    bonds_OH = numpy.where(system.bonds[:,0] == 3)[0]
    # indices of all silanol O-H bonds = type 3
    bonds_SiO = numpy.where(system.bonds[:,0] == 2)[0]
    # indices of all silanol Si-O bonds = type 2

    SiOH = []
    SiOH_left = []
    SiOH_right = []

    for i in bonds_OH:
        a = system.bonds[i,1] # first atom
        b = system.bonds[i,2] # second atom
        if a in Hs:
            H_i = a
            O_i = b
        elif b in Hs:
            H_i = b
            O_i = a
        else:
            print("ERROR: Atom not found in list")
    for j in bonds_SiO:
        c = system.bonds[j,1] # first atom
        d = system.bonds[j,2] # second atom
        if O_i == c: # O is first atom
            Si_i = d
        elif O_i == d: # O is second atom
            Si_i = c
        SiOH.append([Si_i, O_i, H_i])
    SiOH = numpy.asarray(SiOH)

    for i in range(len(SiOH)):
        if SiOH[i,0] in left: # Si atom in left set
            SiOH_left.append(SiOH[i,:])
        elif SiOH[i,0] in right: # Si atom in right set
            SiOH_right.append(SiOH[i,:])
        else:
            print("ERROR: Atom not found in left or right set")

    SiO_left = []
    SiO_right = []
    ##%
    seed(int(randseed))
    for s in range(int(n_deprotonated)):
        index = randint(0, len(SiOH_left)-1)
    # choose random left silanol
    ID = SiOH_left.pop(index)
    # delete from list
    SiO_left.append(ID)
    # add to deprotonated list
    index = randint(0, len(SiOH_right)-1)
    ID = SiOH_right.pop(index)
    SiO_right.append(ID)
    ##% no double dangling silanols (for simplicity)
    SiO_left = numpy.asarray(SiO_left)
    SiO_right = numpy.asarray(SiO_right)

    Siss = numpy.where(system.types == 10)[0]+1
    # all atoms of type 10=Siss
    Siss = numpy.c_[Siss, numpy.zeros(len(Siss), dtype='>i4')]

    for i in range(len(Siss)):
        if Siss[i,0] in SiO_right[:,0]:
            Siss[i,1] -= 1
        elif Siss[i,0] in SiO_left[:,0]:
            Siss[i,1] -= 1
    for i in Siss[:,1]:
```

```

if i < -1:
    print("ERROR: two silanols of a geminal are deprotonated
    in surface charge input file, try different random seed")

%% writing output files
file_Si = open("outputs\Si_surfacecharge.dat", "w")
file_O = open("outputs\O_surfacecharge.dat", "w")
file_H = open("outputs\H_surfacecharge.dat", "w")
for i in range(len(SiO_left)):
    Si_sc = numpy.asarray(SiO_left[i])[0]
    O_sc = numpy.asarray(SiO_left[i])[1]
    H_sc = numpy.asarray(SiO_left[i])[2]
    file_Si.write("{}\n".format(Si_sc))
    file_O.write("{}\n".format(O_sc))
    file_H.write("{}\n".format(H_sc))
for i in range(len(SiO_right)):

```

```

Si_sc = numpy.asarray(SiO_right[i])[0]
O_sc = numpy.asarray(SiO_right[i])[1]
H_sc = numpy.asarray(SiO_right[i])[2]
file_Si.write("{}\n".format(Si_sc))
file_O.write("{}\n".format(O_sc))
file_H.write("{}\n".format(H_sc))
print("Surface charge initialization data files written")
file_Si.close()
file_O.close()
file_H.close()

```

E.2. Creating (de)protonation events input files

```
#!/usr/bin/env
```

```

import numpy
from PyMD.IO import write_lammpsdata, read_lammpsdata
from PyMD.functions import add_water
from PyMD.System import System, Box
import argparse
from random import randint, seed

if __name__ == '__main__':

    parser = argparse.ArgumentParser()

    parser.add_argument('--fin', type=str)
    parser.add_argument('--deprotonatedOfile', type=str)
    # text file with atom numbers of deprotonated O
    parser.add_argument('--seed', type=str)
    parser.add_argument('--steps', type=str)
    parser.add_argument('--k_iso', type=str) # optional
    parser.add_argument('--k_gem', type=str) # optional
    parser.add_argument('--k_vic', type=str) # optional
    parser.add_argument('--style', type=str) # optional

```

```

args = parser.parse_args()

if args.style == None:
    args.style = 'default'
if args.k_iso == None:
    args.k_iso = 1
if args.k_gem == None:
    args.k_gem = 1
if args.k_vic == None:
    args.k_vic = 1

%% uncomment for parser arguments
# system = read_lammpsdata(args.fin, style=args.style)
# file = open(args.deprotonatedOfile, "r")
# randseed = args.seed
# steps = args.steps
# k_iso = args.k_iso # ratio in integers
# k_gem = args.k_gem
# k_vic = args.k_vic

```

```

%% uncomment for manual input arguments
system = read_lammpsdata(
"W:\1235\Initialization\outputs\min.lammpsdata",
style='default')
file = open(
r"W:\1235\Initialization\inputs\O_surfacecharge.dat", "r")
#file = open("outputs\O_1238_50.dat", "r")
randseed = 1238
steps = 20000
k_iso = 1 # ratio in integers
k_gem = 1
k_vic = 1

```

```

%% make SiOH array
left = numpy.where(system.pos[:, 2] < 0)[0]+1 # all left atoms
right = numpy.where(system.pos[:, 2] > 0)[0]+1 # all right atoms
Hs = numpy.where(system.types == 11)[0]+1 # all atoms of type 11=Hs
Os = numpy.where(system.types == 8)[0]+1 # all atoms of type 8=Os
Sib = numpy.where(system.types == 4)[0]+1 # all atoms of type 4=SiB
Si_sil = numpy.append((numpy.where(system.types == 9)[0]+1),
(numpy.where(system.types == 10)[0]+1))
# all atom numbers of Si atoms that are part of a silanol

bonds_OH = numpy.where(system.bonds[:, 0] == 3)[0]
# indices of all silanol O-H bonds = type 3
bonds_SiO = numpy.where(system.bonds[:, 0] == 2)[0]

```

```
# indices of all silanol Si-O bonds = type 2
```

```

SiOH = []
for i in bonds_OH:
    a = system.bonds[i, 1] # first atom
    b = system.bonds[i, 2] # second atom
    if a in Hs:
        H_i = a
        O_i = b
    elif b in Hs:
        H_i = b
        O_i = a
    else:
        print("ERROR: Atom not found in list")
    for j in bonds_SiO:
        c = system.bonds[j, 1] # first atom
        d = system.bonds[j, 2] # second atom
        if O_i == c: # 0 is first atom
            Si_i = d
        elif O_i == d: # 0 is second atom
            Si_i = c
        SiOH.append([Si_i, O_i, H_i, 0])
# add column for probability
SiOH = numpy.asarray(SiOH)

%% assign isolated/geminal/vicinal status
Siss = numpy.where(system.types == 10)[0]+1
# all atoms of type 10=Siss (geminal)
for i in range(len(SiOH)):
    #print("Si atom number", SiOH[i, 0])
    if SiOH[i, 0] in Siss: # if Si is part of geminal
        SiOH[i, 3] = k_gem
        #print("geminal")
    elif SiOH[i, 0] not in Siss:
        bonds = numpy.append(numpy.where(
system.bonds[:, 1] == SiOH[i, 0])[0],
numpy.where(system.bonds[:, 2] == SiOH[i, 0])[0])
        # indices of the bonds where Si atom is present
        #print("bonds=", bonds)
        bridge = []
        # empty list for atom numbers of bridge atoms
        check = []
        for j in bonds:
            a = system.bonds[j, 1] # first atom
            b = system.bonds[j, 2] # second atom
            #print("a=", a, "b=", b)
            if a not in Os and b not in Os:
                # discard the silanol bond
                if a == SiOH[i, 0]:
                    bridge = numpy.append(bridge, b)
                    # add atom number of bonded atom
                elif b == SiOH[i, 0]:
                    bridge = numpy.append(bridge, a)
                    # add atom number of bonded atom
                #print("bridge=", bridge)
            for k in bridge:
                bonds_2 = numpy.append(numpy.where(
system.bonds[:, 1] == k)[0],
numpy.where(system.bonds[:, 2] == k)[0])
                # indices of the bonds where the
                # bridge oxygen atom is present
                #print("bonds_2=", bonds_2)
            for l in bonds_2:
                a = system.bonds[l, 1] # first atom
                b = system.bonds[l, 2] # second atom
                #print("a=", a, "b=", b)
                if a != SiOH[i, 0] and b != SiOH[i, 0]:
                    # discard original Si
                    if a == k:

```

```

        check = numpy.append(check,b)
        # find atom number to check
    elif b == k:
        check = numpy.append(check,a)
        # find atom number to check
    #print("check=",check)
    vic = 0
    for m in check:
        if m in Si_sil:
            vic += 1
    if vic == 0:
        SiOH[i,3] = k_iso
        #print("isolated")
    elif vic != 0:
        SiOH[i,3] = k_vic
        #print("vicinal")

%% make SiO list
Od = file.readlines()      # read deprotonated Os
file.close()
Od = [i.split() for i in Od]
Od = numpy.asarray(Od)

dep = []
for i in range(len(Od)):
    s = int(Od[i])
    index = numpy.where(SiOH[:,1] == s)[0]
    # index where Od is in SiOH list
    ID = SiOH[index]
    # save that row
    SiOH = numpy.delete(SiOH,index,axis=0)
    # delete that row for SiOH list
    dep.append(ID)
    # add to SiO list
    SiO = numpy.zeros([len(dep),4],dtype='>i4')
    # make empty list for deprotonated SiOH
    for i in range(len(dep)):
        # SiO as numpy array
        SiO[i,:] = dep[i]

%% account for geminal silanols
Siss = numpy.where(system.types == 10)[0]+1
# all atoms of type 10=Siss
Siss = numpy.c_[Siss,numpy.zeros(
    len(Siss),dtype='>i4')]
# add row for charge
for i in range(len(Siss)):
    if Siss[i,0] in SiO[:,0]:
        Siss[i,1] -= 1

%% make left and right lists
SiOH_left = []
SiOH_right = []
for i in range(len(SiOH)):
    if SiOH[i,0] in left:      # Si atom in left set
        SiOH_left.append(SiOH[i,:])
    elif SiOH[i,0] in right:  # Si atom in right set
        SiOH_right.append(SiOH[i,:])
    else:
        print("ERROR: Atom not found in left or right set")

SiO_left = []
SiO_right = []
for i in range(len(SiO)):
    if SiO[i,0] in left:      # Si atom in left set
        SiO_left.append(SiO[i,:])
    elif SiO[i,0] in right:   # Si atom in right set
        SiO_right.append(SiO[i,:])
    else:
        print("ERROR: Atom not found in left or right set")

%% assign different probability
for i in range(len(SiO_left)):
    # silanols with higher probability appear more times in the list
    k = SiO_left[i][3]
    for j in range(0,k-1):
        SiO_left.append(SiO_left[i])
for i in range(len(SiOH_left)):
    # silanols with higher probability appear more times in the list
    k = SiOH_left[i][3]
    for j in range(0,k-1):
        SiOH_left.append(SiOH_left[i])
for i in range(len(SiO_right)):
    # silanols with higher probability appear more times in the list
    k = SiO_right[i][3]
    for j in range(0,k-1):
        SiO_right.append(SiO_right[i])
for i in range(len(SiOH_right)):
    # silanols with higher probability appear more times in the list
    k = SiOH_right[i][3]
    for j in range(0,k-1):
        SiOH_right.append(SiOH_right[i])

%% (de)protonate
seed(int(randseed))

deprotonated_left = []
protonated_left = []

for s in range(int(steps)):
    indexd = randint(0, len(SiOH_left)-1)
    # choose random left SiOH to deprotonate
    if SiOH_left[indexd][0] in Siss[:,0]:
        Siss[numpy.where(Siss[:,0] ==
            SiOH_left[indexd][0])[0],1] -= 1
    # reduce charge of Si
    charged = Siss[numpy.where(Siss[:,0] ==
        SiOH_left[indexd][0])[0],1]
    elif SiOH_left[indexd][0] not in Siss[:,0]:
        charged = -1
    else:
        print("ERROR")
    indexp = randint(0, len(SiO_left)-1)
    # choose random left SiO to protonate
    if SiO_left[indexp][0] in Siss[:,0]:
        # if silanol is part of geminal
        Siss[numpy.where(Siss[:,0] ==
            SiO_left[indexp][0])[0],1] += 1
    # charge of Si +1
    chargep = Siss[numpy.where(Siss[:,0] ==
        SiO_left[indexp][0])[0],1]
    elif SiO_left[indexp][0] not in Siss[:,0]:
        chargep = 0

    Od_index = SiOH_left[indexd][1]
    # atom number of deprotonating oxygen
    #print("length=",len(SiOH_left))
    indices = [] # indices of items to be removed
    for i in range(len(SiOH_left)):
        #print("i=",i)
        if SiOH_left[i][1] == Od_index:
            indices.append(i)
        #print("indicesd",indices)
    for j in sorted(indices, reverse=True):
        #print("j=",j)
        IDd = SiOH_left.pop(j)
    # delete that row from left SiOH
    #print("IDd=",IDd)
    SiO_left.append(IDd)
    # append deprotonated row to SiO

    Op_index = SiO_left[indexp][1]
    # atom number of protonating oxygen
    #print("length=",len(SiO_left))
    indices = [] # indices of items to be removed
    for i in range(len(SiO_left)):
        #print("i=",i)
        if SiO_left[i][1] == Op_index:
            indices.append(i)
        #print("indicesp",indices)
    for j in sorted(indices, reverse=True):
        #print("j=",j)
        IDp = SiO_left.pop(j)
    # delete that row from left SiOH
    #print("IDp=",IDp)
    SiOH_left.append(IDp)
    # append deprotonated row to SiO

    deprotonated_left.append(numpy.append(IDd,charged))
    # add to list of deprotonation events
    protonated_left.append(numpy.append(IDp,chargep))
    # add to list of deprotonation events

deprotonated_right = []
protonated_right = []

for s in range(int(steps)):
    indexd = randint(0, len(SiOH_right)-1)
    # choose random left SiOH to deprotonate
    if SiOH_right[indexd][0] in Siss[:,0]:
        Siss[numpy.where(Siss[:,0] ==
            SiOH_right[indexd][0])[0],1] -= 1
    # reduce charge of Si
    charged = Siss[numpy.where(Siss[:,0] ==
        SiOH_right[indexd][0])[0],1]
    elif SiOH_right[indexd][0] not in Siss[:,0]:
        charged = -1
    else:
        print("ERROR")
    indexp = randint(0, len(SiO_right)-1)
    # choose random left SiO to protonate
    if SiO_right[indexp][0] in Siss[:,0]:
        # if silanol is part of geminal
        Siss[numpy.where(Siss[:,0] ==
            SiO_right[indexp][0])[0],1] += 1
    # charge of Si +1
    chargep = Siss[numpy.where(Siss[:,0] ==
        SiO_right[indexp][0])[0],1]

```

```

        SiO_right[indexp][0][0],1]
    elif SiO_right[indexp][0] not in Siss[:,0]:
        chargep = 0

    Od_index = SiOH_right[indexd][1]
    # atom number of deprotonating oxygen
    #print("length=",len(SiOH_right))
    indices = [] # indices of items to be removed
    for i in range(len(SiOH_right)):
        #print("i=",i)
        if SiOH_right[i][1] == Od_index:
            indices.append(i)
    #print("indices=",indices)
    for j in sorted(indices, reverse=True):
        #print("j=",j)
        IDd = SiOH_right.pop(j)
    # delete that row from right SiOH
    #print("IDd=",IDd)
    SiO_right.append(IDd)
    # append deprotonated row to SiO

    Op_index = SiO_right[indexp][1]
    # atom number of protonating oxygen
    #print("length=",len(SiO_right))
    indices = [] # indices of items to be removed
    for i in range(len(SiO_right)):
        #print("i=",i)
        if SiO_right[i][1] == Op_index:
            indices.append(i)
    #print("indicesp",indices)
    for j in sorted(indices, reverse=True):
        #print("j=",j)
        IDp = SiO_right.pop(j)
    # delete that row from right SiOH
    #print("IDp=",IDp)
    SiOH_right.append(IDp)
    # append deprotonated row to SiO

    deprotonated_right.append(numpy.append(IDd,charged))
    # add to list of deprotonation events
    protonated_right.append(numpy.append(IDp,chargep))
    # add to list of deprotonation events

    ##% list of unique SiO- oxygens
    oxygen = []
    for i in range(len(SiO_right)):
        oxygen.append(SiO_right[i][1])
    for i in range(len(SiO_left)):
        oxygen.append(SiO_left[i][1])

    output = []
    for x in oxygen:
        if x not in output:
            output.append(x)

    ##% write output files
    Sip_left = open("outputs\which_Si_protonates.left", "w")
    Op_left = open("outputs\which_O_protonates.left", "w")
    Hp_left = open("outputs\which_H_protonates.left", "w")
    Cp_left = open("outputs\charge_of_protonating_Si.left", "w")
    Sid_left = open("outputs\which_Si_deprotonates.left", "w")
    Od_left = open("outputs\which_O_deprotonates.left", "w")
    Hd_left = open("outputs\which_H_deprotonates.left", "w")
    Cd_left = open("outputs\charge_of_deprotonating_Si.left", "w")

    Sip_right = open("outputs\which_Si_protonates.right", "w")
    Op_right = open("outputs\which_O_protonates.right", "w")
    Hp_right = open("outputs\which_H_protonates.right", "w")
    Cp_right = open("outputs\charge_of_protonating_Si.right", "w")
    Sid_right = open("outputs\which_Si_deprotonates.right", "w")
    Od_right = open("outputs\which_O_deprotonates.right", "w")
    Hd_right = open("outputs\which_H_deprotonates.right", "w")
    Cd_right = open("outputs\charge_of_deprotonating_Si.right", "w")

    for i in range(len(deprotonated_left)):
        charge_deprotonated_left = 0
        charge_deprotonated_right = 0
        charge_protonated_left = 0
        charge_protonated_right = 0

        if deprotonated_left[i][4] == -1:
            charge_deprotonated_left = 0.725000
            # set charge of single dangling Si
        elif deprotonated_left[i][4] == -2:
            charge_deprotonated_left = 0.350000
            # set charge of double dangling Si
        if deprotonated_right[i][4] == -1:
            charge_deprotonated_right = 0.725000
            # set charge of single dangling Si
        elif deprotonated_right[i][4] == -2:
            charge_deprotonated_right = 0.350000
            # set charge of double dangling Si

        if protonated_left[i][4] == 0:
            charge_protonated_left = 1.100000
            # set charge of protonated Si
        elif protonated_left[i][4] == -1:
            charge_protonated_left = 0.725000
            # set charge of single dangling Si
        if protonated_right[i][4] == 0:
            charge_protonated_right = 1.100000
            # set charge of protonated Si
        elif protonated_right[i][4] == -1:
            charge_protonated_right = 0.725000
            # set charge of single dangling Si

        Sip_left.write("{}\n".format(protonated_left[i][0]))
        # write files with atom numbers of which Si protonates
        Op_left.write("{}\n".format(protonated_left[i][1]))
        Hp_left.write("{}\n".format(protonated_left[i][2]))
        Cp_left.write("{}\n".format(charge_protonated_left))
        Sid_left.write("{}\n".format(deprotonated_left[i][0]))
        Od_left.write("{}\n".format(deprotonated_left[i][1]))
        Hd_left.write("{}\n".format(deprotonated_left[i][2]))
        Cd_left.write("{}\n".format(charge_deprotonated_left))

        Sip_right.write("{}\n".format(protonated_right[i][0]))
        Op_right.write("{}\n".format(protonated_right[i][1]))
        Hp_right.write("{}\n".format(protonated_right[i][2]))
        Cp_right.write("{}\n".format(charge_protonated_right))
        Sid_right.write("{}\n".format(deprotonated_right[i][0]))
        Od_right.write("{}\n".format(deprotonated_right[i][1]))
        Hd_right.write("{}\n".format(deprotonated_right[i][2]))
        Cd_right.write("{}\n".format(charge_deprotonated_right))

        Sip_left.close()
        Op_left.close()
        Hp_left.close()
        Cp_left.close()
        Sid_left.close()
        Od_left.close()
        Hd_left.close()
        Cd_left.close()

        Sip_right.close()
        Op_right.close()
        Hp_right.close()
        Cp_right.close()
        Sid_right.close()
        Od_right.close()
        Hd_right.close()
        Cd_right.close()

        oxygen =
        open("outputs\deprotonated_oxygens_at_end.dat", "w")
        for i in range(len(output)):
            oxygen.write("{}\n".format(output[i]))
        oxygen.close()

        print("output files written")

```

E.3. Generating MSD data

```

#!/usr/bin/env

import argparse
import MDAnalysis as mda
from maicos import density_planar, msd_planar
import matplotlib.pyplot as plt

```

```

import numpy as np

plt.style.use('seaborn-colorblind')
plt.rcParams['font.serif'] = "Georgia"
plt.rcParams['font.family'] = "serif"

```

```

counter[0:n-i-1] += 1
msd = msd_planar(u.atoms.select_atoms('type 12'),
verbose=True,membrane_shift=True, varbins=True,
wallwidth=20, sternlayer=10, save=False)
.run(begin=i, end=-1)
# kan ook dz=value, bin width aanpassen
msdxy = (msd.results['msdx'] +
msd.results['msdy'])/2
msdz = msd.results['msdz']
for j in range(nbins):
    dataxy[j,0:n-i-1] += msdxy[j]
    dataz[j,0:n-i-1] += msdz[j]

output = dataxy/counter
file = open("/stokes/fenna/"+path+"/k"+k+
"/outputs/MSDxy_Na.dat", "w")
for i in range(len(output[0])):
    file.write("{} {} {} {} {} {} \n".format(output[1][i],
output[2][i], output[3][i], output[4][i], output[5][i],
output[6][i]))
file.close()
output = dataz/counter
file = open("/stokes/fenna/"+path+"/k"+k+
"/outputs/MSDz_Na.dat", "w")
for i in range(len(output[0])):
    file.write("{} {} {} {} {} {} \n".format(output[1][i],
output[2][i], output[3][i], output[4][i], output[5][i],
output[6][i]))
file.close()
#%% calculate msd Cl
nbins = 8
n = len(u.trajectory)
dataz = np.zeros((nbins,n))
dataxy = np.zeros((nbins,n))
counter = np.zeros((n))
for i in range(n-1):
    if i%100 == 0:
        print("i=",i)
        counter[0:n-i-1] += 1
        msd = msd_planar(u.atoms.select_atoms('type 13'),
verbose=True,membrane_shift=True, varbins=True,
wallwidth=20, sternlayer=10, save=False)
.run(begin=i, end=-1)
# kan ook dz=value, bin width aanpassen
msdxy = (msd.results['msdx'] +
msd.results['msdy'])/2
msdz = msd.results['msdz']
for j in range(nbins):
    dataxy[j,0:n-i-1] += msdxy[j]
    dataz[j,0:n-i-1] += msdz[j]

output = dataxy/counter
file = open("/stokes/fenna/"+path+"/k"+k+
"/outputs/MSDxy_Cl.dat", "w")
for i in range(len(output[0])):
    file.write("{} {} {} {} {} {} \n".format(output[1][i],
output[2][i], output[3][i], output[4][i], output[5][i],
output[6][i]))
file.close()
output = dataz/counter
file = open("/stokes/fenna/"+path+"/k"+k+
"/outputs/MSDz_Cl.dat", "w")
for i in range(len(output[0])):
    file.write("{} {} {} {} {} {} \n".format(output[1][i],
output[2][i], output[3][i], output[4][i], output[5][i],
output[6][i]))
file.close()

```